Appendix II:

LSPC Watershed Model Development for Simulation of Loadings to the Los Angeles/Long Beach Harbors

October 2010

Appendix II Sections

Appendix II Summary

The *Watershed Model Development for Simulation of Loadings to the Los Angeles/Long Beach Harbors* Report describes the approach used to estimate metals and organic pollutant loads from the Los Angeles River, the San Gabriel River, and other nearshore watershed areas. These models, in addition to the Dominguez Channel model, were used to determine the pollutant loadings to Dominguez Channel and Greater Los Angeles and Long Beach Harbor Waters. Key findings of the report include:

- Pollutants of interest include metals such as copper, lead, and zinc, and several organic pollutants (PAHs, DDT, PCBs, and chlordane).
- Separate approaches were used to represent dry- and wet-weather conditions.
- The wet weather analyses are based on an eleven-year simulation using the LSPC watershed model (Section 3). A new model was developed to address nearshore areas, while previously developed models were used for the Los Angeles and San Gabriel River watersheds. Metals loadings were estimated based on direct LSPC simulations (using regionally calibrated modeling parameters). Watershed model parameters were not available to represent organics loadings. To determine PAHs loads, land use-specific EMCs from stormwater monitoring studies were applied to predicted flows. Specifically, stormwater total PAH concentrations for each model subwatershed were predicted using weighted averages of land use EMCs based on area and runoff potential of each land use in each subwatershed. For DDT, PCBs, and chlordane, a different approach was required because no detectable levels of these pollutants were found in the mass emissions monitoring stations (DDT was only detected in stations associated with agricultural runoff). Sediment concentrations from Bight 03 monitoring data were applied to predicted sediment loads to estimate loads of these pollutants.
- Dry-weather models used for TMDL calculations have been typically based on steady-state assumptions for flows and pollutant concentrations and heavily reply on robust monitoring efforts (Section 4). Assumptions for steady-state, dry-weather flows were based on a combination of monitoring data and simplified methods based on land use. Monitoring results from the Los Angeles River, San Gabriel River, and Ballona Creek were extrapolated for prediction of pollutant loads from the remaining watersheds.
- The average daily loadings of metals, PAHs, DDT and PCBs to each receiving waterbody are shown in Figures 30 through 35. These average daily loadings are based on eleven year loads and were ultimately used as inputs to the EFDC receiving water model (see Appendix I). Annual loads for an 11-year period to each receiving waterbody were calculated for each pollutant and are presented in Appendix B.

LSPC Watershed Model Development for Simulation of Loadings to the Los Angeles/Long Beach Harbors

FINAL

October 2010

Prepared for:
USEPA Region 9
Los Angeles Regional Water Quality Control Board

Prepared by:
Tetra Tech, Inc.

1. Introduction

Estimation of pollutant loadings to the Los Angeles and San Gabriel estuaries, Los Angeles and Long Beach Harbors (Harbors), and San Pedro Bay (SPB) requires development of approaches that address both wet and dry conditions. Previous modeling studies performed by Tetra Tech for Los Angeles River (LAR) and San Gabriel River (SGR) supported calculation of metals loadings to those waterbodies. Recent modeling of Dominguez Channel (DC) by the Southern California Coastal Water Research Project (SCCWRP) will be based on consistent modeling approaches for metals (SCCWRP, unpublished results). For the remaining watershed area not included in the LAR, SGR, and DC models (hereafter referred to as nearshore areas), including areas draining to estuaries of LAR and SGR, Tetra Tech worked with SCCWRP, Los Angles Regional Water Quality Control Board (Regional Board) staff, and EPA to develop and implement an approach to calculate pollutant loadings from the nearshore areas (see Figure 1).

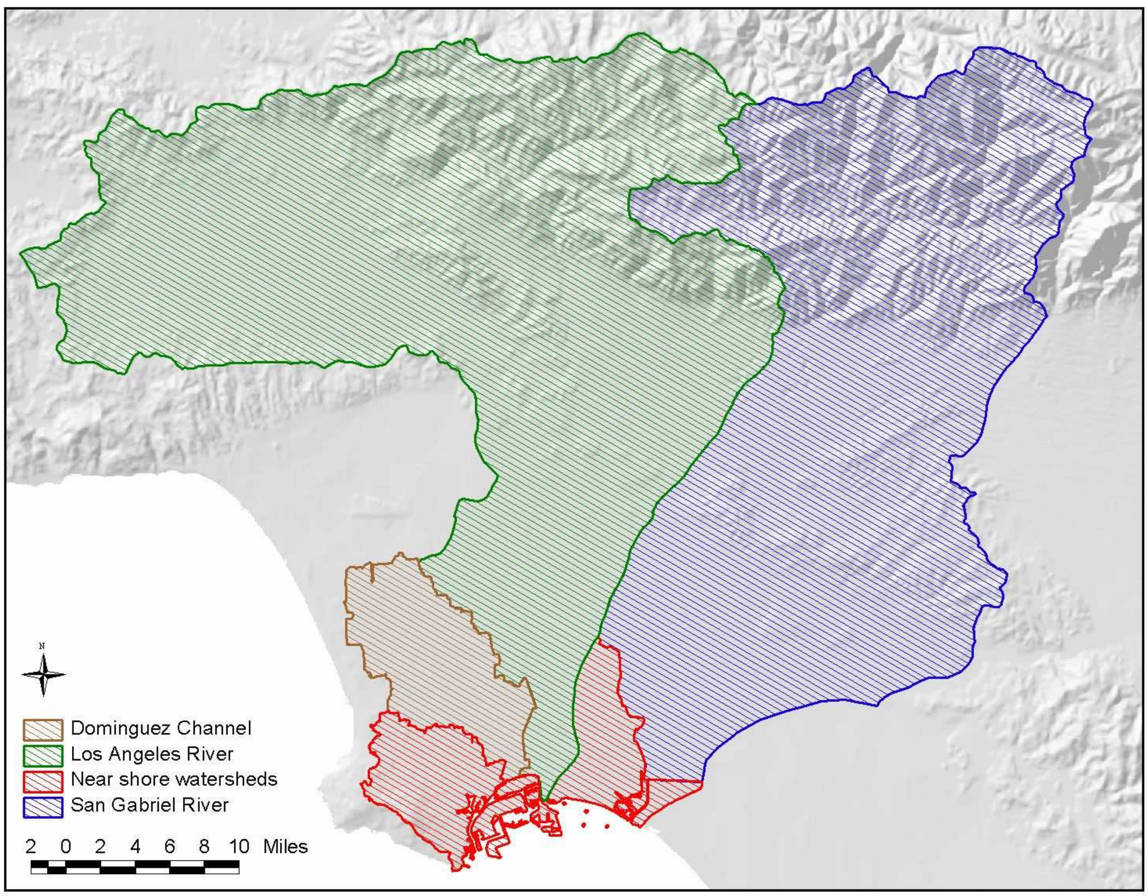

Figure 1. Watersheds of the Harbors and San Pedro Bay

This report provides a summary of the approach Tetra Tech used for estimation of metals and organic pollutant loads (polycyclic aromatic hydrocarbons [PAHs], dichlorodiphenyltrichloroethane [DDT], polychlorinated biphenyls [PCBs], and chlordane) from LAR, SGR, and nearshore areas. Pollutant loadings from the DC Los Angeles Harbor were estimated in a separate study performed by SCCWRP (SCCWRP, unpublished results).

2. Model Domain

The entire watershed modeling domain for the current study is depicted in Figure 1. As discussed, this study utilized previously developed models of LAR and SGR, as well as a model of DC developed through a separate study performed by SCCWRP. The remaining nearshore areas required development of new models for simulation of runoff pollutant loads to SGR and LAR estuaries, the Harbors, and SPB (depicted in red in Figure 1). As opposed to the LAR, SGR, and DC models of major watersheds and associated rivers/channels discharging to estuaries, the nearshore watersheds are representative of smaller tributaries and sewersheds discharging directly to receiving waters.

Tetra Tech delineated the nearshore subwatersheds based on a combination of sewersheds provided by the POLA and the Port of Long Beach (POLB); monitoring locations; model domains of LAR, SGR, and DC watersheds; receiving water model domain of the Harbors and SPB; and a USGS digital elevation model (Figure 2). These subwatershed boundaries were used in development of hydrologic and water quality models of these areas.

Because the pollutant sources and their means of transport to receiving waters vary between wet and dry conditions (McPherson et al., 2005a; LARWQCB, 2005a, 2005b, 2005c, Stein et al., 2003), Tetra Tech developed technical approaches that are consistent with our understanding of the processes for each weather condition—this assumption is consistent with most other TMDLs adopted in the Los Angeles Region. The following sections describe our technical approach and estimated pollutant loads for each condition.

3. Wet Weather

The transport of metals and organic pollutants during wet-weather events is generally believed to be associated with the detachment and transport of sediment (Buffleben et al., 2002; CALTRANS, 2003; Hoffman et al., 1982; Lau and Stenstrom, 2005; Logonathan et al., 1997; Stein et al., 2005; Yunker et al., 2002). Specifically, during rainy periods, these pollutant loads are delivered to the waterbody through creeks and stormwater collection systems.

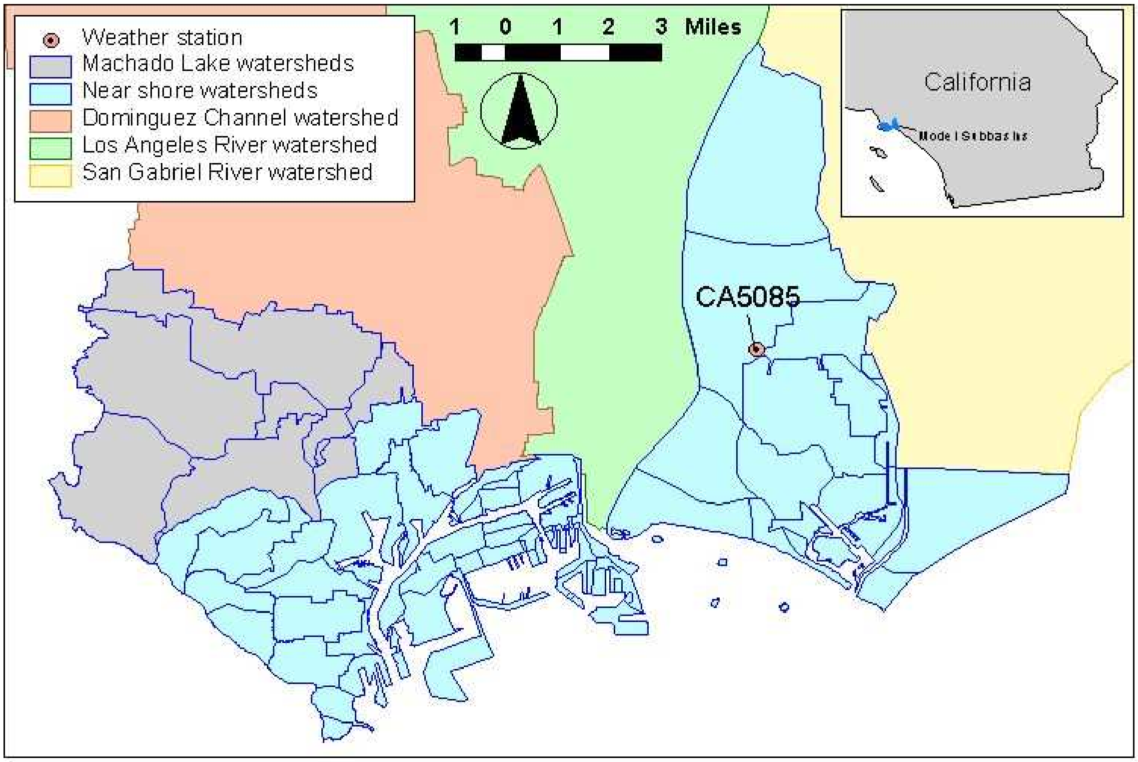

Figure 2. Subwatershed Delineation for the Nearshore Watersheds

Specific watershed sources of metals and organic pollutants vary based on location and pollutant and, for some pollutants, concentration "hot spots" are present. These "hot spots" are typically associated with spills or other events that lead to higher pollutant concentrations and their presence and impact to receiving waters are difficult to identify/characterize. Additionally, available data to characterize the pollutant sources are often limited. Metals and organic pollutants can also be linked to specific land use types that have higher relative accumulation rates of the pollutant(s), higher relative loads of sediment from the land surface, or are more likely to deliver sediment and associated pollutants to waterbodies due to delivery through stormwater collection systems.

To assess the link between sources of sediment, metals, and organic pollutants and the impaired waters, a modeling system was utilized that simulates land use-based sources of sediment and associated metals loads and the hydrologic and hydraulic processes that affect delivery. The hydrology and sediment model results along with monitoring data were utilized to determine organic pollutant loads to the Harbors.

The U.S. Environmental Protection Agency's (USEPA) Loading Simulation Program C++ (LSPC) (Shen et al., 2004; USEPA, 2003a) was used to represent the hydrologic and water quality conditions in the Harbors' watersheds. LSPC is a component of the USEPA's TMDL Modeling Toolbox (USEPA, 2003b), which has been developed through a joint effort between USEPA and Tetra Tech, Inc. It integrates a geographical information system (GIS), comprehensive data storage and management capabilities, a dynamic watershed model (a re-coded version of USEPA's Hydrological Simulation Program – FORTRAN [HSPF] [Bicknell et al., 2001]), and a data analysis/post-processing system into a convenient PC-based windows interface that dictates no software requirements.

LSPC is capable of representing loading and both flow and water quality from non-point and point sources as well as simulating in-stream processes. LSPC can simulate flow, sediment, metals, nutrients, pesticides, and other conventional pollutants for pervious and impervious lands and waterbodies. The model has been successfully applied and calibrated in Southern California for the Los Angeles River, the San Gabriel River, the San Jacinto River, and multiple watersheds draining to impaired beaches of the San Diego Region. For the nearshore watersheds, LSPC was used to simulate sediment and metals (copper, lead, and zinc) for determining loads to the Harbors.

Previous wet-weather watershed modeling and TMDL efforts by Tetra Tech and SCCWRP have led to the development of a regional watershed modeling approach to simulate hydrology, sediment, and metals transport in Los Angeles watersheds. The regional modeling approach assumes that metals loadings can be dynamically simulated based on hydrology and sediment transported from land uses in a watershed. Development of the approach resulted from application and testing of models for multiple small-scale land use sites and larger watersheds in the Los Angeles Region. SCCWRP developed watershed models, based on HSPF (Bicknell et al., 2001), of multiple homogeneous land use sites in the region. Sufficient stormflow and water quality data were available at these locations to facilitate calibration of land-use-specific HSPF modeling parameters. These parameters were validated in an additional HSPF model of Ballona Creek (Ackerman et al., 2005a; SCCWRP, 2004), and similar models of LAR (Tetra Tech, Inc., 2004) and SGR (Tetra Tech, Inc, 2005a) based on LSPC. These models were used to calculate TMDLs for each of these waterbodies (LARWQCB, 2005a, 2005c, and 2006; USEPA, 2007).

Wet-weather days were determined based on flow criteria for each subwatershed. Specifically, for the nearshore areas, all days with flow greater than the dry-weather flow calculated in Section 4 are designated as wet days. Similarly, for LAR and SGR, all days with flow greater than the 50^{th} percentile observed flow in the watershed are designated as wet days (Section 4), which is consistent with the designation of wet days in the LAR Metals TMDL (LARWQCB, 2005c). All wet days in the model were assigned pollutant loads based on the approaches described in Section 3.3, while all dry days in the model were assigned loads based on the approaches described in Section 4.

Wet-weather events for the study areas were simulated using previously calibrated LSPC models of the LAR and SGR watersheds (illustrated in green and blue in Figure 1, respectively) and newly developed LSPC models for the nearshore areas (Figure 2). The simulation time frames for the LAR and SGR watershed models were extended to overlap with the current study period. To perform this temporal extension, updated flow, copper, lead, and zinc point source data for the major dischargers in the watershed were required. With these data, simulations were performed to obtain flow, total suspended solid (TSS), and total metals model output for the LAR and SGR watersheds.

The following sections describe wet-weather model configuration, calibration, validation, and application. While they focus largely on the newly developed models of the nearshore areas, details associated with the extension of the LAR and SGR models and their application to determine loadings to their respective estuaries are also provided, where pertinent.

3.1. Model Configuration

The watershed model represented the variability of wet-weather runoff source contributions through dynamic representation of hydrology and land practices. It included all point and non-point source contributions. Key components of the watershed modeling that are discussed below are:

- Watershed segmentation
- Meteorological data
- Land use representation
- Soils
- Reach characteristics
- Point source discharges
- Hydrology representation
- Pollutant representation
- Flow data

3.1.1. Watershed Segmentation

To evaluate sources contributing to an impaired waterbody and to represent the spatial variability of these sources, the contributing drainage area was represented by a series of sub-watersheds. This subdivision was primarily based on the stream networks and topographic variability, and secondarily on the locations of flow and water quality monitoring stations, consistency of hydrologic factors, land use consistency, and existing watershed boundaries (e.g., CALWTR 2.2 watershed boundaries and municipal storm sewersheds). The nearshore watersheds were divided into 76 sub-watersheds for appropriate hydrologic connectivity and representation (Figure 2). Nine additional watersheds that drain to Machado Lake were delineated, but are not assumed to be hydrologically connected to areas draining to the Harbors except during extremely large and rare meteorological events.

3.1.2. Meteorological Data

Meteorological data are a critical component of the watershed model. LSPC requires appropriate representation of precipitation and potential evapotranspiration (ET). In general, hourly precipitation (or finer resolution) data are recommended for nonpoint source modeling. Therefore, only weather stations with hourly-recorded data were considered in the precipitation data selection process. Rainfall-runoff processes for each subwatershed were driven by precipitation data from the most representative station. These data provide necessary input to LSPC algorithms for hydrologic and water quality representation.

National Climatic Data Center (NCDC) precipitation data were reviewed based on geographic location, period of record, and missing data to determine the most appropriate meteorological stations to represent the nearshore areas. Hourly rainfall data were obtained from the Long Beach weather station (CA5085) located in the eastern portion of the nearshore watersheds (Figure 2). Precipitation data were obtained for January 1, 1990 through July 31, 2005.

Additional localized precipitation data were obtained from the Ports of Long Beach and Los Angeles. These data were specific to monitoring locations and storm events. (See Section 3.1.9 for more information on the monitoring locations.) Data from these local stations were used to replace the CA5085 precipitation data for the particular storm events to create separate weather files for each monitoring location and its surrounding subwatersheds.

Because rainfall gages are not always in operation and accurately recording data, the resulting dataset may contain various intervals of accumulated, missing, or deleted data. Missing or deleted intervals are periods over which either the rainfall gage malfunctioned or the data records were somehow lost. Accumulated intervals represent cumulative precipitation over several hours, but the exact hourly distribution of the data is unknown. To address the incomplete portions of CA5085, which accounted for less than 5 percent of the records during the model period, it was necessary to patch the rainfall data with information from nearby gages.

Specifically, to address days that had accumulated intervals, the daily rainfall total was summed and treated as an accumulated interval for that entire 24-hour period. The normal-ratio method (Dunne & Leopold, 1978) was used to disaggregate these daily totals to hourly based on hourly rainfall distributions at nearby gages. To apply this normal-ratio method, a composite hourly distribution was first estimated for station *A* (where accumulated, missing, or deleted data exist). This distribution was determined by using a weighted average from surrounding *n* stations with similar rainfall patterns and where unimpaired data were measured for the same time period.

Subsequently, the observed daily values were distributed across the resulting hourly time series, keeping the original rainfall volume intact. Using this same methodology, missing or deleted intervals in the data were patched using the normal-weighted hourly distributions at nearby gages. Because the normal ratio considers the long-term average rainfall as the weighting factor, this method is adaptable to regions where there is large orographic precipitation variation since elevation differences will not bias the predictive capability of the method.

Potential evapotranspiration, which is also required by the LSPC model, was calculated from data obtained from NCDC. Specifically, long-term hourly wind speed, cloud cover, temperature, and dew point data available for the Los Angeles International Airport (WBAN #23174) were used to calculate potential evapotranspiration for the weather station representing the nearshore areas.

In addition to developing the new weather file for the nearshore model, weather files for the LAR and SGR models were extended to cover the entire modeling period. The original weather files for LAR and SGR ended in 2001 and 2004, respectively. Data associated with each of the LAR and SGR stations were obtained and updated weather files were created consistent with methods used in development of the original models (Tetra Tech, Inc., 2004 and 2005a).

3.1.3. Land Use Representation

The watershed model requires a basis for distributing hydrologic and pollutant loading parameters. This is necessary to appropriately represent hydrologic variability throughout the basin, which is influenced by land surface and subsurface characteristics. It is also necessary to represent variability in pollutant loading, which is highly correlated with land practices. The basis for this distribution was provided by the land use coverage of the entire watershed. The land use data used to represent the nearshore areas was the Southern California Association of Governments (SCAG) 2000 land use dataset that covers Los Angeles and Orange Counties.

Although the multiple categories in the land use coverage provide much detail regarding spatial representation of land practices in the watershed, such resolution is unnecessary for watershed modeling if many of the categories share hydrologic or pollutant loading characteristics. Therefore, many land use categories were grouped into similar classifications, resulting in a subset of eight categories for modeling: agriculture, commercial, high-density residential, industrial, low-density residential, mixed urban, open, and port activities. Selection of these land use categories was based on the availability of monitoring data and literature values that could be used to characterize individual land use contributions and critical metal-contributing practices associated with different land uses. The distributions of the eight land uses in the 76 subwatersheds are presented in Table 1.

LSPC algorithms require that land use categories be divided into separate pervious and impervious land units for modeling. The division of the eight land use categories identified above to represent impervious and pervious areas in the model was based on typical impervious percentages associated with different land use types as defined in the TR-55 Manual (USDA, 1986). This division resulted in 14 unique pervious or impervious land uses in the nearshore watersheds.

Table 1. Land Use Areas (acres) of each Subwatershed

Sub-watershed number	Agri-culture	Com-mercial	High density residential	Industrial	Low density residential	Mixed urban	Open	Port activities
1	0.0	0.0	0.0	0.0	0.0	0.0	0.0	254.2
2	0.0	0.0	0.0	0.0	0.0	0.0	0.0	17.1
3	0.0	0.0	0.0	8.6	0.0	5.7	0.0	128.5
4	0.0	0.0	0.0	0.0	0.0	0.0	0.0	22.9
5	0.0	22.9	0.0	0.0	0.0	0.0	0.0	25.7
6	0.0	0.0	0.0	0.0	0.0	0.0	0.0	80.0
7	0.0	0.0	0.0	2.9	0.0	0.0	0.0	54.3
8	0.0	2.9	0.0	0.0	11.4	0.0	0.0	74.3
9	0.0	0.0	0.0	0.0	0.0	0.0	0.0	5.7
10	0.0	0.0	0.0	0.0	0.0	0.0	0.0	20.0
11	0.0	2.9	0.0	5.7	20.0	8.6	14.3	171.4
12	0.0	0.0	0.0	0.0	0.0	0.0	0.0	8.6
13	0.0	0.0	0.0	0.0	0.0	0.0	0.0	2.9
14	0.0	0.0	0.0	0.0	0.0	0.0	0.0	14.3
15	0.0	0.0	0.0	5.7	0.0	0.0	0.0	0.0
16	0.0	0.0	0.0	0.0	0.0	0.0	0.0	5.7
17	0.0	57.1	0.0	8.6	14.3	42.8	20.0	11.4
18	0.0	0.0	0.0	0.0	0.0	40.0	0.0	0.0
19	0.0	1.0	0.0	86.0	0.0	5.7	10.7	300.9
20	0.0	0.0	0.0	0.0	0.0	0.0	0.0	2.9
21	0.0	0.0	0.0	63.8	0.0	1.5	12.7	6.9
22	0.0	0.0	0.0	0.0	0.0	2.6	0.0	177.9
23	0.0	0.0	0.0	21.9	0.0	44.0	7.3	4.1
24	0.0	0.0	0.0	20.0	0.0	5.7	0.0	117.1
25	0.0	0.0	0.0	20.0	0.0	0.0	0.0	128.5
26	0.0	0.0	0.0	0.0	0.0	0.0	0.0	62.8
27	0.0	0.0	0.0	0.0	0.0	0.0	0.0	31.4
28	0.0	0.0	0.0	0.0	0.0	0.0	0.0	31.4
29	0.0	0.0	0.0	0.0	0.0	0.0	0.0	8.6
30	0.0	0.0	0.0	0.0	0.0	0.0	0.0	154.2
31	0.0	0.0	0.0	0.0	0.0	0.0	0.0	108.5
32	0.0	0.0	0.0	0.0	0.0	0.0	0.0	108.5

Sub-watershed number	Agri-culture	Com-mercial	High density residential	Industrial	Low density residential	Mixed urban	Open	Port activities
33	0.0	0.0	0.0	48.6	0.0	14.3	48.6	208.5
34	0.0	11.4	0.0	137.1	0.0	42.8	20.0	102.8
35	0.0	34.3	0.0	17.1	25.7	5.7	5.7	237.1
36	0.0	0.0	0.0	97.1	0.0	11.4	2.9	397.0
37	0.0	0.0	0.0	0.0	0.0	0.0	0.0	614.1
38	0.0	0.0	0.0	185.7	0.0	31.4	34.3	2.9
39	0.0	117.1	277.1	160.0	77.1	237.1	57.1	71.4
40	0.0	97.1	114.3	148.5	71.4	65.7	11.4	222.8
41	8.6	108.5	85.7	468.4	91.4	68.6	57.1	568.4
42	0.0	177.1	494.1	5.7	94.3	28.6	11.4	0.0
43	0.0	60.0	251.4	25.7	108.5	51.4	142.8	37.1
44	5.7	85.7	339.9	45.7	74.3	14.3	45.7	0.0
45	0.0	74.3	568.4	0.0	262.8	2.9	179.9	0.0
46	0.0	11.4	185.7	0.0	419.9	40.0	397.0	0.0
47	0.0	68.6	0.0	25.7	142.8	0.0	31.4	28.6
48	0.0	214.2	199.9	2.9	391.3	22.9	14.3	0.0
49	0.0	11.4	0.0	20.0	51.4	2.9	85.7	140.0
50	0.0	71.4	277.1	0.0	345.6	0.0	22.9	0.0
51	0.0	14.3	288.5	0.0	120.0	2.9	134.2	0.0
52	0.0	22.9	331.3	0.0	71.4	8.6	122.8	0.0
53	0.0	5.7	65.7	0.0	122.8	37.1	51.4	0.0
54	0.0	0.0	40.0	0.0	40.0	2.9	40.0	0.0
101	0.0	0.0	0.0	5.7	0.0	0.0	0.0	0.0
102	0.0	0.0	0.0	14.3	0.0	0.0	0.0	0.0
103	0.0	0.0	0.0	11.4	0.0	0.0	0.0	0.0
104	0.0	0.0	0.0	8.6	0.0	0.0	0.0	0.0
105	0.0	291.3	285.6	0.0	448.4	131.4	154.2	5.7
106	0.0	288.5	674.1	165.7	585.5	54.3	42.8	0.0
107	0.0	8.6	125.7	0.0	179.9	8.6	85.7	0.0
108	0.0	0.0	0.0	0.0	71.4	0.0	0.0	0.0
109	0.0	40.0	68.6	0.0	85.7	2.9	2.9	0.0
110	0.0	157.1	585.5	11.4	239.9	2.9	302.8	0.0
111	8.6	77.1	297.1	2.9	151.4	2.9	74.3	0.0
112	0.0	34.3	137.1	0.0	11.4	5.7	20.0	0.0
113	0.0	80.0	17.1	262.8	14.3	14.3	62.8	0.0
114	0.0	40.0	11.4	102.8	0.0	0.0	40.0	0.0
115	0.0	45.7	142.8	0.0	82.8	2.9	62.8	0.0
116	0.0	140.0	188.5	194.2	734.1	225.6	971.1	0.0
117	0.0	828.3	1,105.4	22.9	145.7	188.5	74.3	0.0
118	0.0	48.6	211.4	0.0	17.1	22.9	0.0	0.0
119	0.0	239.9	551.3	0.0	0.0	34.3	0.0	0.0
120	0.0	219.9	1,062.5	0.0	0.0	14.3	102.8	0.0
121	0.0	1,322.5	1,216.8	782.6	77.1	105.7	534.1	0.0
122	80.0	976.9	2,433.6	371.3	748.4	122.8	97.1	0.0

3.1.4. Soils

Soil data for the watershed were obtained from the State Soil Geographic Data Base (STATSGO). There are four main Hydrologic Soil Groups (Groups A, B, C, and D). These groups, which are described below, range from soils with low runoff potential to soils with high runoff potential (USDA, 1986).

The total area associated with each specific soil type was determined for all 76 subwatersheds. The representative soil group for each model subwatershed was based on the dominant soil type found in that subwatershed.

<u>Group A Soils</u> have low runoff potential and high infiltration rates even when wet. They consist chiefly of sand and gravel and are well drained to excessively-drained.

<u>Group B Soils</u> have moderate infiltration rates when wet and consist chiefly of soils that are moderately-deep to deep, moderately- to well-drained, and moderately course.

<u>Group C Soils</u> have low infiltration rates when wet and consist chiefly of soils having a layer that impedes downward movement of water with moderately-fine to fine texture.

<u>Group D Soils</u> have high runoff potential, very low infiltration rates and consist chiefly of clay soils. These soils also include urban areas.

3.1.5. Reach Characteristics

Each delineated subwatershed was represented with a single stream assumed to be a completely mixed, one-dimensional segment with a trapezoidal cross-section. While some reach segments were based on EPA's Reach File, Version 3 (RF3), most of the reaches are based on storm sewer systems, since much of the flow in the nearshore watersheds drains through storm sewers. Once the representative reach was identified for each subwatershed, slopes were calculated based on Digital Elevation Model (DEM) data, and stream lengths measured from the reach coverage. Because much of the area surrounding POLA/POLB has no topographic variation, several subwatersheds had a slope of zero. To ensure that the model would predict flow through these areas, a slope of 0.001 was assigned.

In addition to stream slope and length, mean depths and channel widths are required to route flow and pollutants through the hydrologically connected subwatersheds. Mean stream depth and channel width were estimated using regression curves that relate upstream drainage area to stream/sewer dimensions. An estimated Manning's roughness coefficient of 0.02 was also applied to each representative stream reach.

3.1.6. Point Source Discharges

During watershed model configuration, National Pollutant Discharge Elimination System (NPDES) discharges can be incorporated into the model as point sources of flow and pollutants. There were no major point sources located in the nearshore watersheds, so this step was excluded during model development.

To extend the LAR and SGR models through the entire modeling period, the NPDES discharge data for flow, copper, lead, and zinc were extended. The dischargers and time periods associated with these data are presented in Table 2. Many of the discharge datasets had missing months or other missing flow and water quality data. In the previously calibrated LAR and SGR models, water quality was incorporated as a constant value based on the discharge effluent concentrations. These constant concentrations were extended to cover the entire modeling period. For dischargers with variable flow that had missing or limited flow data, daily averages calculated from the existing data was used in the model. For dischargers with nearly constant flows, longer averages (e.g., monthly) were included in the model. These averaged flows are identified in the modeling database and can be easily modified if more complete flow data become available.

Table 2. LAR and SGR Point Source Dischargers and Date Ranges

San Gabriel River			
NPDES #	**Facility**	**Pipe**	**Period**
CA0053619	Pomona WWRP	PO001	01/1986–01/2006
CA0053716	Whittier Narrows WWRP	WN001	01/1986–12/ 2005
CA0053911	San Jose Creek WWRP	SJC001e	01/1986–07/2005
		SJC001w	12/1992–09/2005
		SJC002	01/1986–12/ 2005
		SJC003	12/1992–12/ 2005
CA0054011	Los Coyotes WWRP	LC001	01/1986–12/ 2005
CA0054119	Long Beach WWRP	LB001	01/1986–12/ 2005
Los Angeles River			
NPDES #	**Discharger**	**Facility**	**Period**
CA0001309	The Boeing Company	Rocketdyne Div. - Santa Susana	01/1988–12/2005
CA0052949	Southern California Edison	Dominguez Hills Fuel Oil Facility	01/1988–12/2005
CA0053953	LA City Bureau of Sanitation	L.A.-Glendale WWRP, NPDES	01/1988–12/2005
CA0055531	Burbank, City Of Public Works	Burbank WWRP, NPDES	01/1988–12/2005
CA0056227	LA City Bureau of Sanitation	Tillman WWRP, NPDES	01/1988–12/2005
CA0064271	Las Virgenes MWD	Tapia Park WWRP, NPDES	01/1988–12/2005

3.1.7. Hydrology Representation

Watershed hydrology plays an important role in the determination of nonpoint source flow and ultimately nonpoint source loadings to a waterbody. The watershed model must appropriately represent the spatial and temporal variability of hydrologic characteristics within a watershed. Key hydrologic characteristics include interception storage capacities, infiltration properties, evaporation and transpiration rates, and watershed slope and roughness. LSPC's algorithms are identical to those in HSPF. The LSPC/HSPF modules used to represent watershed hydrology for TMDL development included PWATER (water budget simulation for pervious land units) and IWATER (water budget simulation for impervious land units). A detailed description of relevant hydrological algorithms are presented in the HSPF User's Manual (Bicknell et al., 2001).

Key hydrologic parameters in the PWATER and IWATER modules are infiltration, groundwater flow, and overland flow. The nearshore models were initially populated using hydrologic parameters for the LAR watershed model (LARWQCB, 2005c; Tetra Tech, Inc., 2004). These parameters were refined as part of model calibration since there were some relevant hydrology data available in the nearshore watersheds.

3.1.8. Watershed Runoff Pollutant Representation

The various pollutants draining to the Harbors were represented through their association with sediment and/or flow. Therefore, to simulate sediment contributions to the nearshore watersheds, the SEDMNT, SOLIDS, and SEDTRN modules were implemented and are discussed below. The sediment model results were then incorporated into the loading estimates and sensitivity analyses for each pollutant. The pollutant-specific approaches and results are discussed in Section 3.3.

The SEDMNT module simulates the production and removal of sediment from all pervious land segments in the model. The removal of sediment by water is simulated as washoff of detached sediment and scour of the soil matrix. Both processes are highly dependent on land use. Washoff depends on both the amount of detached sediment available to be carried away by the overland flow and the transport capacity of the overland flow. The amount of detached sediment available to be transported depends primarily on the rainfall intensity. The transport capacity of the overland flow depends on surface water storage and surface water flow.

The SOLIDS module represents the accumulation and removal of sediment/solids from impervious lands. The removal of sediment/solids is simulated by washoff of available sediment. Sediment/solids accumulation represents atmospheric fallout and general land surface accumulation for urban areas.

Once the sediment is transported to the stream channel by overland flow, the SEDTRN module simulates the transport, deposition, and scour of sediment in the stream channels. These processes depend primarily on sediment characteristics, e.g. settling velocity, critical shear stress for deposition, critical shear stress for resuspension, and predicted bottom shear stresses.

3.1.9. Flow Data

Three storm events were monitored by POLB and POLA. Information about each flow station, including outflow subwatershed, the station identification number, and period used for model calibration, is presented in Table 3, and their locations are illustrated in Figure 3.

Table 3. Flow Data Used for LSPC Model Calibration and Validation

Station ID	Model subwatershed	Dates
Forest Industries	27	2/24/03–2/25/03
Maritime Museum (MM)	48	3/17/02
Pier A	22	2/24/03–2/25/03

3.2. Model Calibration and Validation

After the model was configured, model calibration and validation were performed. This is generally a two-phase process, with hydrology calibration and validation completed before repeating the process for water quality. Upon completion of the calibration and validation at selected locations, a calibrated dataset containing parameter values for each modeled land use and pollutant was developed.

Calibration refers to the adjustment or fine-tuning of modeling parameters to reproduce observations. Calibration was performed for different LSPC modules at the Forest subwatershed (Figure 3). Subsequently, model validation was performed to test the calibrated parameters at different locations (Pier A and Maritime Museum [Figure 3]), without further adjustment.

3.2.1. Hydrology Calibration and Validation

Hydrology is the first model component calibrated because estimation of sediment loading relies heavily on flow prediction. The hydrology calibration involves a comparison of model results to in-stream flow observations at selected locations. After comparing the results, key hydrologic parameters were adjusted and additional model simulations were performed. This iterative process was repeated until the simulated results closely represented the system and reproduced observed flow patterns and magnitudes.

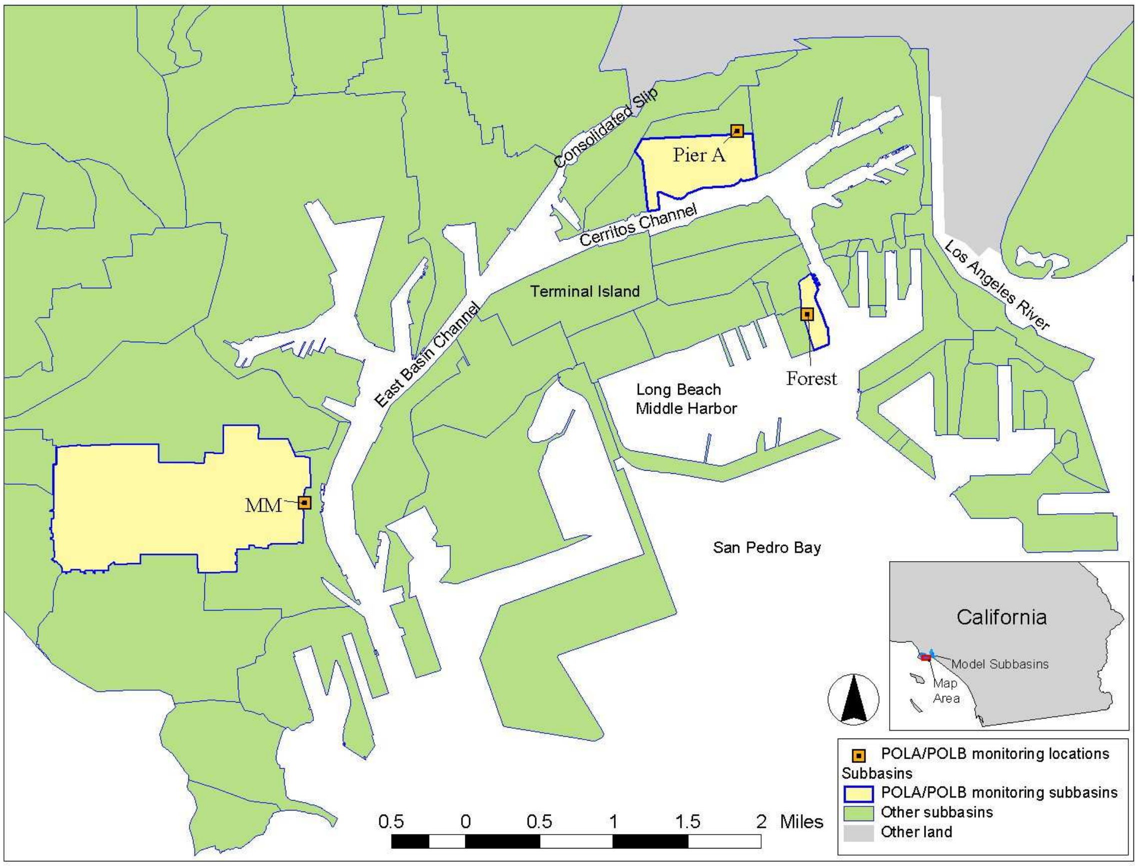

Figure 3. Locations of Monitoring Stations Used for Model Calibration

The nearshore models were initially populated using hydrologic parameters for the LAR watershed model (LARWQCB, 2005c; Tetra Tech, Inc., 2004). The LAR watershed had very similar land uses to the nearshore watersheds, so the parameters were easily transferred. However, the Port Activities land use was not present in the LAR watershed. Therefore, this land use was initially parameterized with the LAR watershed industrial land use parameters and subsequently adjusted during model calibration.

For the nearshore watersheds, predicted hydrology was compared to observed flow from a single storm event at each of three monitoring stations (Forest, Pier A, and Maritime Museum), which are identified in Figure 3. The Forest site was considered a calibration location, while Pier A and Maritime Museum were used as validation locations.

The model's accuracy was primarily assessed through interpretation of the time-variable plots. Time-variable plots of observed versus modeled flow provided insight into the model's representation of storm hydrographs, baseflow recession, and time distribution. Time-variable plots for each station are shown in Figure 4 through Figure 6.

During low flow conditions, the model is unable to predict dry urban runoff associated with human activities (e.g., lawn irrigation, car washing) without data quantifying the spatial distribution, flow, and loadings associated with these sources. As a result, the LSPC watershed model is not used for dry-weather load estimates and a separate methodology was used to calculate dry weather loadings (see Section 4).

3.2.1.1. Hydrology Calibration

Figure 4 shows the calibration results for the Forest monitoring station, which is entirely represented by the Port Activities land use. The plot shows modeled and measured flow versus time. As this plot indicates, the predicted flow for the Forest subwatershed has a similar pattern, but slightly higher peaks than the observed flow at the POLA/POLB stormwater sampling station. This small discrepancy in flow is well within acceptable modeling ranges.

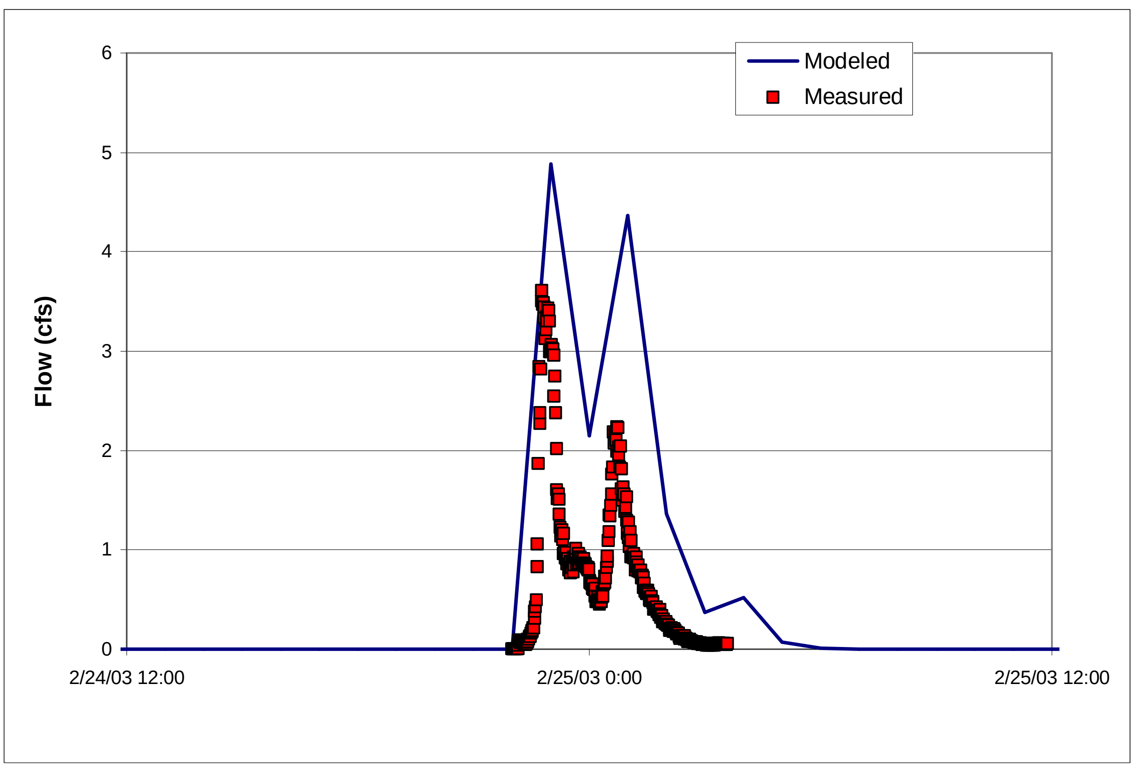

Figure 4. Modeled and Observed Flow for the Forest Subwatershed

3.2.1.2. Hydrology Validation

After calibrating hydrology, a validation of the hydrologic parameters was made through a comparison of model output to different monitoring locations. Model validation essentially confirmed the applicability of the watershed-based hydrologic parameters derived during the calibration process. Validation results were assessed in a similar manner to calibration. At the Pier A monitoring station, flow was simulated fairly well (Figure 5). The initial peak was low; however, the second peak was fairly close.

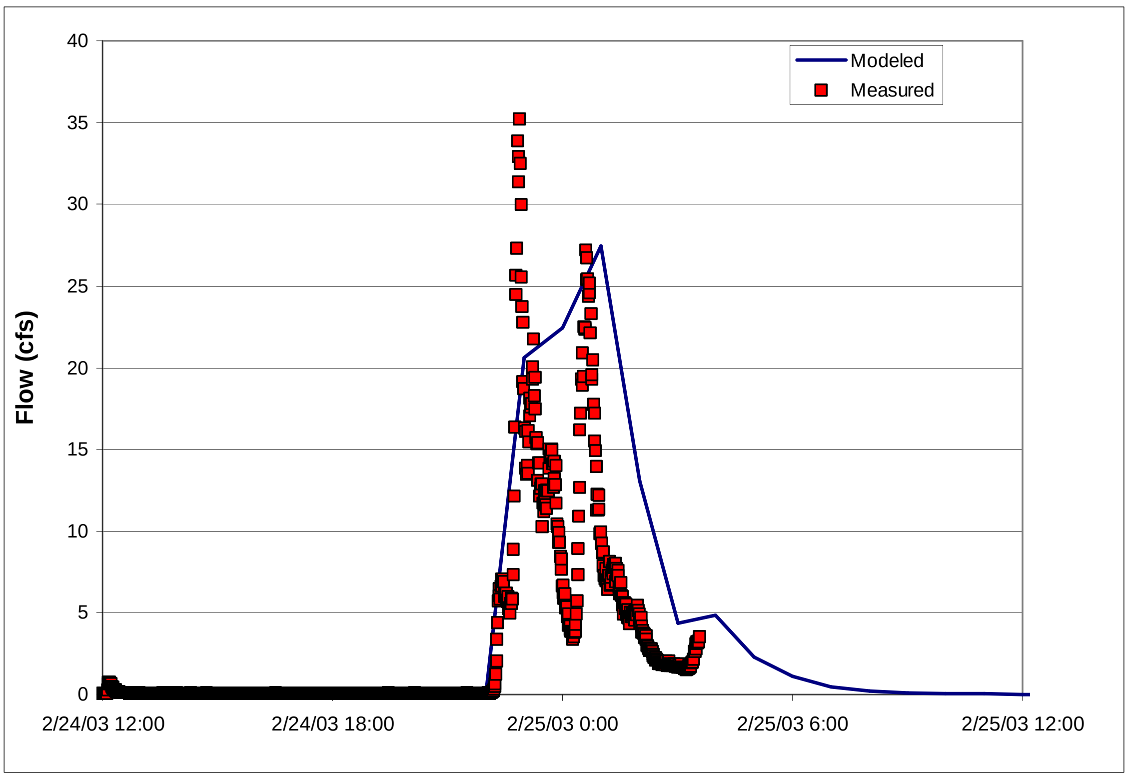

Figure 5. Modeled and Observed Flow for the Pier A Subwatershed

For the Maritime Museum station, the validation results did not match the measured flow (Figure 6). An effort was made to further calibrate the hydrology parameters to more closely match the measured data; however, such efforts would have caused some of the previously calibrated LAR watershed parameters to be adjusted outside of recommended ranges. Although the results at Maritime Museum were poor, there were not enough data to justify re-calibration of the calibrated and validated parameters for the LAR watershed model (Tetra Tech, Inc, 2004). Therefore, the calibrated nearshore hydrology parameters remained unchanged.

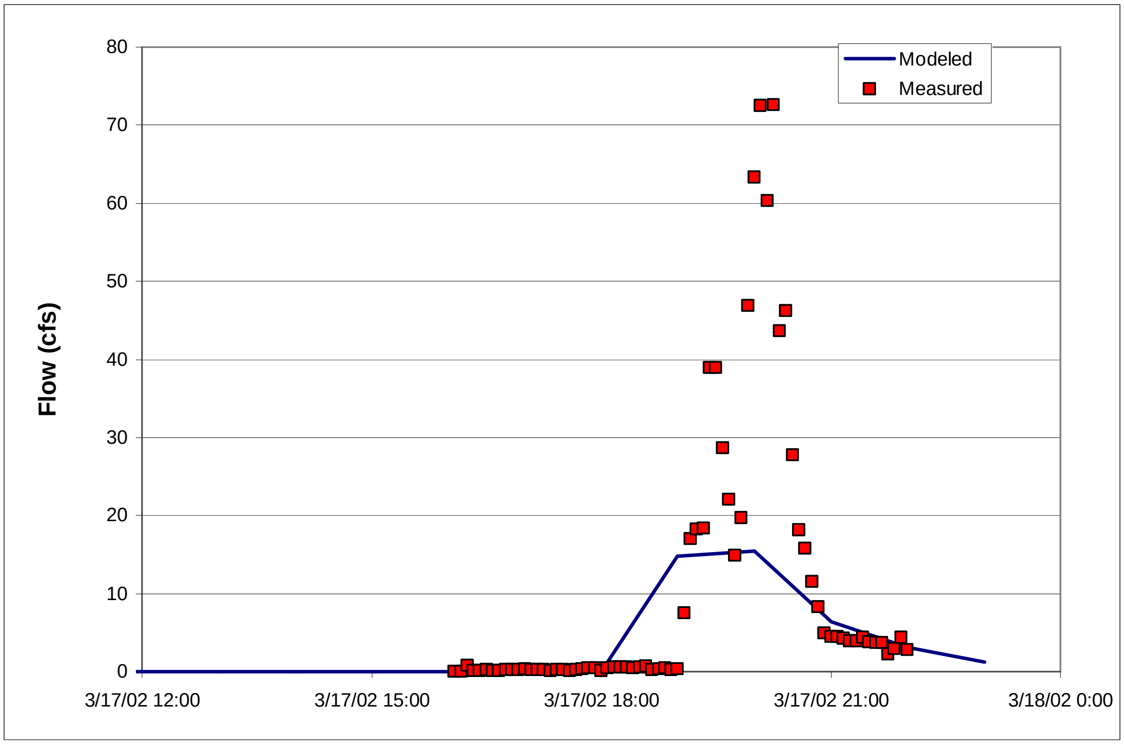

Figure 6. Modeled and Observed Flow for the Maritime Museum Subwatershed

3.2.2. Sediment Calibration and Validation

Once the model was calibrated and validated for hydrology, the regional modeling approach was applied to simulate sediment in the nearshore areas. The robust calibration and validation process previously performed for land use sites, Ballona Creek, LAR, and SGR are considered sufficient for documenting the performance of modeling parameters and verifying the transferability of the parameters among models of adjacent watersheds in the region. The application of the regional modeling approach provides increased opportunity for verification as additional datasets become available for comparison with model predictions.

Similar to the hydrology simulations, for the nearshore watersheds, predicted TSS was compared to observed TSS from a single storm event at each of three monitoring stations (Forest, Pier A, and Maritime Museum), which are identified in Figure 3. The Forest site was considered a calibration location, while Pier A and Maritime Museum were used as validation locations.

3.2.2.1. <u>Sediment Calibration</u>

For this study, the sediment parameters from the regional modeling approach (SCCWRP, 2004; Tetra Tech, Inc, 2004 & 2005a) were applied to the appropriate land uses in the nearshore watersheds. The Port Activities land use was initially assigned the same sediment parameter values as the heavy industrial land use, and further adjusted through the model calibration process that included adjustment of the KEIM and JEIM parameter values, which are the coefficient and exponent in the solids washoff equation, respectively. Final model parameter values, including newly calibrated parameters for the Port Activities land use, are presented in Table 4.

Table 4. Sediment Parameters in the Nearshore Watershed Model

Parameter	Agri-culture	Commer-cial	High density residential	Industrial	Low density residential	Mixed urban	Open	Port activities
PERVIOUS LAND USE								
Splash detachment								
SMPF	1	1	1	1	1	1	1	1
KRER	0.02	0.02	0.02	0.02	0.02	0.02	0.02	0.02
JRER	2	2	2	2	2	2	2	2
AFFIX	0.003	0.003	0.003	0.003	0.003	0.003	0.003	0.003
COVER	0	0	0	0	0	0	0	0
NVSI	20	20	20	20	20	20	20	20
Soil matrix scouring								
KSER	8	8	8	8	8	8	8	8
JSER	2	2	2	2	2	2	2	2
KGER	0	0	0	0	0	0	0	0
JGER	2	2	2	2	2	2	2	2

IMPERVIOUS LAND USE						
Parameter	**Commercial**	**High density residential**	**Industrial**	**Low density residential**	**Mixed urban**	**Port activities**
KEIM	0.05	0.1	0.35	0.15	0.05	0.35
JEIM	2	2	2	2	2	1.75
ACCSDP	0.004	0.004	0.004	0.004	0.004	0.004
REMSDP	0.025	0.025	0.025	0.025	0.025	0.025

Parameter Descriptions:

- *SMPF* is the supporting management practice factor.
- *KRER* is the coefficient in the soil detachment equation.
- *JRER* is the exponent in the soil detachment equation.
- *AFFIX* is the fraction by which detached sediment storage decreases each day as a result of soil compaction.
- *COVER* is the fraction of land surface which is shielded from rainfall erosion.
- *NVSI* is the rate at which sediment enters detached storage from the atmosphere negative value may be used to simulate removal by human activity or wind.
- *KSER* is the coefficient in the detached sediment washoff equation.
- *JSER* is the exponent in the detached sediment washoff equation.
- *KGER* is the coefficient in the matrix soil scour equation, which simulates gully erosion.
- *JGER* is the exponent in the matrix soil scour equation, which simulates gully erosion.
- *KEIM* is the coefficient in the solids washoff equation.
- *JEIM* is the exponent in the solids washoff equation.
- *ACCSDP* is the rate at which solids accumulate on the land surface.
- *REMSDP* is the fraction of solids storage which is removed each day when there is no runoff.

To assess the predictive capability of the model, the output was graphically compared to observed data. The sediment calibration results at Forest are presented in Figure 7. The modeled TSS in the Forest subwatershed has a higher peak and a more gradual decline than the observed data. Similar to the hydrology results, these discrepancies are well within acceptable modeling ranges.

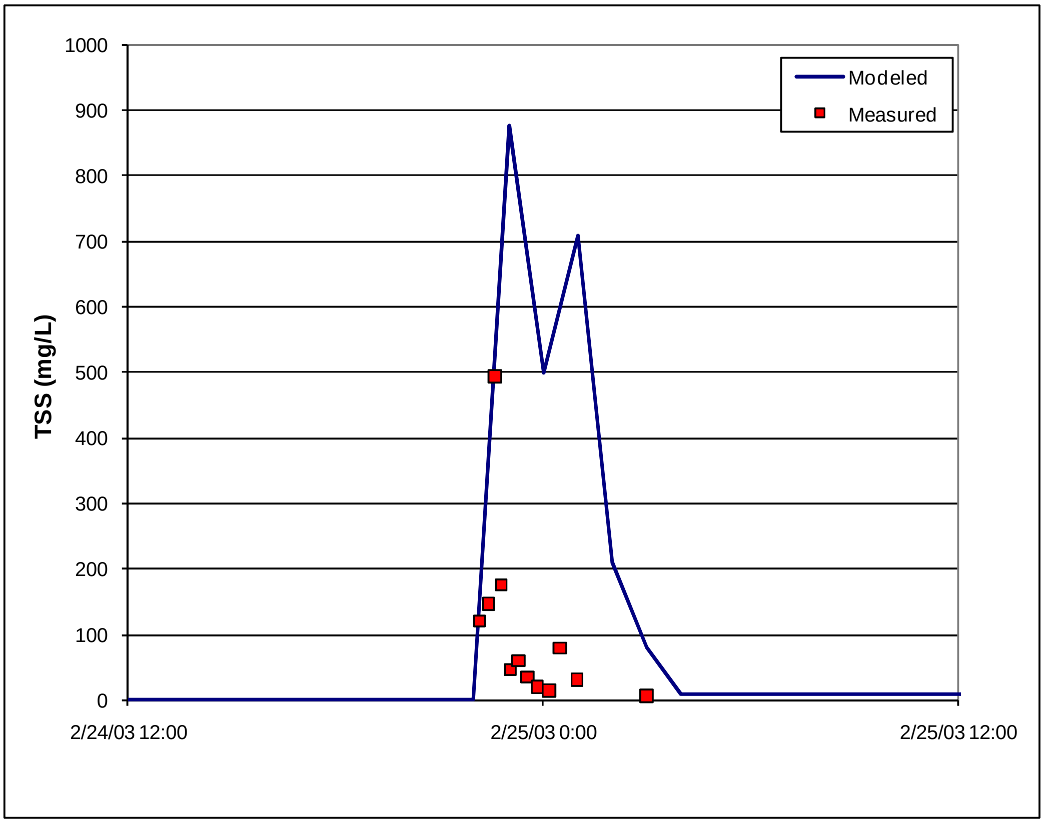

Figure 7. Modeled and Observed TSS for the Forest Subwatershed

3.2.2.2. Sediment Validation

The sediment validation results at Pier A and Maritime Museum are presented in Figure 8 and Figure 9, respectively. The modeled TSS in the Pier A subwatershed has a higher peak and a more gradual decline than the observed data. Overall, the validation at Pier A had similar results to the Forest calibration.

The Maritime Museum discrepancy between modeled and predicted results was expected because the model did not predict observed flow well (Figure 6) and would, therefore, not simulate TSS accurately. In addition, multiple land uses are represented in the Maritime Museum, including commercial (26%), high-density residential (24%), low-density residential (47%), and mixed urban (3%). These land uses were represented based on the regionally calibrated land-use-specific parameters listed in Table 4. Note that this site does not include the Port Activities land use, with associated parameters calibrated and validated for Forest and Pier A, respectively. Based on the land use distribution in the Maritime Museum watershed, it was impossible to isolate impacts from individual land use assumptions and therefore determine which parameters could have contributed to the error and subsequently required further calibration. If the regionally calibrated parameters are to be validated for all land uses surrounding the harbors, more monitoring is recommended at different sites that isolate land uses. Additional monitoring is also recommended at the Maritime Museum site to determine if the storm flows previously monitored are anomalous, or if the model consistently under-predicts flows for this location.

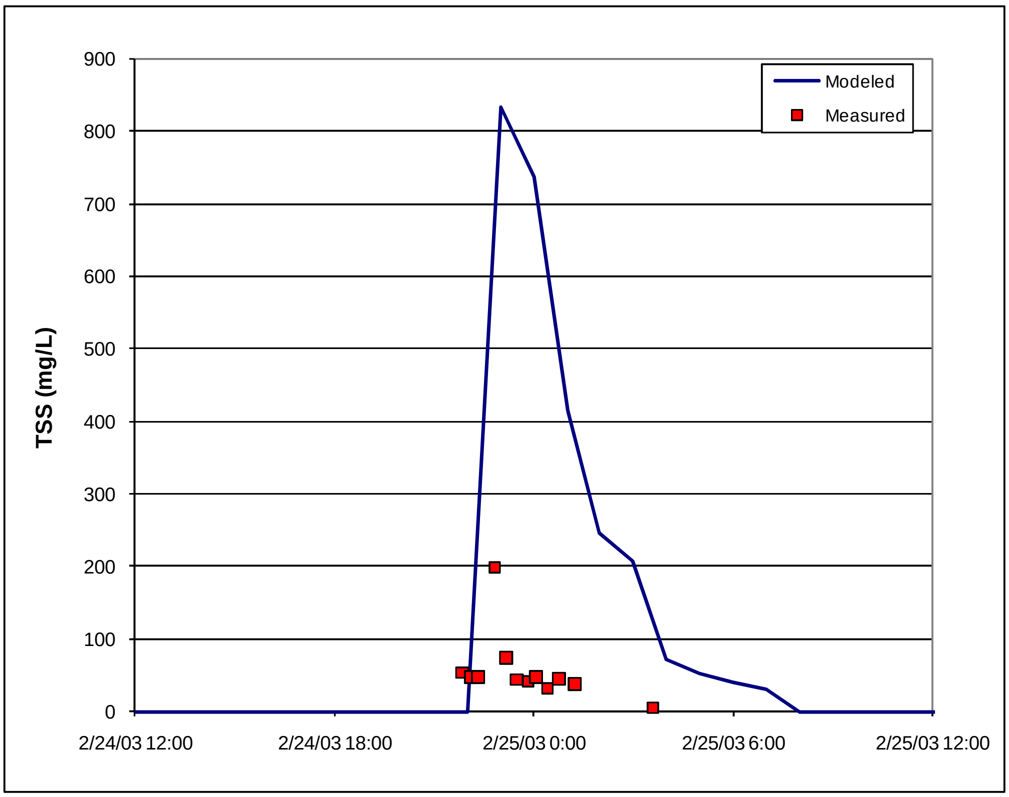

Figure 8. Modeled and Observed TSS for the Pier A Subwatershed

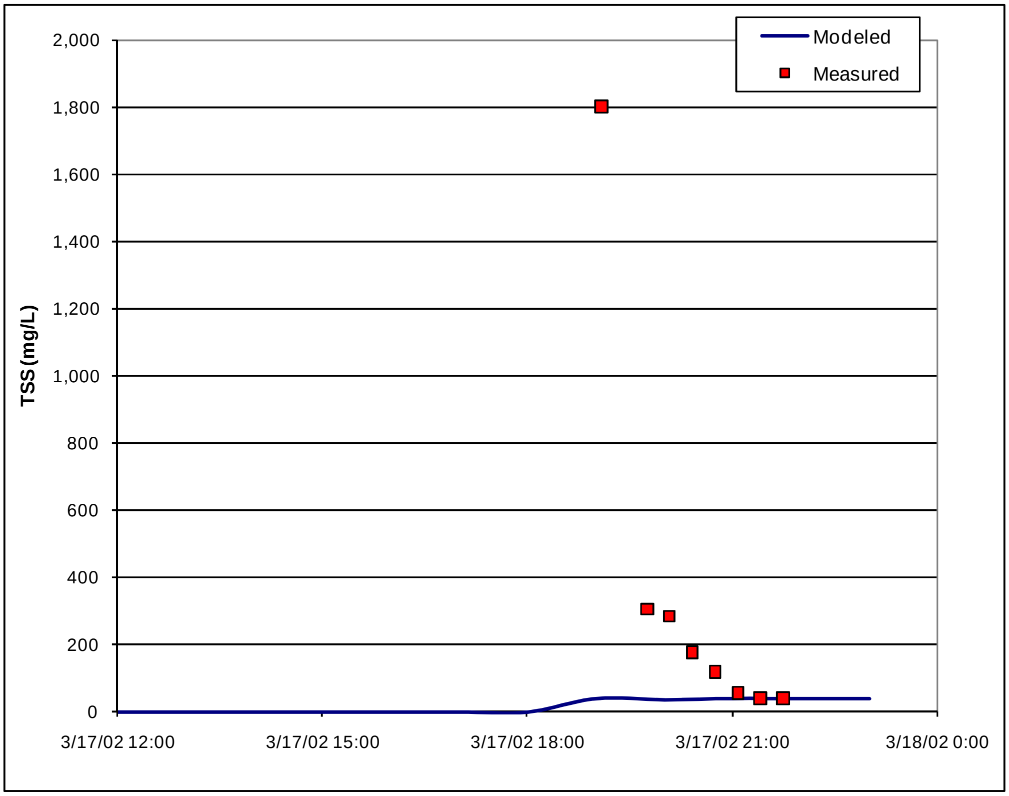

Figure 9. Modeled and Observed TSS for the Maritime Museum Subwatershed

To further validate the nearshore model, model TSS results and observed data were compared using time-series plots at several POLB stormdrain monitoring stations in the nearshore watersheds. Figure A-1 of Appendix A illustrates the sampling stations in the nearshore areas, while Figures A-2 through A-15 of Appendix A present the time-series plots. These figures indicate that the model predicts TSS concentrations generally within the range of observed data.

Overall, the model appears to reproduce the magnitude of observed data reasonably well. Deviations from the observed data may be caused by localized conditions that are not captured as input to the model.

3.3. Application of Wet-Weather Watershed Model

As described below, metals for both the LAR and SGR watersheds and nearshore areas were simulated directly using LSPC. To determine loadings for PAHs, DDT, PCBs, and chlordane, it was necessary to develop pollutant-specific approaches. These approaches, which are described in detail below, all use LSPC model output from January 1995 through July 2005 for the LAR and SGR watersheds and nearshore areas. Specifically, for PAHs, the simulated flow is combined with land-use specific event mean concentrations (EMCs) to calculate loadings in the nearshore areas, while watershed-specific observed concentrations were applied to the LAR and SGR watersheds. Simulated TSS results are combined with pollutant concentrations associated with sediment samples to determine DDT, PCBs, and chlordane loads. In addition, for the PAH, DDT, PCB, and chlordane analyses, the LSPC subwatersheds were further combined (i.e. all upstream subwatersheds were merged) so that each subwatershed represented a direct loading to the Harbors. The pollutant-specific wet-weather approaches and results for the Forest, Pier A, and Maritime Museum subwatersheds are presented in the following sections and annual loads to the receiving waterbodies for each pollutant are provided in Appendix B.

3.3.1. Metals

The previously calibrated models of the LAR and SGR watersheds (LARWQCB, 2005c; Tetra Tech, Inc, 2004 & 2005b) were expanded to determine metal loads to their respective estuaries in the receiving water model for the entire Los Angeles Region modeling period. For modeling wet-weather metals loads from nearshore areas (Figure 2), Tetra Tech developed LSPC models based on the regionally calibrated land use modeling parameters described above. Metals loadings from the calibrated and validated nearshore model were determined for the entire modeling period and ultimately applied as direct loadings to the Harbors in the receiving water model.

The regional modeling approach described above for sediment was also applied to simulate metals in the nearshore watersheds. Copper, lead, and zinc were represented in the model through their association with sediment. In order to simulate sediment contributions to the nearshore watersheds, the SEDMNT, SOLIDS, and SEDTRN modules were implemented. After using the sediment module to simulate TSS, metals associated with sediment were simulated using the LSPC water quality module. The relationships between sediment and copper, lead, and zinc were simulated using the POTFW parameter. POTFW is the washoff potency factor or the ratio of constituent yield to sediment outflow. A unique value for POTFW can be assigned for each constituent and these values can vary by land use.

After sediment was calibrated and validated (see Section 3.2.2), the metals parameters based on the regional modeling approach (SCCWRP, 2004; Tetra Tech, Inc, 2004 & 2005b) were applied to the nearshore areas. Similar to the previous simulations, predicted copper, lead, and zinc were compared to observed concentrations from a single storm event at each of three monitoring stations (Forest, Pier A, and Maritime Museum), which are identified in Figure 3. The Forest site was considered a calibration location, while Pier A and Maritime Museum were used as validation locations.

3.3.1.1. Metals Calibration

For this study, the metals parameters reported in SCCWRP (2004) and Tetra Tech, Inc. (2005b) were applied to the appropriate land uses in the nearshore watersheds. The Port Activities land use was initially assigned the same metals parameter values as the heavy industrial land use, and calibration was performed for the Forest subwatershed to develop specific parameters for Port Activities. Specifically, model results were compared to stormwater sampling data and slight adjustments were made to the metals parameters to more closely match the observed data at the Forest station. This methodology is consistent with the minor calibrations performed in the SGR model (Tetra Tech, Inc, 2005b) to more closely match the local conditions in the watershed. Calibrated POTFW parameter values are presented in Table 5.

To assess the predictive capability of the model, the output was graphically compared to observed data. Model results for metals concentrations in the Forest subwatershed are presented in Figure 10 and their associated loads are presented in Figure 11. These graphs illustrate that, for copper, lead, and zinc, the predicted concentrations are slightly lower than the observed concentrations. The predicted loads are fairly close to the observed POLA/POLB stormwater data. These model results are within acceptable modeling ranges.

Table 5. Metals Washoff Potency Factors in the Nearshore Wet-Weather Watershed Model

Land Use	Copper	Lead	Zinc
Agriculture	0.3	0.1	2.5
Commercial	1	1	10.2
Commercial (impervious)	1	1	10.2
High density residential	0.80	0.80	7.50
High density residential (impervious)	0.80	0.80	7.50
Industrial	0.3	0.18	4
Industrial (impervious)	0.3	0.18	4
Low density residential	0.62	0.27	1.93
Low density residential (impervious)	0.62	0.27	1.93
Mixed urban	0.8	0.25	5
Mixed urban (impervious)	0.8	0.25	5
Open	0.3	0.1	2.5
Port activities	0.175	0.15	1.5
Port activities (impervious)	0.175	0.15	1.5

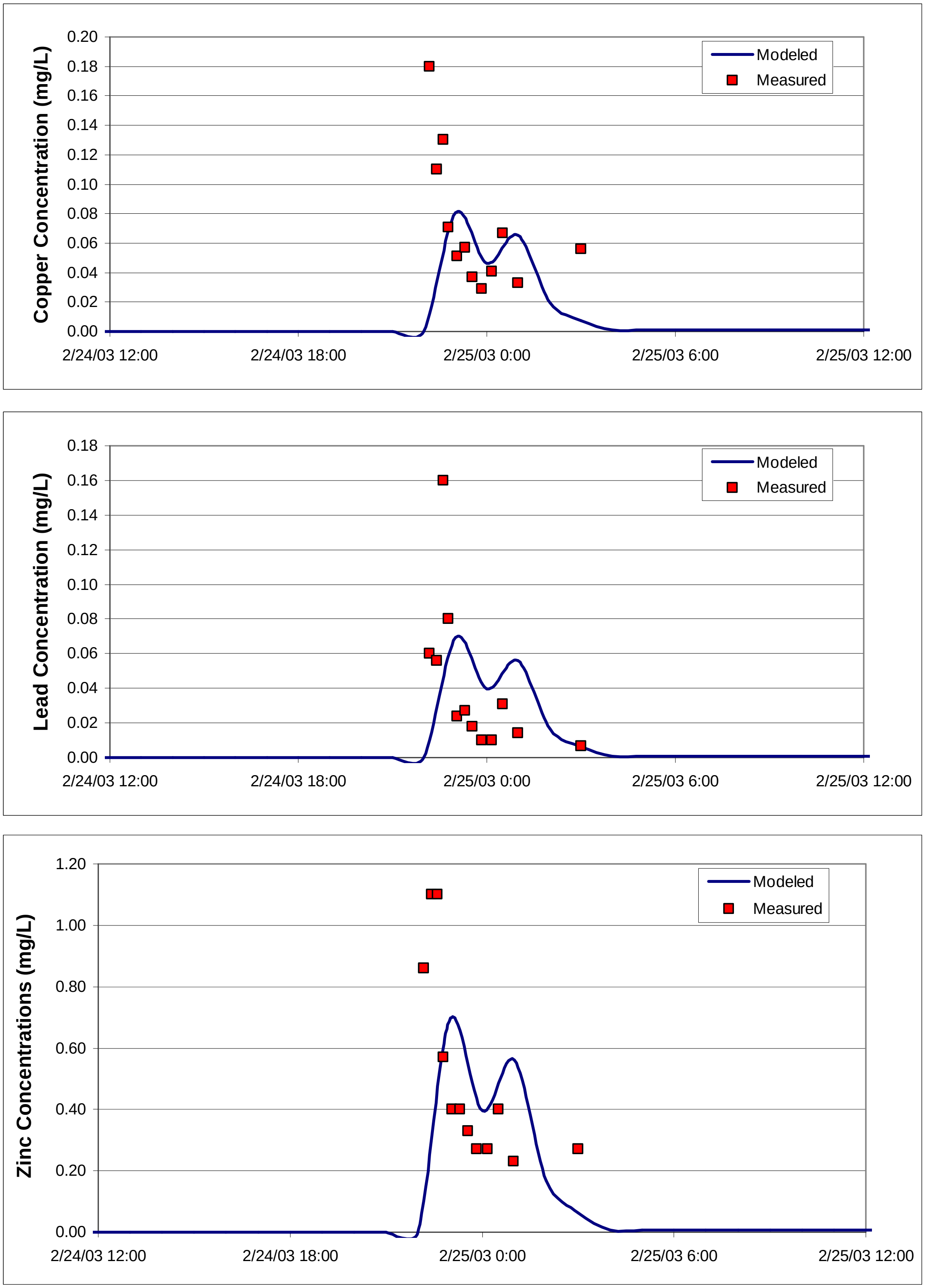

Figure 10. Modeled and Observed Copper, Lead, and Zinc Concentrations for the Forest Subwatershed

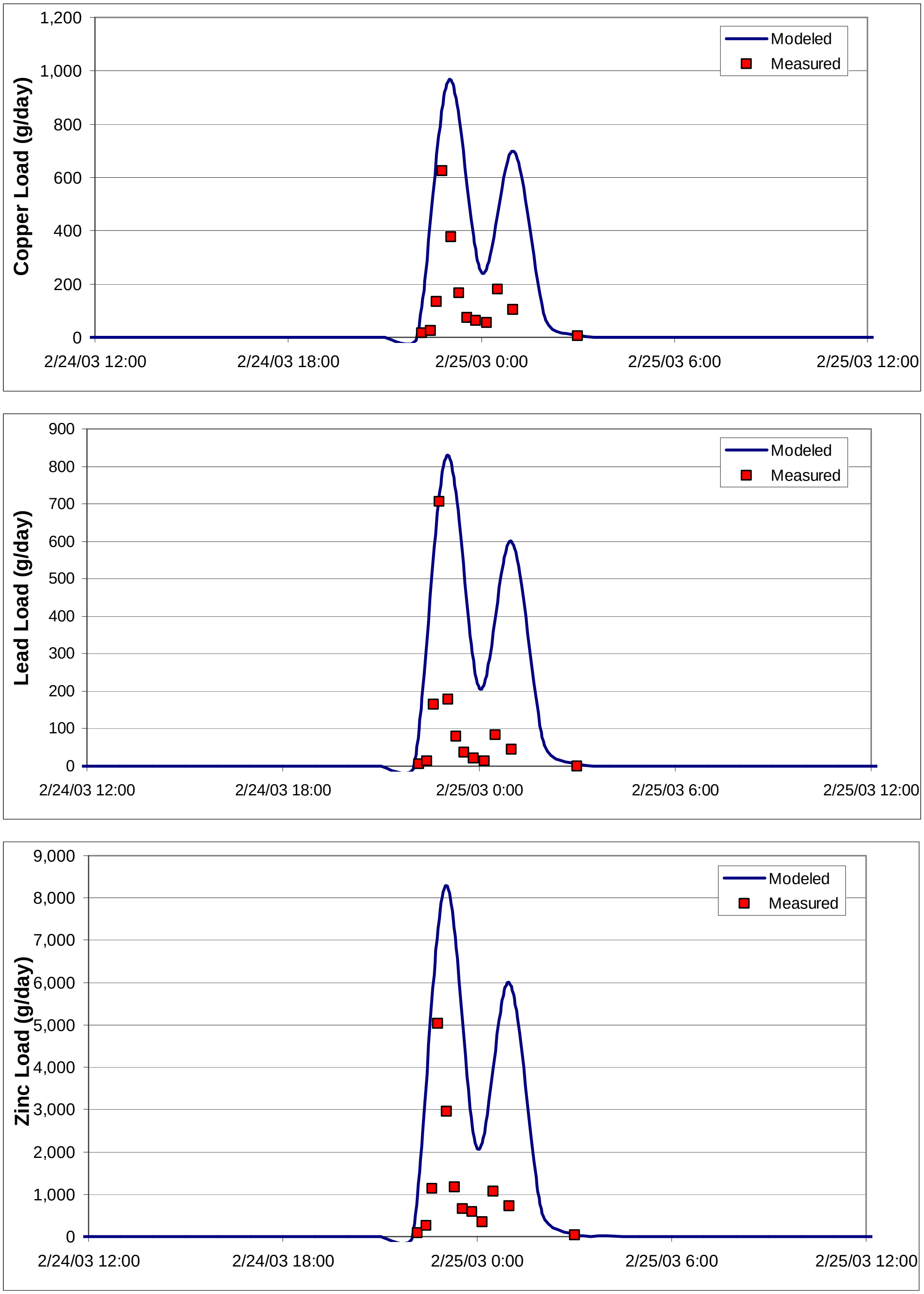

Figure 11. Modeled and Observed Copper, Lead, and Zinc Loads for the Forest Subwatershed

To further assess overall model performance in predicting pollutographs and associated metals loads, observed event mean concentrations (EMCs) were compared to EMCs calculated using hourly model output (Figure 12). EMC comparisons at Forest showed that the model EMCs were similar to observed EMCs (percent differences ranging from 3 to 20%) (Table 6).

Table 6. Modeled and Observed Copper, Lead, and Zinc Event Mean Concentrations at Forest, Pier A, and Maritime Museum

Date	Copper (mg/L)			Lead (mg/L)			Zinc (mg/L)		
	Measured	Modeled	Percent Difference	Measured	Modeled	Percent Difference	Measured	Modeled	Percent Difference
Forest Industries	0.057	0.059	3%	0.042	0.050	20%	0.440	0.505	15%
Pier A	0.059	0.047	-20%	0.040	0.040	1%	0.460	0.406	-12%
Maritime Museum	0.098	0.014	-86%	0.093	0.012	-87%	0.701	0.114	-84%

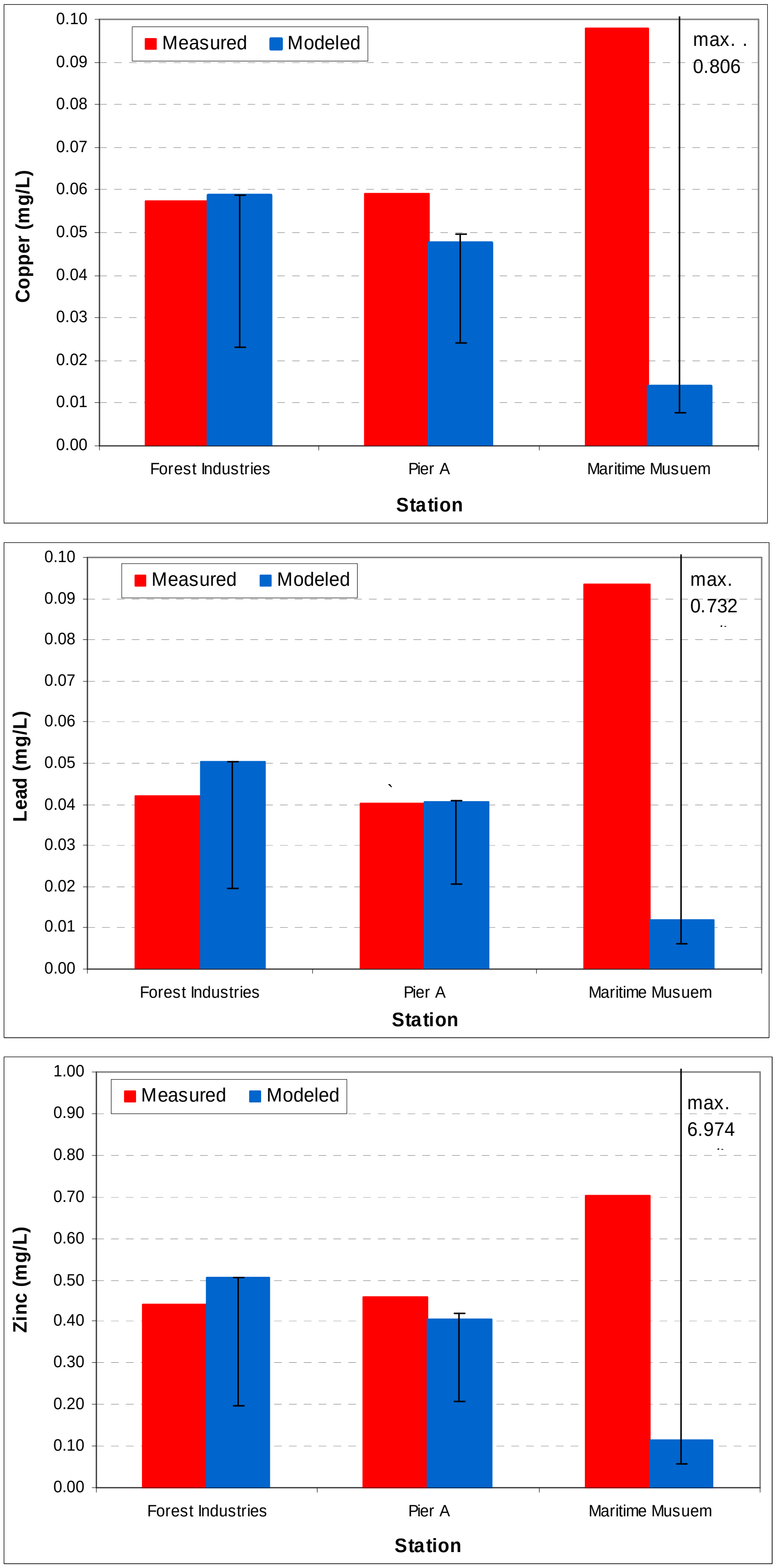

Figure 12. Modeled and Observed Copper, Lead, and Zinc Event Mean Concentrations for Forest, Pier A, and Maritime Museum

3.3.1.2. Metals Validation

The validation results for metals concentrations for the Pier A subwatershed are presented in Figure 13 and their associated loads are presented in Figure 14. Similarly, the concentration and load results for the Maritime Museum subwatershed are presented in Figure 15 and Figure 16, respectively. The modeled concentrations in the Pier A subwatershed have lower peaks than the observed data (Figure 13) and the peak for the copper and zinc predicted loads were very similar to those for the observed loads (Figure 14). The predicted concentrations and loads have a smooth curve over the course of the storm, but the observed data do not follow such a pattern, making it difficult to directly compare the modeled and observed results. Overall, the validation at Pier A show that the model results were well within the ranges of observed data.

For the Maritime Museum validation, the model results did not capture the observed peak in either concentrations or loads (Figure 15 and Figure 16, respectively). The Maritime Museum discrepancy between modeled and predicted results was expected because the model did not predict observed flow and TSS well and would, therefore, not simulate metals accurately. However, there were not enough data to justify re-calibration of the well-validated regional parameter ranges.

Similar to the model calibration at the Forest subwatershed, observed storm EMCs were compared to EMCs calculated using hourly model output for Pier A and Maritime Museum (Figure 12). EMC comparisons at Pier A showed that the model EMCs were very similar to observed EMCs (percent differences range from -20 to 1%) (Figure 12 and Table 6). At Maritime Museum, the model consistently under-predicted metals EMCs (percent differences range from -87 to -84%) (Figure 12 and Table 6).

To further validate the nearshore model, modeled copper, lead, and zinc results and observed data were compared using time-series plots at several POLB stormdrain monitoring stations in the nearshore watersheds. Figure A-1 of Appendix A illustrates the sampling stations in the nearshore areas, while Figures A-16 through A-27 present the time-series plots. Figures A-16 through A-27 of Appendix A indicate that the model predicts copper, lead, and zinc concentrations generally similar to or below the observed range of data.

Overall, the model appears to reproduce the magnitude of observed data reasonably well. Deviations from the observed data may be caused by localized conditions that are not captured as inputs to the model.

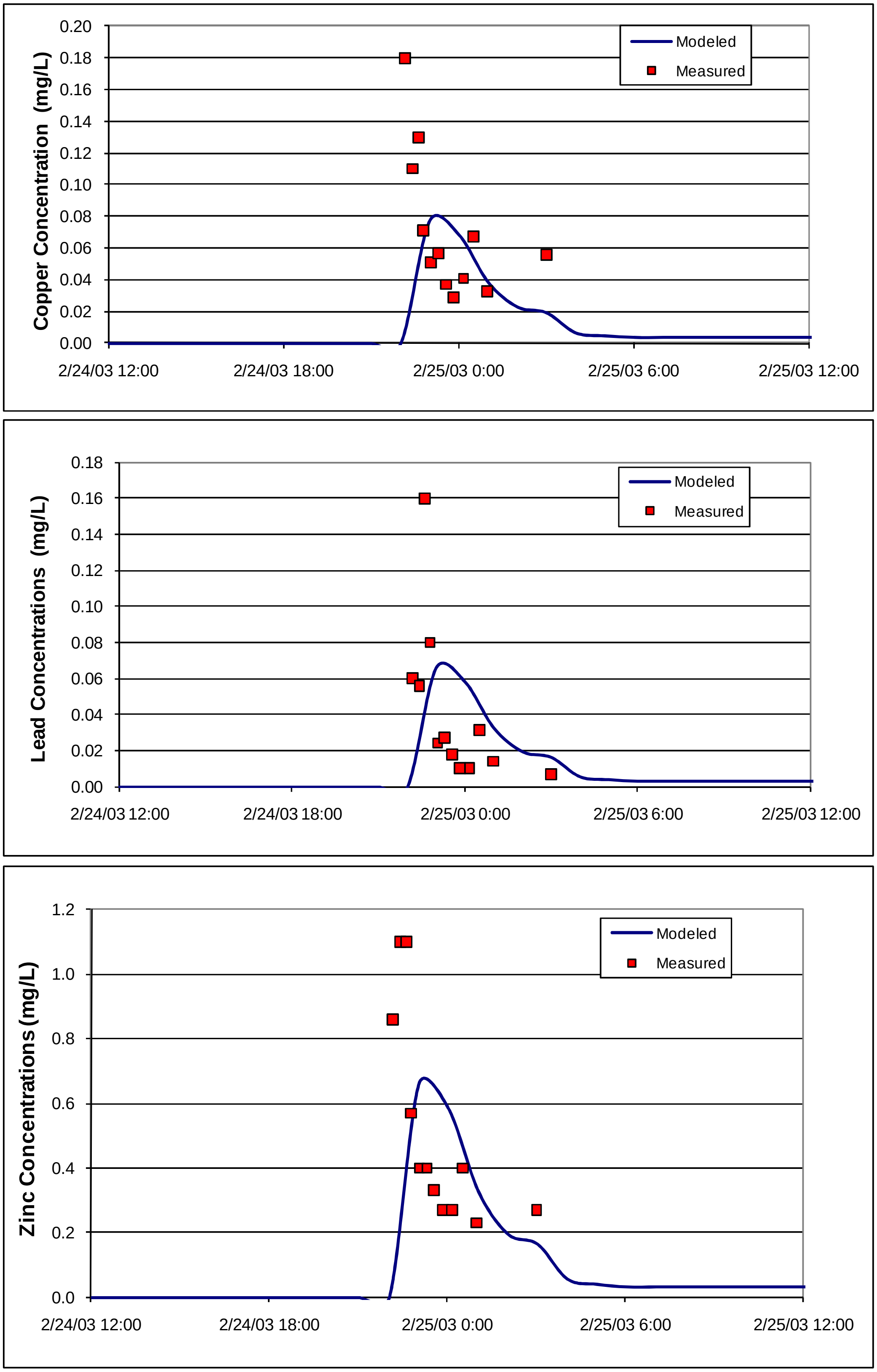

Figure 13. Modeled and Observed Copper, Lead, and Zinc Concentrations for the Pier A Subwatershed

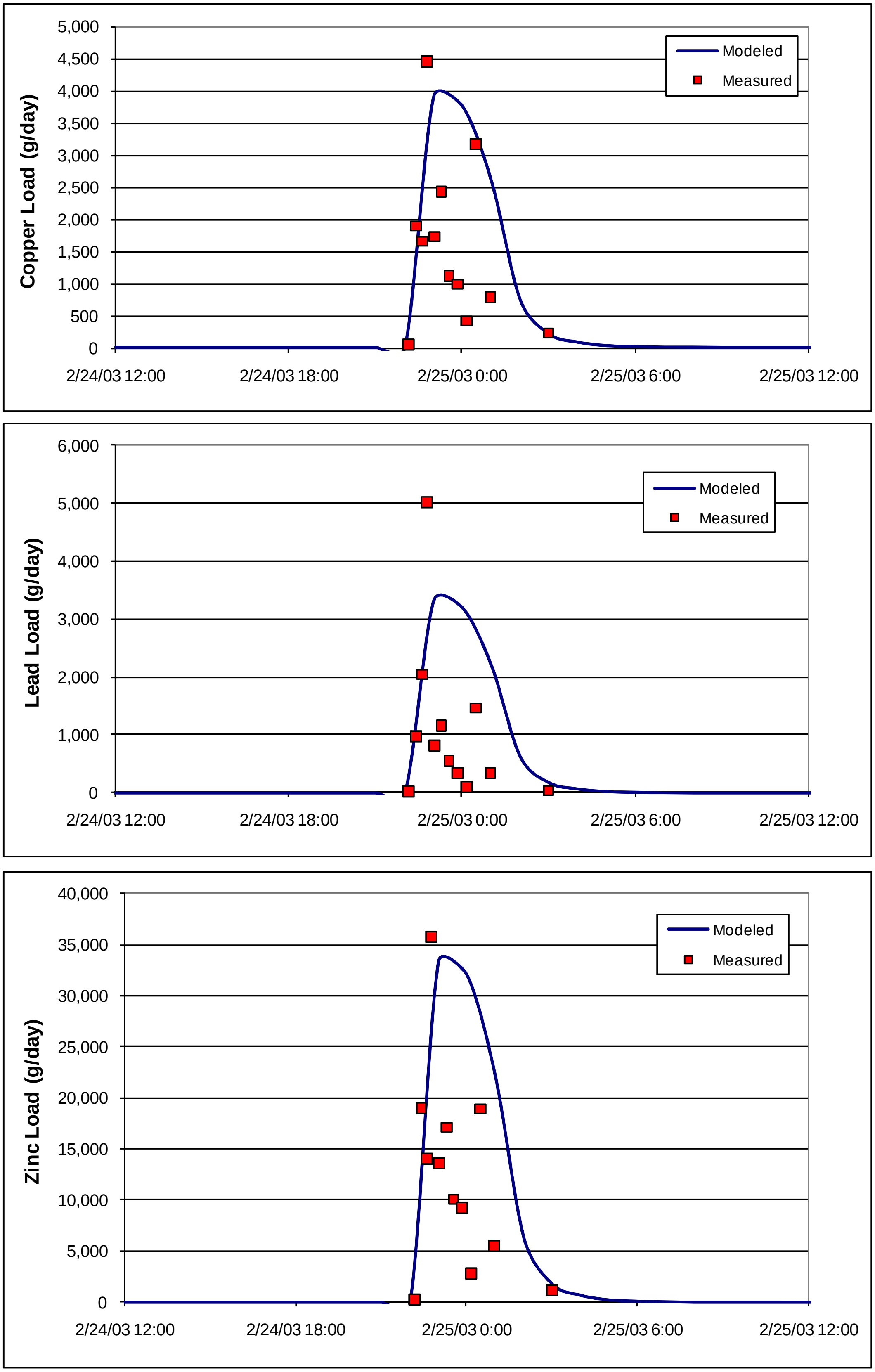

Figure 14. Modeled and Observed Copper, Lead, and Zinc Loads for the Pier A Subwatershed

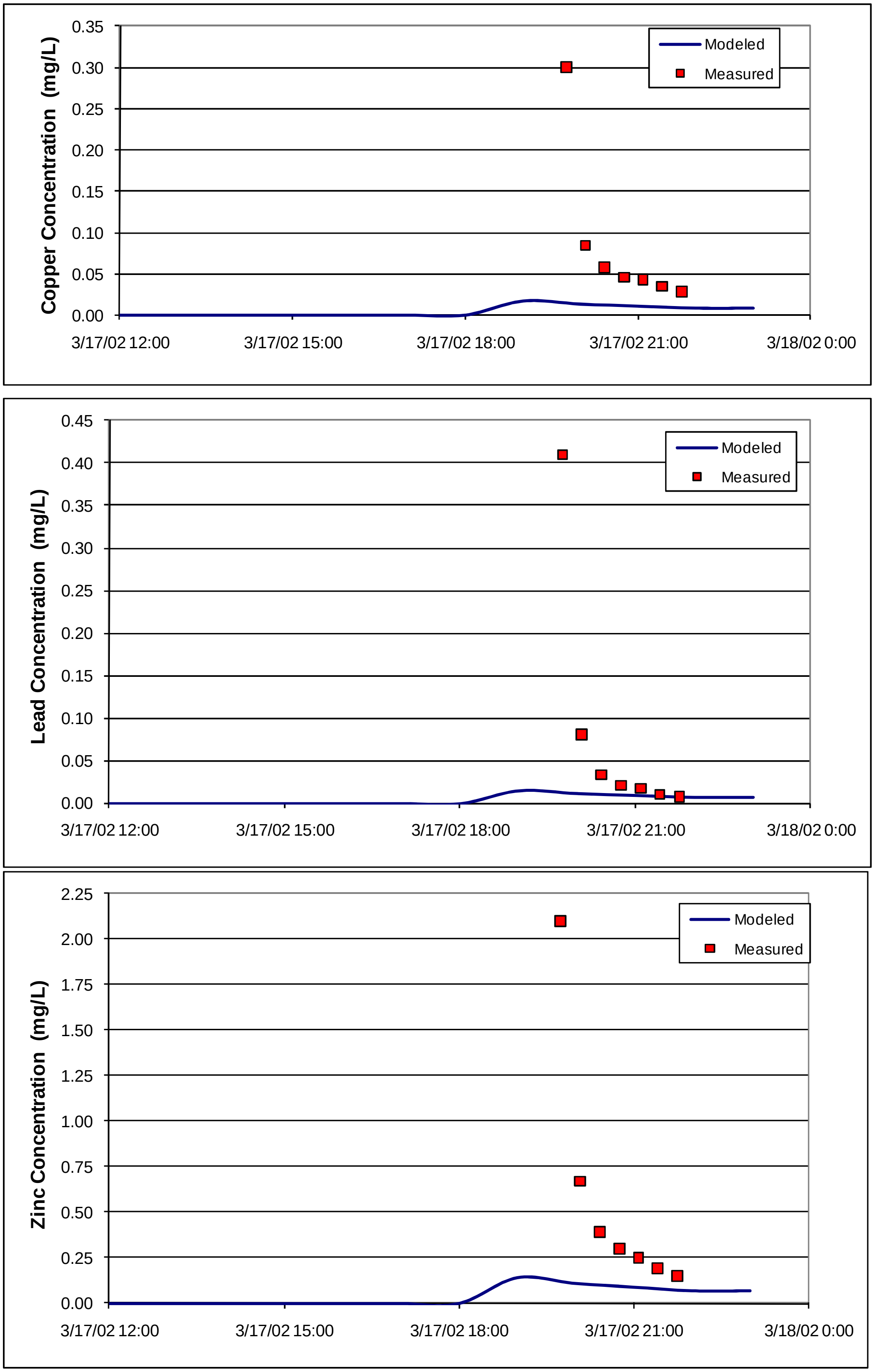

Figure 15. Modeled and Observed Copper, Lead, and Zinc Concentrations for the Maritime Museum Subwatershed

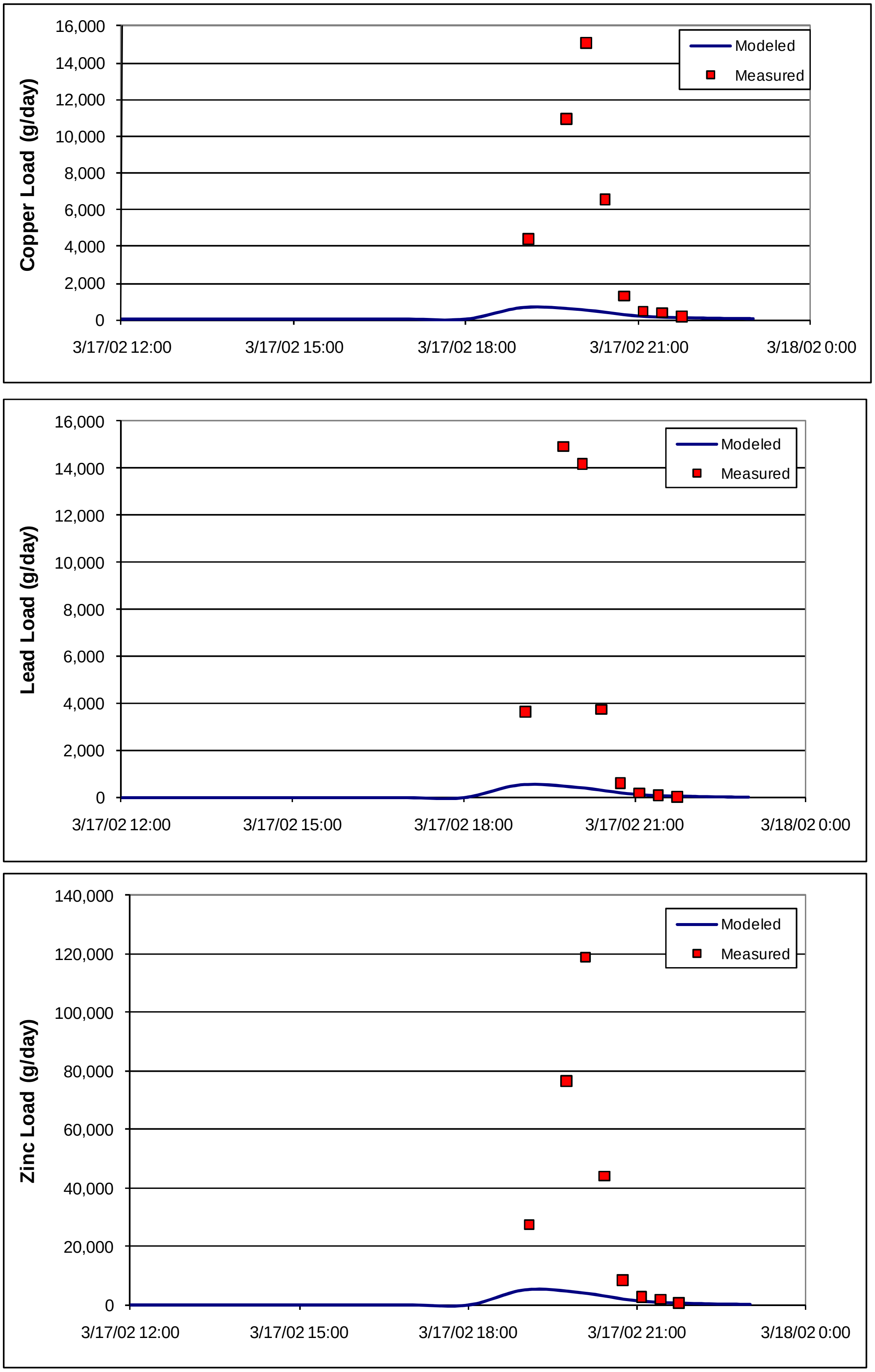

Figure 16. Modeled and Observed Copper, Lead, and Zinc Loads for the Maritime Museum Subwatershed

3.3.1.3. Metals Sensitivity Analysis

Sensitivity analyses were performed for comparison with model results. These analyses included modifying the KEIM and JEIM sediment parameters and re-running the model. KEIM is the coefficient in the solids washoff equation and JEIM is the exponent in the same equation. These parameters, which were part of the regionally calibrated parameters provided by SCCWRP (2004), vary by land use and help define the rate at which built-up solids wash off of the land surface. During the SGR modeling effort, analyses were performed to determine the acceptable ranges of these parameters for the SGR watershed (Tetra Tech, Inc, 2005a).

To assess their sensitivity on model output for the nearshore areas, model runs were performed using the minimum and maximum KEIM and JEIM values from the SGR model (Tetra Tech, Inc, 2005a). These analyses should only be used as a relative comparison of parameter sensitivity on TSS, and ultimately, metals, concentrations. The results of these analyses are represented by the error bars on the metals EMCs in Figure 12. While the KEIM and JEIM parameters are important factors associated with the TSS levels output by the model, the error bars indicate that the minimum and maximum values have more of an impact on metals when the TSS concentrations are higher.

3.3.2. PAHs

Presently, no land-use-based watershed models have been developed for simulation of wet-weather sources of PAHs in the Los Angeles Region. However, monitoring at land use sites throughout the Los Angeles Region has yielded information that can be used for the present study. Stein et al. (2005) report EMCs of total PAHs for various land uses based on land use sites monitored in the Los Angeles Region. At each location, 10 to 15 grab samples were collected at a frequency of 30 to 60 minutes during storm events. The Port Activities land use was not included in the land use monitoring performed by Stein et al. (2005); therefore, storm monitoring data provided by POLA/POLB for the Forest and Pier A monitoring stations, which are surrounded by the Port Activities land use, were analyzed to determine a land use-specific PAH EMC.

The land use categories associated with the EMCs described by Stein et al. (2005) and calculated from the POLA/POLB data are slightly different than those from the regional modeling approach for metals (Table 7). Therefore, the SCAG 2000 land use data were used to represent the study area and were reclassified to maintain consistency with the EMC land use categories (Table 7).

Table 7. Land Use Categories

LSPC watershed model land use categories	PAH wet weather assumptions land use categories
Mixed urban	Transportation
Industrial	Industrial
Commercial	Commercial
Low-density residential	Low-density residential
High-density residential	High-density residential
Agriculture	Agriculture
Open	Open
	Recreational
Port activities	Port activities

The average EMCs and respective standard deviations reported by Stein et al. (2005) and calculated from the POLA/POLB data for each land use are listed in Table 8. As shown in this table, PAH concentrations are commonly observed in stormflows from each land use. Stein et al. (2005) indicated that some apparent differences in PAH EMCs and fluxes were observed between land uses, with no significant differences in EMCs and fluxes among land use categories.

Table 8. Average EMCs for PAHs at Land Use Sites (Stein et al., 2005)

Land use	EMC (ng/L)	Standard deviation
Industrial	1.50E+03	8.60E+02
Commercial	1.20E+03	5.80E+02
Low-density residential	1.40E+03	6.00E+02
High-density residential	4.40E+03	2.60E+03
Agricultural	8.60E+02	1.00E+03
Open	1.38E+02	0.00E+00
Recreational	4.60E+02	3.00E+02
Transportation	4.80E+02	2.80E+02
Port Activities*	1.70E+03	7.40E+02

* Based on analysis of POLA/POLB storm monitoring data

To estimate loading of PAHs from subwatersheds, LSPC flow predictions were combined with EMCs listed in Table 8. Specifically, stormwater total PAH concentrations for each model subwatershed were predicted using weighted averages of land use EMCs based on area and runoff potential of each land use in each subwatershed. The following equation (1) was used to determine representative EMCs for each subwatershed:

$$EMC_{avg.} = \frac{\sum_{i=LU} A_i C_i (EMC_i)}{\sum_{i=LU} A_i C_i} \qquad (1)$$

where, EMC_{avg} = average subwatershed EMC
LU = land use category
A = land use area
C = runoff coefficient

Runoff coefficients for each land use are based on values reported by Ackerman and Schiff (2003) for modeling stormwater mass emissions in Southern California and are presented in Table 9. These land uses do not correlate exactly to the EMC land use categories. To overcome this limitation, the residential runoff coefficient was assigned to both the high density and low density residential land uses, the open runoff coefficient was assigned to the open and recreation land uses, and the other urban runoff coefficient was assigned to the transportation and the port activity land use.

Table 9. Runoff Coefficients by Land Use (Ackerman and Schiff, 2003)

Land use	Runoff coefficient
Industrial	0.64
Commercial	0.61
Residential	0.39
Agriculture	0.10
Open	0.06
Other urban	0.41

EMCs determined for each subwatershed are assumed to be constant for all stormflows. These EMCs were multiplied by hourly flows predicted by LSPC models for estimation of dynamic loads of total PAHs from the watersheds. Although the total PAH concentrations are assumed to be constant, variability of model-predicted stormflows resulted in likewise variable loadings to the Harbors and SPB. Table 10 presents the average PAH EMC calculated for the Forest, Pier A, and Maritime Museum subwatersheds. These concentrations were used to predict loads for their respective subwatersheds. Figure 17 through Figure 19 show the time-variable flows, constant EMC, and resulting time-variable loads for Forest, Pier A, and Maritime Museum, respectively. These figures illustrate that the predicted PAH concentrations are generally within the range of observed data. This methodology was applied to the model output from all other model nearshore subwatersheds and the resulting loads were included as input to the receiving water model.

Table 10. Wet-Weather PAH Concentrations

Watershed	Concentration
Forest	1.68 ± 0.74 (range 0.94-2.42) (μg/L)
Pier A	1.59 ± 0.76 (range 0.82-2.35) (μg/L)
Maritime Museum	1.84 ± 0.94 (range 0.90-2.77) (μg/L)

For the LAR watershed, an EMC value from the LAR at Wardlow monitoring station was obtained from Stein et al. (2005). The values included in the LAR PAH analysis were obtained by averaging the two EMCs and standard deviations presented for the station. The PAH EMC was then multiplied by the modeled flows to calculate LAR loadings.

To obtain EMCs for the SGR watershed, PAH monitoring data for multiple storms on the SGR and Coyote Creek were utilized (Stein, 2006). The observed concentrations for each storm were multiplied by their respective flows, summed, and then divided by the total storm flow to determine the EMC for each storm at each stream reach. Final EMC values for SGR and Coyote Creek were obtained by averaging the three storm EMCs and their respective standard deviations for each reach. The SGR and Coyote Creek EMCs were multiplied by their LSPC modeled flow and then summed to obtain watershed-wide SGR wet-weather PAH loads.

Although in reality total PAH concentrations are typically higher during the rising limb of the storm hydrograph due to first flush, mass loading exhibits only a moderate first flush for storms monitored in Los Angeles (Stein et al., 2005). Therefore, assuming constant total PAH concentrations for stormflows is reasonable. Based on a similar method of using EMCs assigned to dynamic flows predicted for Ballona Creek using EPA's Storm Water Management Model (SWMM) to predict wet-weather nutrient loads, McPherson et al. (2005b) state that in most cases, the total load estimated using EMCs for long-term simulation can have similar accuracy as more complex models (e.g., HSPF/LSPC).

To assess the uncertainty of model predictions based on EMCs, sensitivity analyses of assumed values were performed. For each subwatershed, upper and lower ranges of average EMCs (based on equation (1)) were determined using land-use-specific EMCs plus/minus one standard deviation, as listed in Table 8. Resulting ranges of wet-weather loadings to the Harbors and SPB were quantified to provide understanding of the sensitivity of loads potentially due to uncertainty of modeling assumptions. For the Forest, Pier A, and Maritime Museum subwatersheds, the PAH EMC and upper and lower ranges are provided in Table 10 and presented graphically in Figure 17 though Figure 19, respectively. Sensitivity analyses for LAR and SGR were performed by determining the loads associated with EMCs plus/minus one standard deviation.

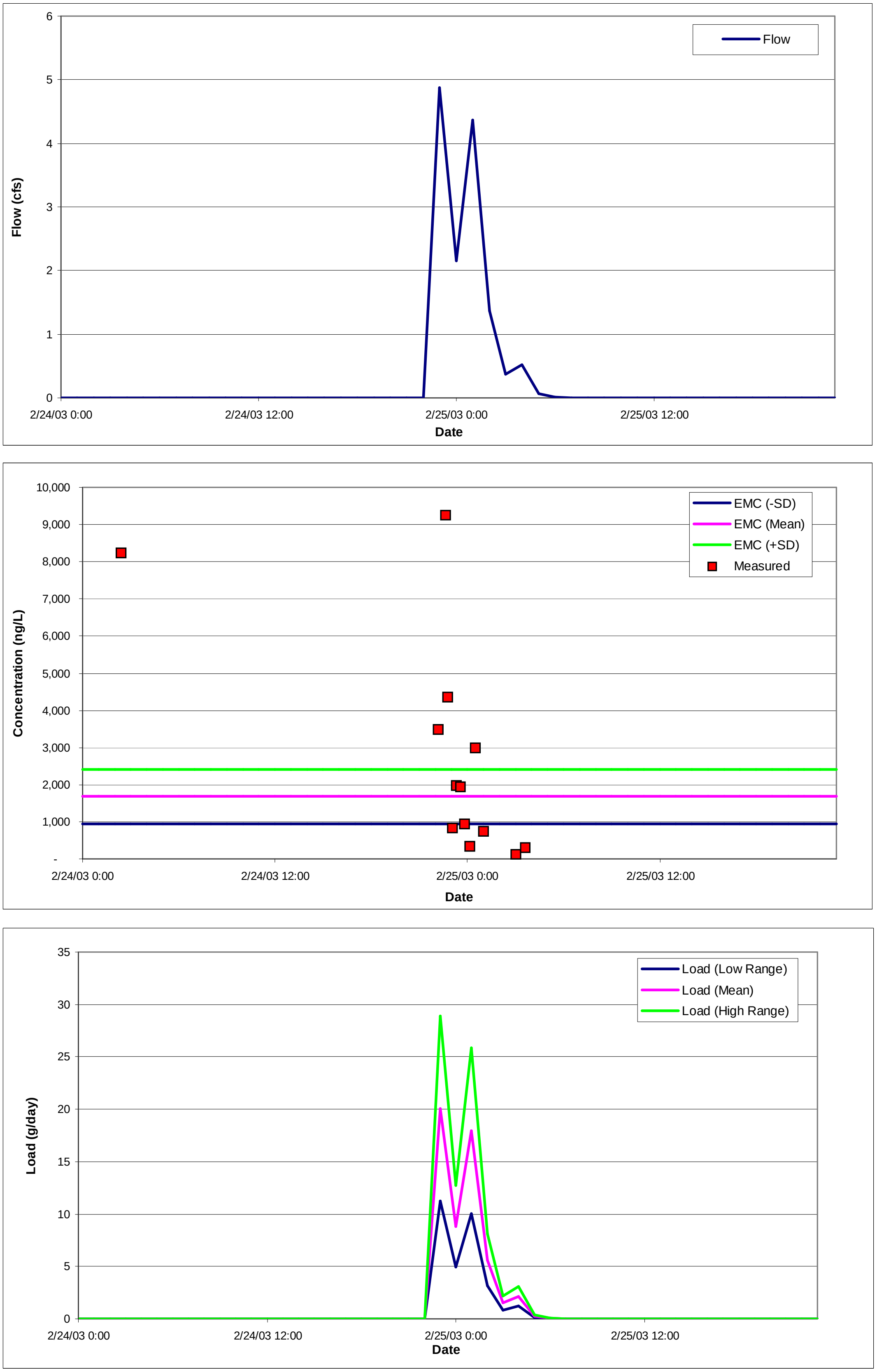

Figure 17. Modeled and Observed PAH Concentrations and Loads for the Forest Subwatershed

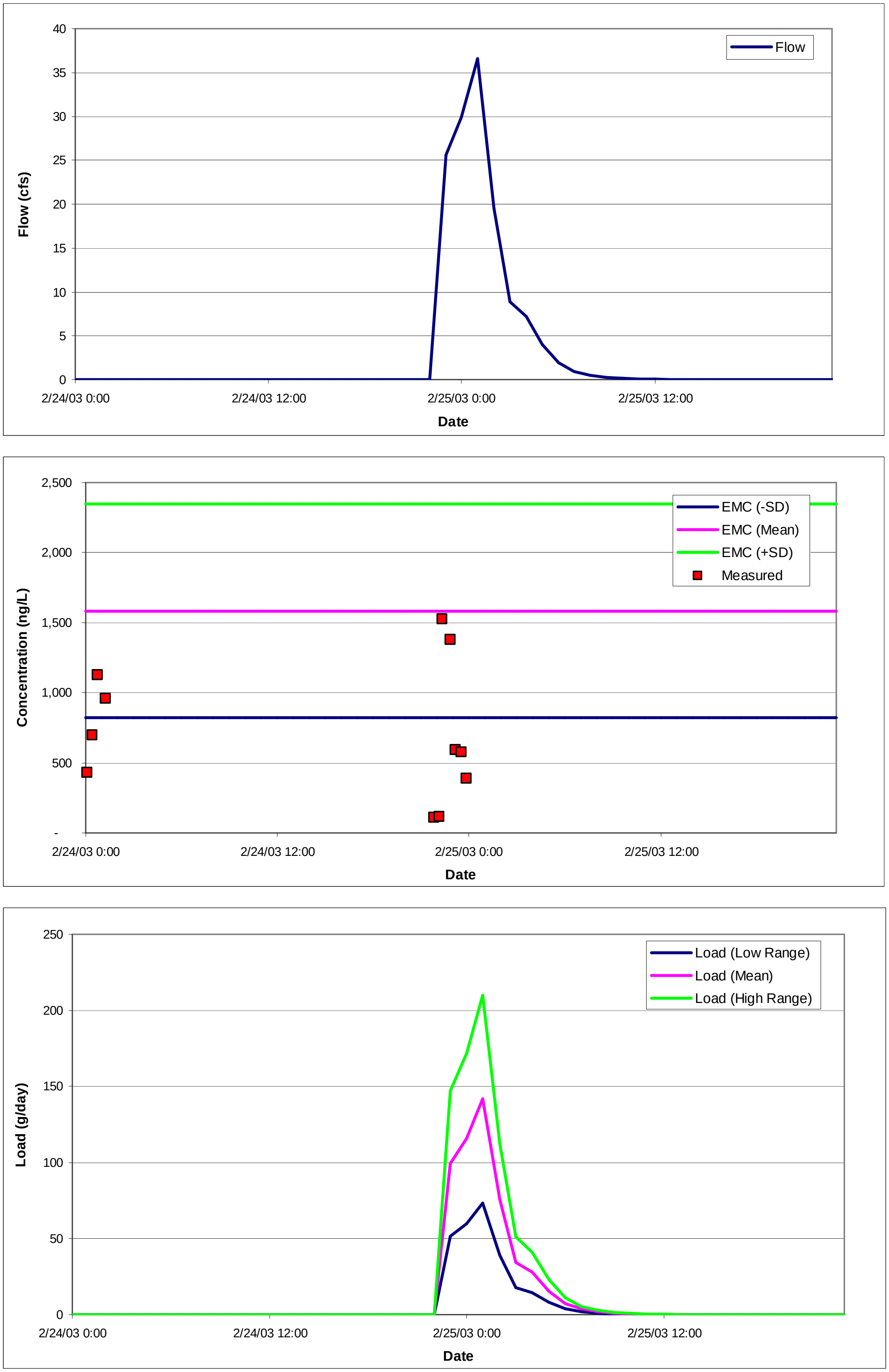

Figure 18. Modeled and Observed PAH Concentrations and Loads for the Pier A Subwatershed

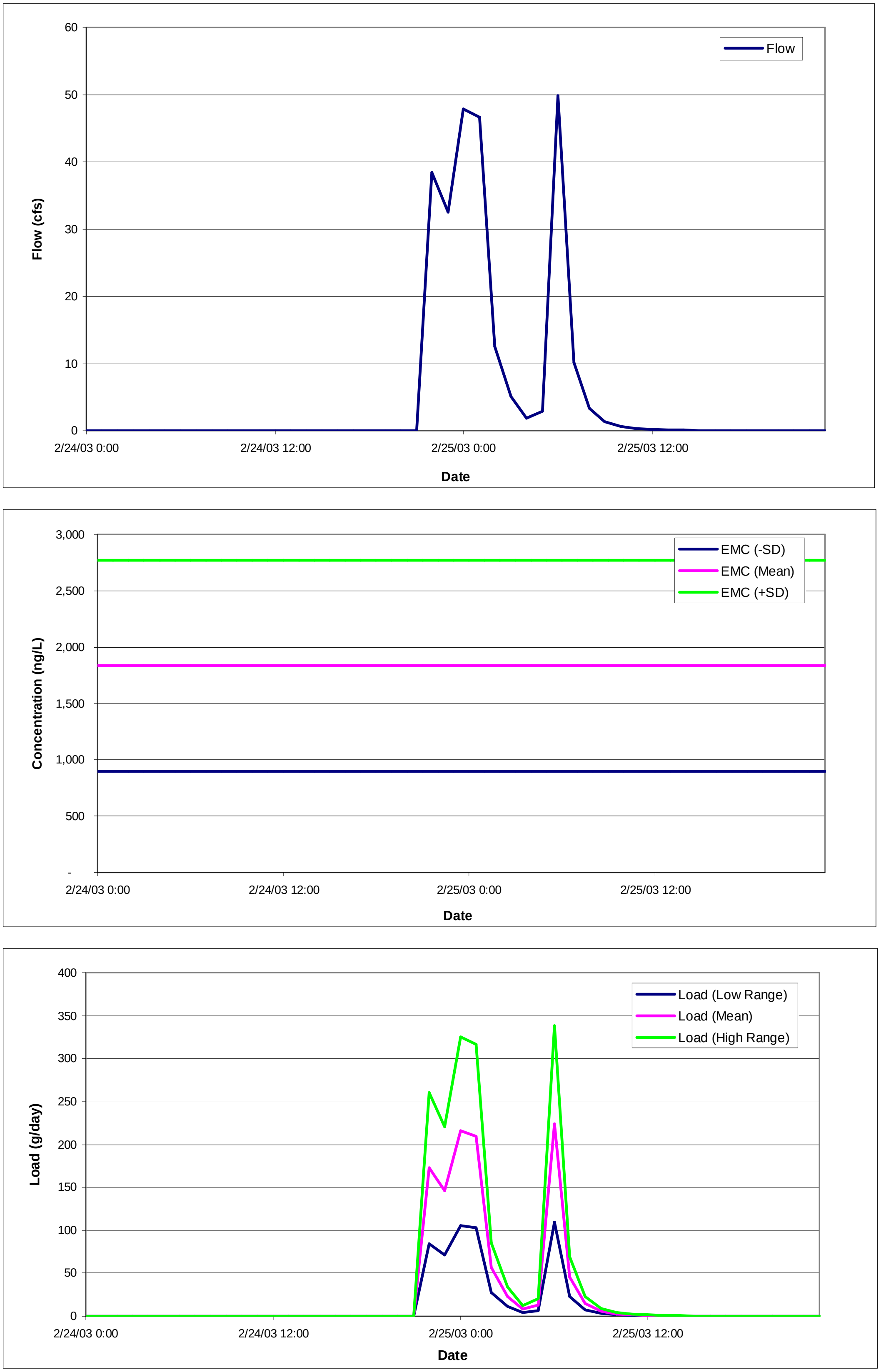

Figure 19. Modeled PAH Concentrations and Loads for the Maritime Museum Subwatershed

PAHs were modeled as total PAHs, and not separately based on molecular weight. The benefit of this approach is the simplicity of assumptions, and the resulting ease at which these assumptions can be understood and utilized in following efforts for modeling to support TMDL implementation and BMP planning. Assumptions will be made for the region during the source identification process, based on whether the pollutant is a high molecular weight PAH or a low molecular weight PAH. Although the use of EMCs assumes no variability in storm concentrations, first flush, and indication of sediment association that are important considerations for planning and assessment of BMP effectiveness, they are regularly used by municipalities for assessment and planning activities, and reduce the need for using more-complex watershed models for load estimation.

3.3.3. DDT, Chlordane, and PCBs

While the sources and land uses associated with DDT, chlordane, and PCBs differ, their transport mechanisms are generally similar. Therefore, these pollutants were modeled using a similar approach and with similar data. DDT is considered a legacy pollutant because it is believed that active uses/sources of the pollutant do not exist. However, because of the persistence of DDT in the environment, reservoirs of the pollutant are often present in the watershed and in the receiving waters. Few detectable levels of DDT have been observed at mass emissions stations in the Los Angeles Region (4,4'-DDD, 4,4'-DDE, and 4,4'-DDT were measured, each with a detection limit of 0.1 μg/L) (LADPW, 2006). Ackerman and Schiff (2003) report EMCs for DDT for land use monitoring performed by San Diego, Ventura, and Los Angeles municipalities as part of their NPDES permit programs. These EMCs resulted from flow-weighted composite samples collected throughout the duration of storm events. Of the five land uses analyzed (agriculture, commercial, industrial, open, and residential), only agricultural land use was shown to have detectable levels of DDT in runoff. PCBs and chlordane are also referred to as legacy pollutants, and similar to DDT, watershed sources of these pollutants may exist. However, no detectable levels of PCBs and chlordane have been observed at County mass emissions stations (LADPW, 2006) (detection limits for PCBs and chlordane are 0.05 and 0.5 μg/L, respectively).

More-detailed study and collection of stormwater concentrations of DDT, PCBs, and chlordane (at lower detection limits) may provide necessary information for development of a detailed regional modeling approach similar to the metals or land use specific EMCs similar to the PAHs. In the absence of such datasets to characterize wet-weather loads from the watersheds, sediment concentrations were used to model these pollutants in the Harbor watersheds. Similar to methods used in prediction of existing DDT, PCBs, and chlordane loads to support development of the Newport Bay Toxics TMDL (SARWQCB, 2000), loads can be predicted as a sediment concentration assigned to all sediment loads transported from watersheds to the receiving waters. For the current study, sediment loads to the Harbors and SPB are predicted based on LSPC models of SGR, LAR, and nearshore areas.

Additional assumptions for sediment concentrations of DDT, PCBs, and chlordane, expressed as constant values for all sediment transported from each watershed, are required. Sediment concentrations for the Harbor region have been calculated for the Bight 03 sediment stations. Figure 20 through Figure 22 illustrate the range of sediment concentrations found at these stations for DDT, PCBs, and chlordane. These figures show that, for the LAR estuary, DDT, PCBs, and chlordane concentrations are all higher near the mouth of the river than throughout the rest of the estuary. This trend does not persist in the SGR estuary, which tends to have lower concentrations of all three organics compared to the rest of the Harbor and SPB, where, as expected, higher concentrations are generally seen in areas with reduced circulation and flushing.

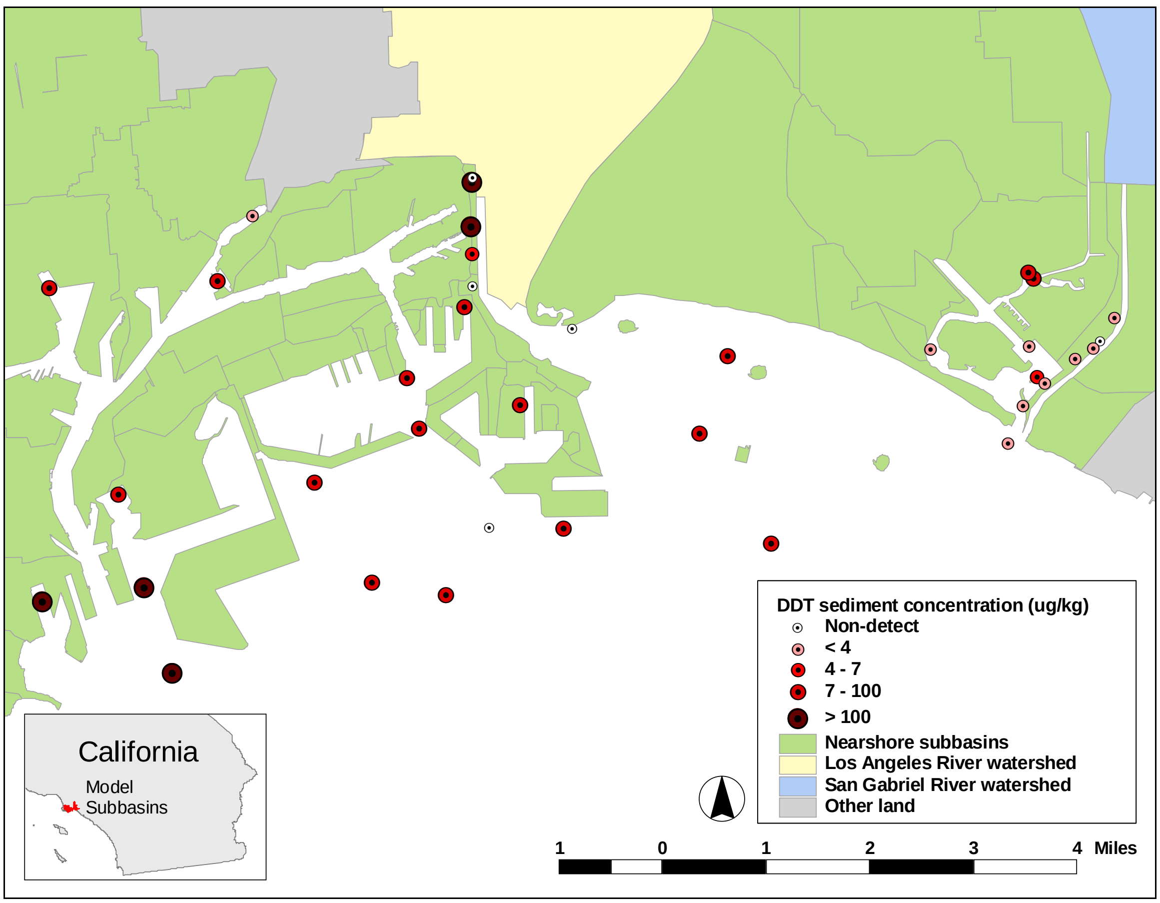

Figure 20. DDT Gradients at the Harbor Bight 03 Sampling Stations

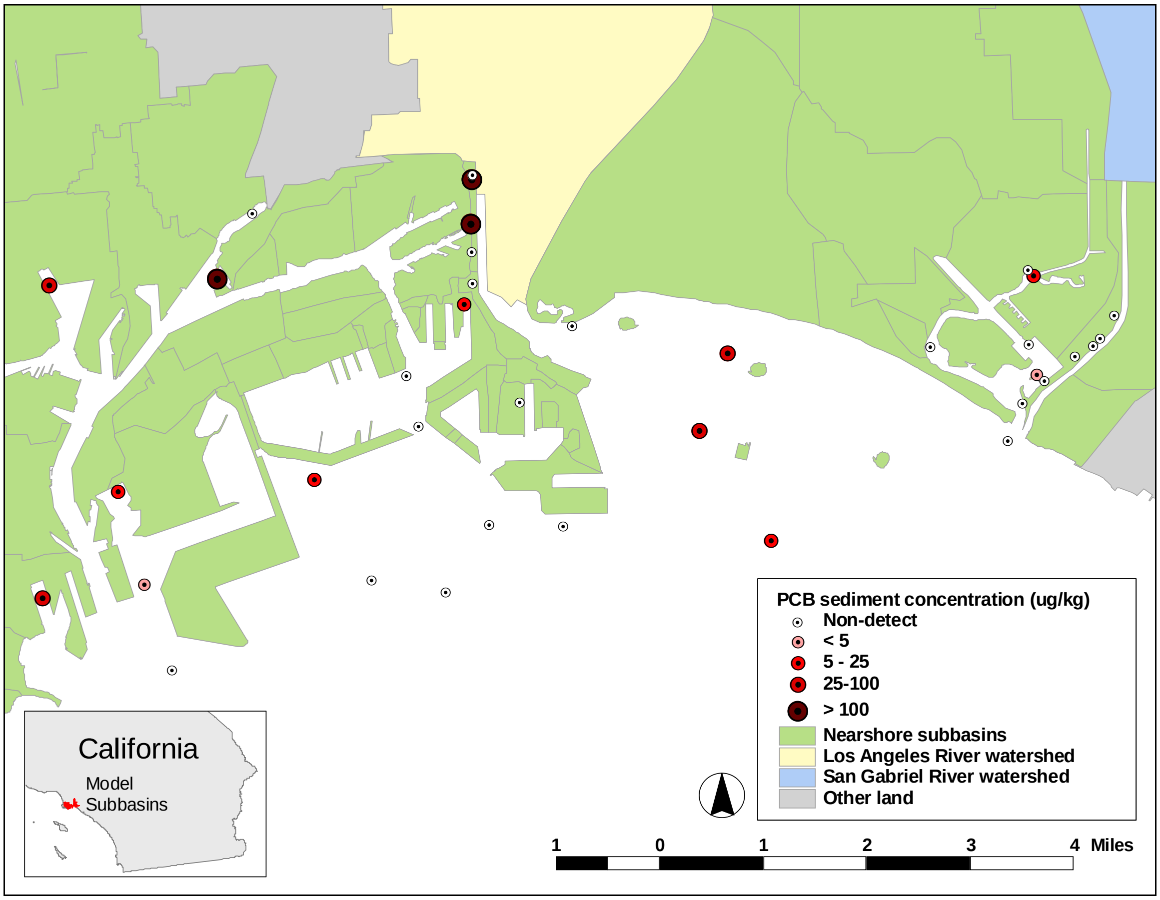

Figure 21. PCBs Gradients at the Harbor Bight 03 Sampling Stations

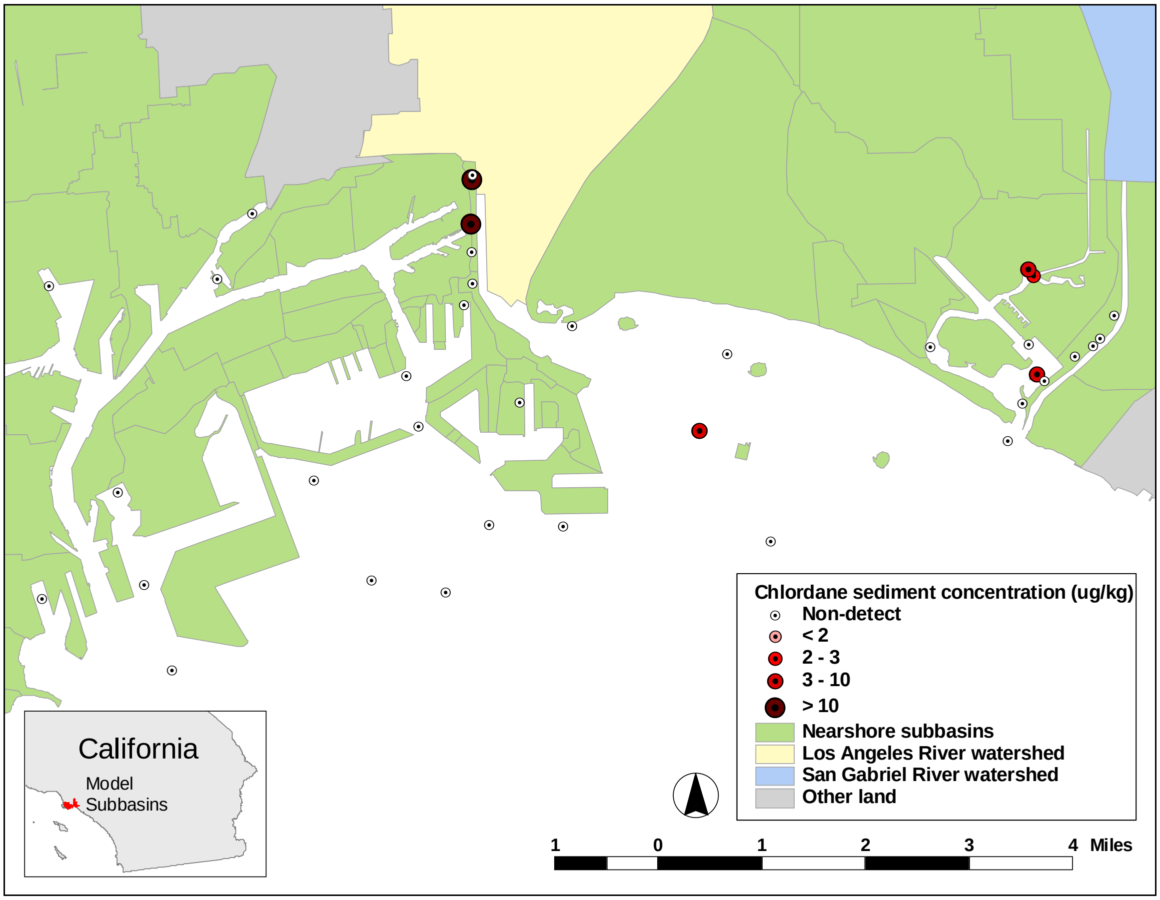

Figure 22. Chlordane Gradients at the Harbor Bight 03 Sampling Stations

The nearshore, LAR, and SGR subwatersheds were all assigned a representative waterbody. These assignments were primarily based on which waterbody was the receiving water of the representative reach. If there were no Bight 03 stations within the representative waterbody, the closest waterbody that contained Bight 03 stations was selected. Figure 23 illustrates the waterbody assignments for all subwatersheds and the Bight 03 stations used to represent these waterbodies (also identified in Table 11). Although Fish Harbor contains a Bight 03 station, the representative reaches for the model subwatersheds surrounding this waterbody drained directly to the Inner Harbor. Therefore, none of the model subwatersheds were assigned to Fish Harbor and its Bight 03 station (station BRI-03) was excluded from the analyses. Similarly, Cabrillo Marina contains a Bight 03 station (station 4138) that was not used in the analyses. There was just a single sample representing this waterbody, while all other waterbodies had multiple stations that could be combined for a more robust analysis, including ranges based on standard deviations. Therefore, the Inner Harbor stations were assigned to the watersheds draining to Cabrillo Marina (note: the results for the single sample in Cabrillo Marina were higher than the average from the Inner Harbor stations, but within the same order of magnitude and generally in the same range).

The Bight 03 DDT, PCB, and chlordane samples within each waterbody were averaged to determine their representative concentrations (for non-detected results, one-half of the Bight 03 detection limit was assigned as the representative concentration). Standard deviations were also calculated for each pollutant-waterbody combination, where enough data were available. Table 12 presents the representative concentrations, which were subsequently applied to each subwatershed assigned to a particular waterbody. The sediment concentration value from the Bight 03 data was then multiplied by the subwatershed's in-stream sediment concentrations (predicted based on LSPC models), resulting in an estimated in-stream concentration of DDT, PCB, and chlordane.

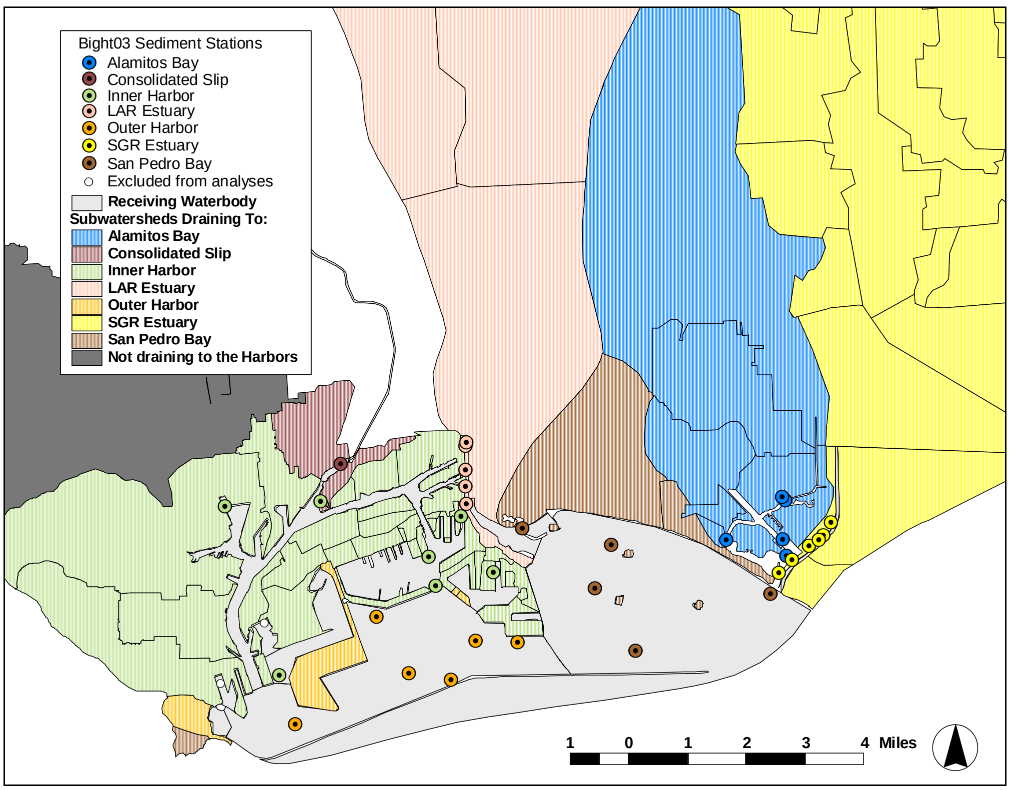

Figure 23. Waterbodies and Bight 03 Stations Assigned to Model Subwatersheds

Table 11. Bight 03 Stations by Waterbody

Waterbody	Bight 03 Station Identification Number
Alamitos Bay	4018
	4130
	4386
	4424
	4456
Los Angeles Harbor - Consolidated Slip	BRI-05
Los Angeles/Long Beach Inner Harbor	4010
	4050
	4146
	4210
	4266
	4338
	4354
Los Angeles River Estuary	4142
	4440
	4600
	4788
	4856
Los Angeles/Long Beach Outer Harbor (inside breakwater)	4178
	4242
	4306
	4400
	4162
	4370
San Gabriel River Estuary	4002
	4258
	4520
	4194
	4322
	4034
San Pedro Bay Near/Off Shore Zones	BRI-06
	4066
	4098
	4274
	4408

The Forest, Pier A, and Maritime Museum subwatersheds were all assigned to the Inner Harbor and Table 12 presents the average DDT, PCBs, and chlordane sediment concentrations for the Inner Harbor. These concentrations were multiplied by the variable subwatershed-specific TSS values from the LSPC model to obtain a water column concentration for Forest, Pier A, and Maritime Museum, which are presented in Figure 24 through Figure 26, respectively. The graphs showing concentrations for each pollutant are on the left side of the figures. These graphs illustrate the predicted concentrations based on the modeled TSS and the Bight 03 sediment concentrations. The POLA/POLB detection limits are included in the graphs for reference (they were excluded from the Maritime Museum graphs [Figure 26] because no organics data were available for this station). The predicted chlordane values are below the POLA/POLB detection limits because these samples were all non-detects for the Inner Harbor. For PCBs and DDT, the predicted concentrations were initially below the observed detection limit, but increased as the TSS peaked during the storm. The resulting loads are also presented for each pollutant on the right side of Figure 24 through Figure 26. The loads for the entire modeling period will be applied to the receiving water model. This methodology was applied to the model output from all other model subwatersheds (LAR, SGR, and other nearshore subwatersheds).

Table 12. Bight 03 DDT, PCB, and Chlordane Sediment Concentrations by Waterbody

Waterbody	Lower range	Mean	Upper range	Notes
DDT (µg/kg)				
Alamitos Bay	1.92	7.71	13.51	a
Los Angeles Harbor - Consolidated Slip	1.30	1.30	1.30	b
Los Angeles/Long Beach Inner Harbor	9.58	45.14	80.69	a
Los Angeles River Estuary	0.00	88.48	200.19	a
Los Angeles/Long Beach Outer Harbor (inside breakwater)	13.64	56.41	99.19	a
San Gabriel River Estuary	1.56	2.35	3.14	a
San Pedro Bay Near/Off Shore Zones	2.65	26.83	51.02	a
Chlordane (µg/kg)				
Alamitos Bay	0.58	2.26	3.93	a
Los Angeles Harbor - Consolidated Slip	0.00	0.50	1.00	c
Los Angeles/Long Beach Inner Harbor	0.00	0.29	0.58	c
Los Angeles River Estuary	16.46	16.60	16.74	d
Los Angeles/Long Beach Outer Harbor (inside breakwater)	0.00	0.29	0.58	c
San Gabriel River Estuary	0.00	0.43	0.86	c
San Pedro Bay Near/Off Shore Zones	0.78	1.09	1.41	d
PCBs (µg/kg)				
Alamitos Bay	3.48	3.78	4.08	d
Los Angeles Harbor - Consolidated Slip	0.00	0.50	1.00	c
Los Angeles/Long Beach Inner Harbor	0.00	31.63	78.17	a
Los Angeles River Estuary	245.66	246.34	247.02	d
Los Angeles/Long Beach Outer Harbor (inside breakwater)	1.10	1.88	2.66	d
San Gabriel River Estuary	0.00	0.63	1.26	c
San Pedro Bay Near/Off Shore Zones	0.00	13.31	29.12	a

[a] Upper and lower ranges based on calculated standard deviations

[b] Only one sample was available; therefore upper and lower ranges were not calculated.

[c] Results were all non-detects. Lower ranges are set equal to zero and upper ranges are set equal to the average detection limit.

[d] Limited detected samples were available to calculate standard deviations; therefore, the average lower ranges were calculated using zero for the non-detected samples and average upper ranges were calculated using the detection limit for the non-detected samples.

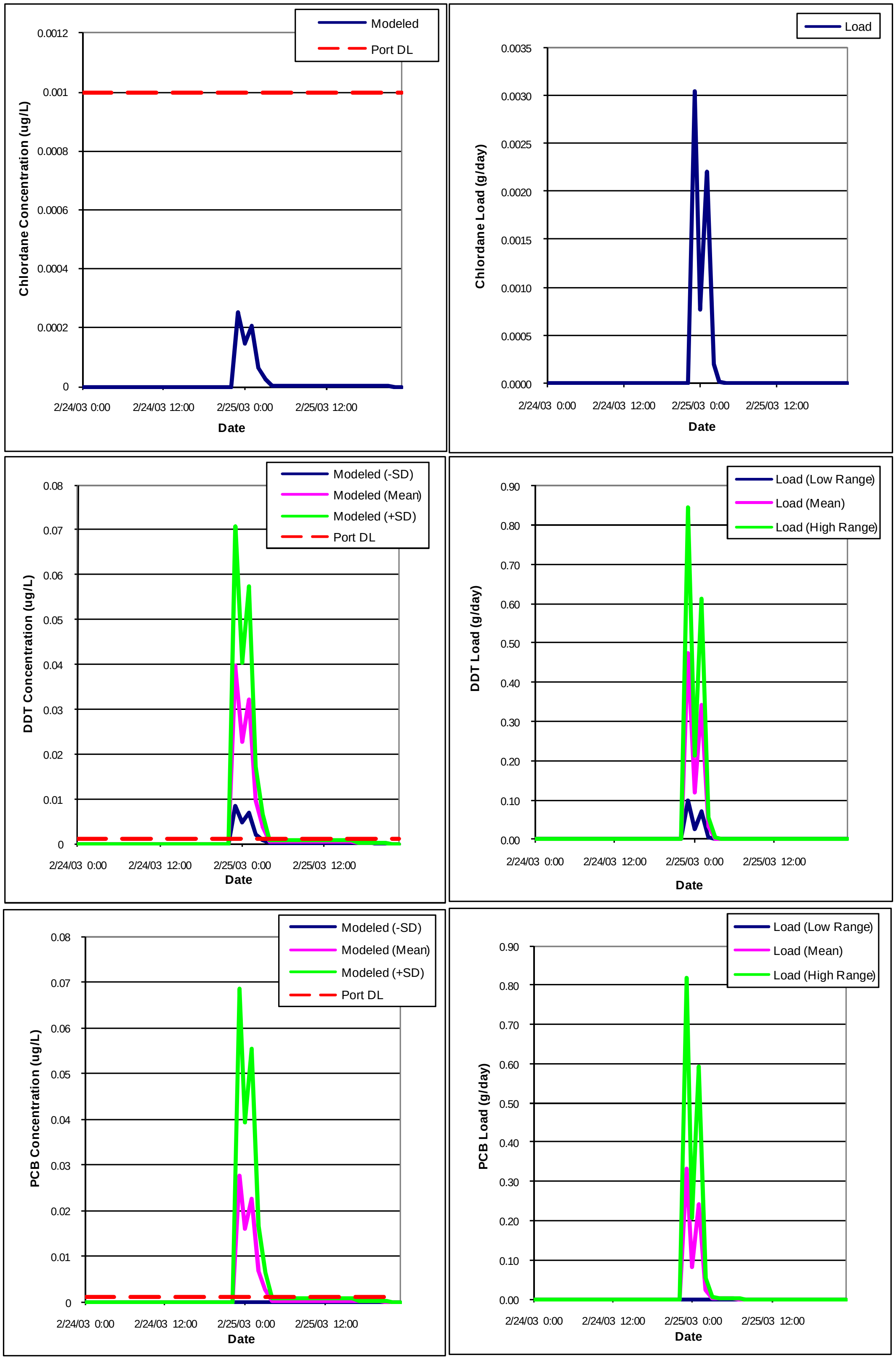

Figure 24. Modeled and Observed Chlordane, DDT, and PCBs Concentrations and Loads for the Forest Subwatershed

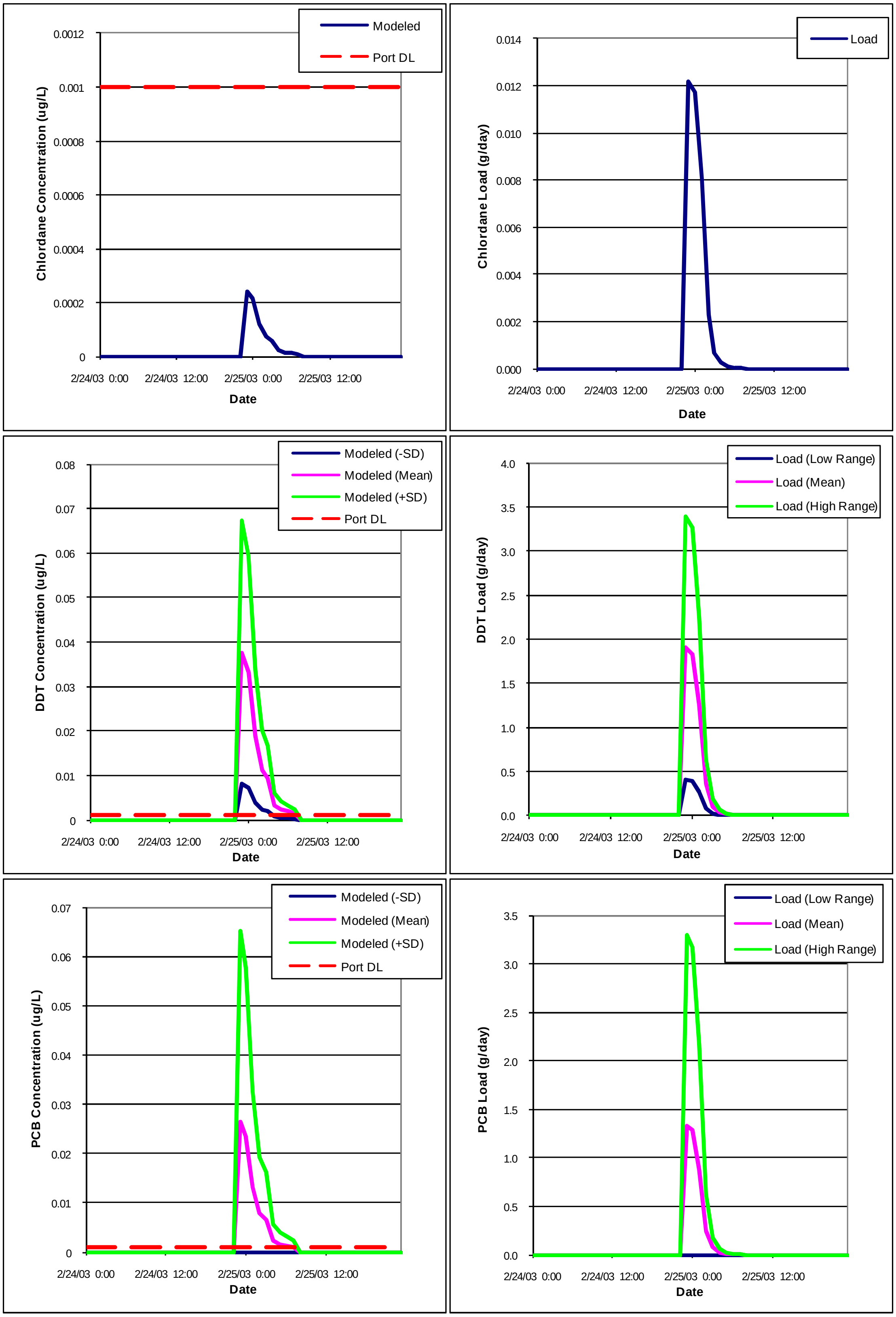

Figure 25. Modeled and Observed Chlordane, DDT, and PCBs Concentrations and Loads for the Pier A Subwatershed

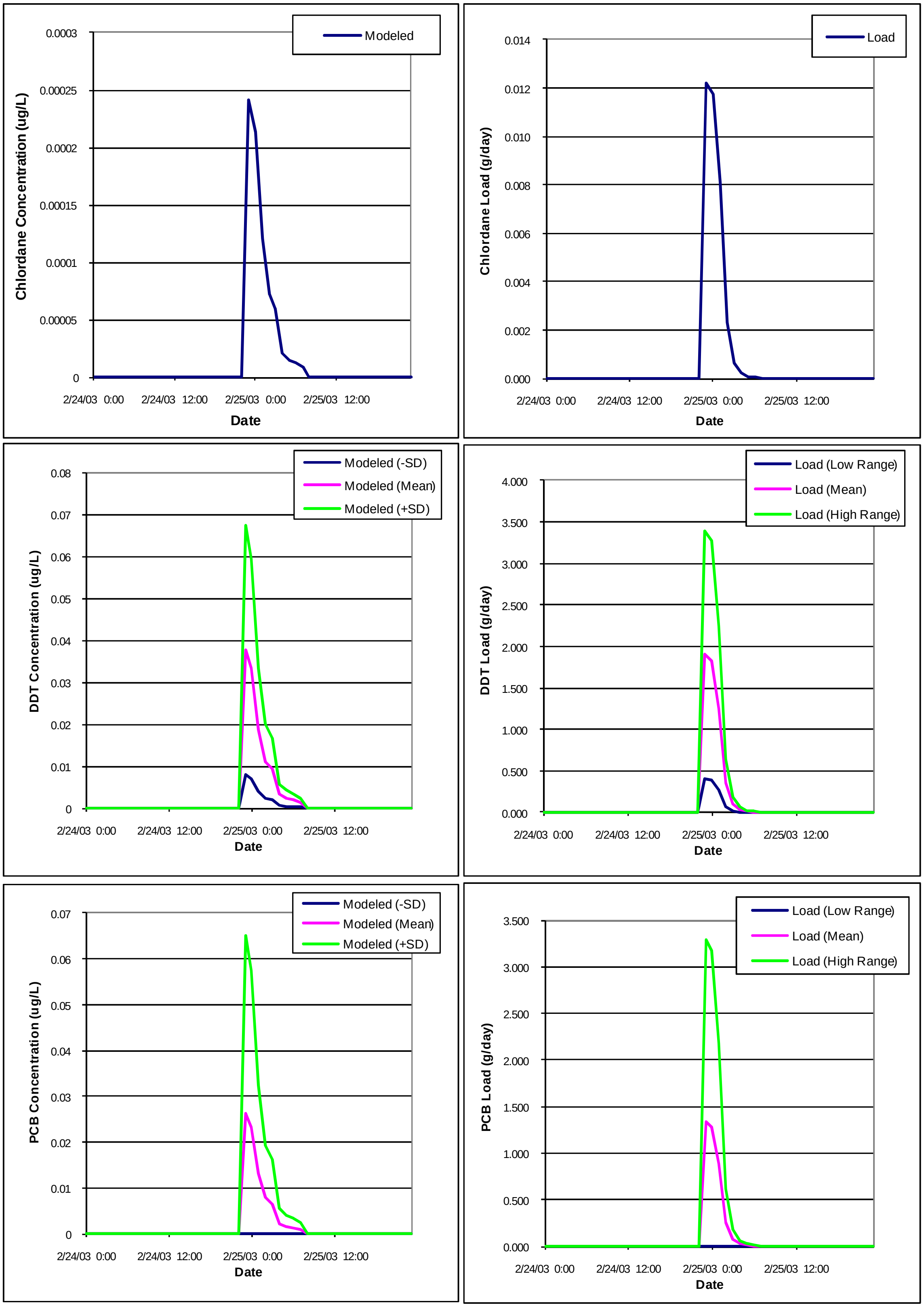

Figure 26. Modeled Chlordane, DDT, and PCBs Concentrations and Loads for the Maritime Museum Subwatershed

To assess the uncertainty of model predictions based on average sediment concentrations, sensitivity analyses of assumed values were performed. For each subwatershed, upper and lower ranges of average concentrations were determined using the average Bight 03 concentration plus/minus one standard deviation or using assumptions to represent non-detected samples, as listed in Table 12. Specifically, if three or more samples were detected, standard deviations were calculated and used to determine upper and lower ranges in the sensitivity analyses. However, if all of the samples were non-detects, the lower range was set equal to zero and the upper range was equal to the detection limit. Similarly, if less than three samples were detects, the non-detected samples were set equal to zero for the lower range and equal to the detection limit for the upper range. The average concentrations were then calculated to represent the upper and lower ranges.

Resulting ranges of wet-weather loadings to the Harbors and SPB were quantified to provide understanding of the sensitivity of loads potentially due to uncertainty of modeling assumptions. For the Forest, Pier A, and Maritime Museum subwatersheds, the DDT, PCB, and chlordane upper and lower ranges for concentrations and loads are presented graphically in Figure 24 though Figure 26, respectively. Sensitivity analyses for LAR, SGR, and the other nearshore areas were similarly performed.

4. Dry Weather

During dry weather, watershed flows are dominated by wastewater reclamation plants (WWRP) effluent, groundwater inflow, and discharges to the stormwater conveyance system from illicit connections, excess irrigation, and other residential and commercial practices (McPherson et al., 2005a; Stein and Ackerman, 2007). Although dry-weather flows are substantially less than stormflows in the region, their long-term contribution of pollutants can be substantial (McPherson et al., 2005a; Stein et al., 2003). Model representation of dry-weather pollutant loads in the region for calculation of TMDLs has been typically based on steady-state assumptions for flows and pollutant concentrations (LARWQCB, 2005a and 2005c; Tetra Tech, Inc, 2005b). Thus far, these approaches have relied heavily on robust monitoring efforts in LAR (Ackerman et al., 2003), SGR (Ackerman et al., 2005b), and Ballona Creek (Stein and Tiefenthaler, 2005). Results of these studies can be extrapolated for prediction of pollutant loads from the remaining watersheds of the Harbors and SPB.

Assumptions for steady-state, dry-weather flows are based on a combination of monitoring data and simplified methods based on land use. Observed flow data were ultimately used to represent the LAR (rather than modeled inflows);

therefore, these measured dry flows were considered appropriate for use in the dry weather loading estimates. For estimation of dry-weather river flows into the SGR estuary, the LSPC modeled flows were used.

Additional assumptions are required for prediction of dry-weather loads from the nearshore areas, which have much smaller subwatersheds and are largely impervious urban areas. A regional comparison of dry-weather flows performed by Stein and Ackerman (2007) provides insight into patterns for dry urban runoff in the region. For six watersheds in the Los Angeles Region, measured flows were reported for multiple sampling events. These watersheds include the LAR, SGR, Coyote Creek, San Jose Creek, Walnut Creek, and Ballona Creek. Ballona Creek was monitored during a single day during the dry season, whereas the remaining watersheds were monitored twice during consecutive dry seasons. Dry flows in LAR, SGR, Coyote Creek, and San Jose Creek were influenced by WWRP effluent flows. For each watershed, Stein and Ackerman summarized the relative contribution of flows from WWRPs, stormdrains, and upstream boundaries of the study domain. Adding the measured boundary and stormdrain flows, and averaging the combined flows for those watersheds with two sampling events, we determined a single representative flow for each watershed. These flows represent a combination of all runoff, baseflow, etc. that does not include WWRP contributions. A regression analysis of these flows verses urban area (summation of commercial, high-density residential, low-density residential, industrial, and mixed urban land uses) in each watershed revealed a noticeable relationship ($R^2 = 0.96$) between dry-weather flows and urban land use (Figure 27). Dry-weather flows for all nearshore areas were estimated based on the following equation (2) determined through the regression analysis.

$$Flow = 0.0024 \times (UrbanArea) \qquad (2)$$

where, *Flow* is in cubic meters per second (m^3/s) and *UrbanArea* is in square kilometers (km^2).

The Forest subwatershed has an urban area of 0.16 km^2. Using this equation, the estimated dry-weather flow is 0.0004 m^3/s or 0.014 cfs for the Forest subwatershed. Similar calculations were performed for the Pier A and Maritime Museum subwatersheds. When the applicable urban areas were assigned, the estimated dry weather flow for the Pier A subwatershed is 0.0025 m^3/s or 0.088 cfs, while the Maritime Museum subwatershed had an estimated flow of 0.0380 m^3/s or 1.343 cfs.

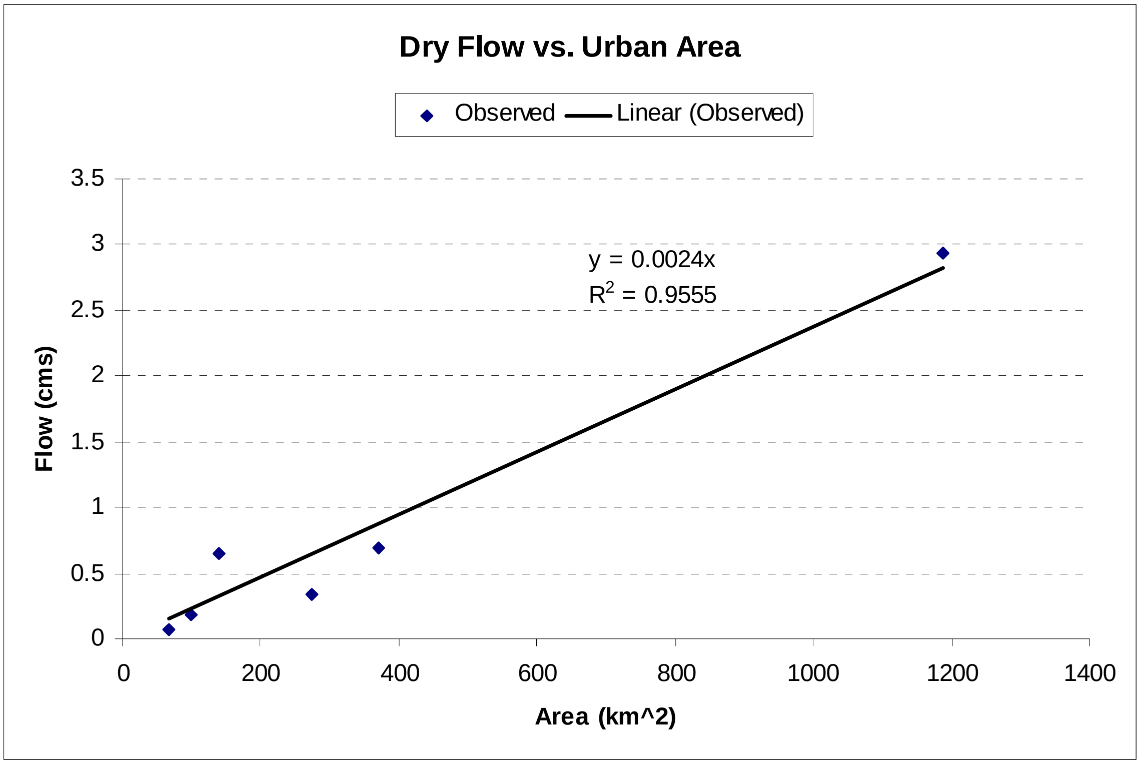

Figure 27. Regression Analysis of Dry-Weather Flows Verses Urban Area

To calculate pollutant loads based on the above flow predictions, additional assumptions for water quality concentrations were required. The availability of water quality data varies by pollutant; therefore, resulting assumptions for water quality predictions are discussed separately in the following sections.

4.1. Metals

Average dry-weather in-stream and stormdrain concentrations of metals in LAR and SGR, based on dry-weather monitoring organized by SCCWRP, are reported by Ackerman et al. (2003), Ackerman et al. (2005b), and Stein and Ackerman (2007). These results were used to estimate existing conditions for dry-weather loadings in LAR and SGR to support development of metals TMDLs for the rivers (LARWQCB, 2005c, 2006; USEPA, 2007). For the current study, metals concentrations for flows to estuaries from LAR and SGR were based on the LSPC metals simulations. These concentrations were multiplied by their respective dry-weather flows to determine loadings to the receiving water model.

To address dry-weather metals loadings in the nearshore areas, average concentrations and standard deviations were calculated using available stormdrain data. These data consisted of 255 stormdrain samples collected between 2000 and 2003 in the LAR and SGR watersheds (Ackerman et al., 2003; Ackerman et al., 2005b). Because these data represented runoff from various land uses, they were used to estimate average representative metals concentrations for all of the nearshore subwatersheds. The average dry-weather metals concentrations along with ranges based on the mean plus/minus the standard deviation are presented in Table 13.

Table 13. Dry-Weather Metals Concentrations Included in Loading Analyses (Ackerman et al., 2003; Ackerman et al., 2005b)

Region-Wide Concentrations			
	Mean minus the standard deviation	**Mean**	**Mean plus the standard deviation**
Copper concentration (mg/L)	0	0.037	0.159
Lead concentration (mg/L)	0	0.011	0.067
Zinc concentration (mg/L)	0	0.152	0.877

Table 14 presents the associated loads for the Forest, Pier A, and Maritime Museum subwatersheds. These were obtained by multiplying the average metals concentrations presented in Table 13 by the subwatershed-specific constant dry-weather flows. This methodology was repeated for all other nearshore model subwatersheds to determine metals loads to the Harbors, which will be input to the receiving water model.

Table 14. Dry-Weather Metals Loads for the Forest, Pier A, and Maritime Museum Subwatersheds

Subwatershed	Pollutant (grams/day)	Low Range	Mean	High Range
Forest Subwatershed	Copper Load	0	1.22	5.23
	Lead Load	0	0.36	2.20
	Zinc Load	0	5.02	28.90
Pier A Subwatershed	Copper Load	0	7.97	34.23
	Lead Load	0	2.43	14.43
	Zinc Load	0	32.86	189.11
Maritime Museum Subwatershed	Copper Load	0	34.00	145.96
	Lead Load	0	9.98	61.52
	Zinc Load	0	140.10	806.36

Sensitivity analyses were performed for the dry-weather loadings to assess the uncertainty of predictions based on average metals concentrations. For each subwatershed, the upper and lower concentrations (Table 13) based on the mean metals concentration plus/minus one standard deviation were multiplied by the subwatershed-specific flow to determine the associated loads. Resulting ranges of dry-weather loadings to the Harbors and SPB were quantified to provide understanding of the sensitivity of loads potentially due to uncertainty of analysis assumptions. For the Forest, Pier A, and Maritime Museum subwatersheds, the metals loading ranges are presented in Table 14.

4.2. PAHs, DDT, Chlordane, and PCBs

No detectable levels of organic pollutants are typically observed during dry weather based on LADPW mass emissions stations in the region (LADPW, 2006). In the absence of local detectable levels, assumptions may be based on values from studies performed outside of the Los Angeles Region. However, organic pollutant concentrations are assumed to be zero for dry-weather runoff since evidence suggests that sources are not prevalent during these conditions.

5. Model Assumptions

Assumptions are inherent to the modeling process as the model user attempts to represent the actual system as accurately as possible. The assumptions associated with the LSPC model and its algorithms are described in the HSPF User's Manual (Bicknell et al., 2001). There were several additional modeling assumptions used in the model of the watersheds draining to the Harbor, which are described below.

- Land use practices are consistent for all that fall within a given category and associated modeling parameters are transferable between subwatersheds.
- The average flows (daily or monthly) assigned from the point source data used to extend the LAR and SGR models were similar to actual discharger flows.
- The previously developed models of LAR and SGR were representative of the loadings from their respective watersheds without further validation.
- Sediment wash off from pervious areas occurred via detachment of the soil matrix for the wet-weather model. This process was considered uniform regardless of the land use type or season.
- Sediment in the watershed consisted of 5% sand, 40% clay, and 55% silt.
- For the wet-weather model, trace metals were linearly related to total suspended solids. As described in SCCWRP (2004), analysis of stormwater data supports this assumption.
- Trace metals were bound to a particle during wet-weather wash off until they dissociated upon reaching the receiving waterbody.
- The wet-weather PAH EMCs were representative of the watershed PAH loadings. Use of EMCs assumes no variability in storm concentrations, first flush, and indication of sediment association.
- PAHs were modeled as total PAHs, and not separately based on molecular weight.

- Non-detected values of DDT, PCBs, and chlordane were assigned a value of one-half of the detection limit while calculating wet-weather sediment concentrations.
- DDT, PCB, and chlordane sediment concentrations were assumed to be representative of DDT, PCB, and chlordane in-stream concentrations.
- Sensitivity analyses were performed for DDT, PCB, and chlordane using standard deviations, where possible, and variations on the detection limits when data were limited or results were non-detects.
- Dry-weather flows were predicted based on a relationship between flow and urban land use area for all nearshore areas.
- Dry-weather metals data collected from storm drains in the LAR and SGR watersheds were considered representative of the concentrations in the nearshore areas.
- Dry-weather metals concentrations measured at the bottom of the LAR and SGR watersheds in monitoring surveys provided by SCCWRP (Ackerman et al. 2003; Ackerman et al., 2005b) are sufficient for characterizing typical concentrations for all dry periods.

6. Conclusions

Loads from the wet- and dry-weather metals, PAHs, DDT, PCB, and chlordane analyses described above were summed to determine annual loads for each subwatershed draining to the Harbors and SPB. To assess the uncertainty of model predicted loadings to each receiving waterbody, sensitivity analyses of the assumed values were performed. Upper and lower concentrations based on the pollutant-specific approaches described above were combined with LSPC model output for wet-weather and estimated flows for dry-weather to determine the loading ranges associated with the varying concentrations.

Figure 28 and Figure 29 identify the model subwatersheds and their associated receiving waterbody for the major drainage areas and the nearshore areas, respectively (specifics on the distribution methodology are described in the receiving water modeling report). It should be noted that Dominguez Channel was not included in this study, and therefore associated loads to Consolidated Slip are not presented in this report (SCCWRP, unpublished results). Ultimately, hourly loadings for LAR, SGR, and DC and daily loadings for the nearshore areas were incorporated into the receiving water model of the Harbors. The calibration and validation of the hydrodynamic and sediment-contaminant portions of the receiving water model is discussed in a separate report.

Figure 30 through Figure 35 present the average daily loadings to each receiving waterbody (based on eleven year loads) for metals, PAHs, DDT, and PCBs, . The loadings for the Consolidated Slip and Los Angeles River Estuary include loadings from the near shore watersheds as well as their larger drainage areas (Dominguez Channel and Los Angeles River watersheds, respectively). Annual loads for an 11-year period to each receiving waterbody were calculated for each pollutant and are presented in Appendix B.

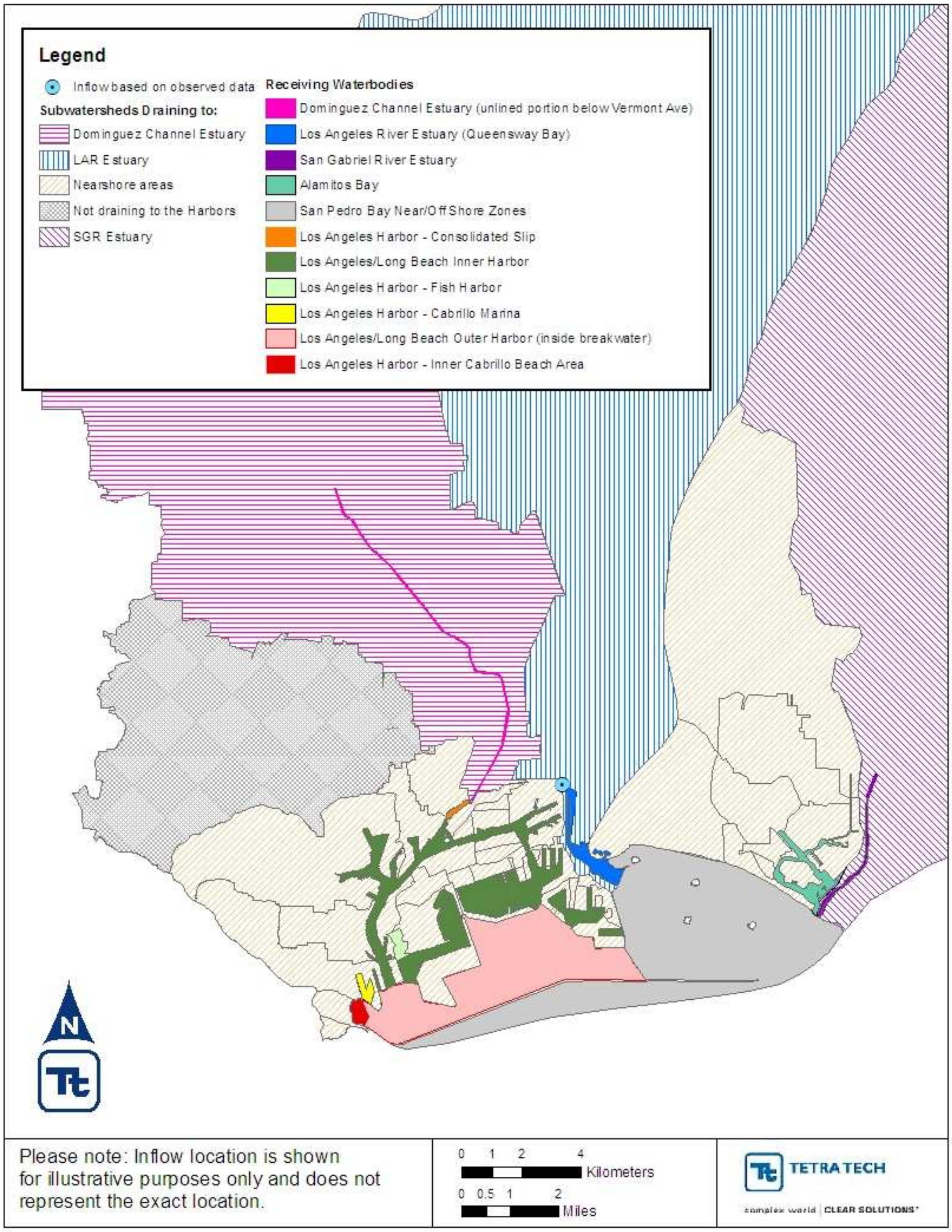

Figure 28. Major Drainage Areas and Waterbody Designations

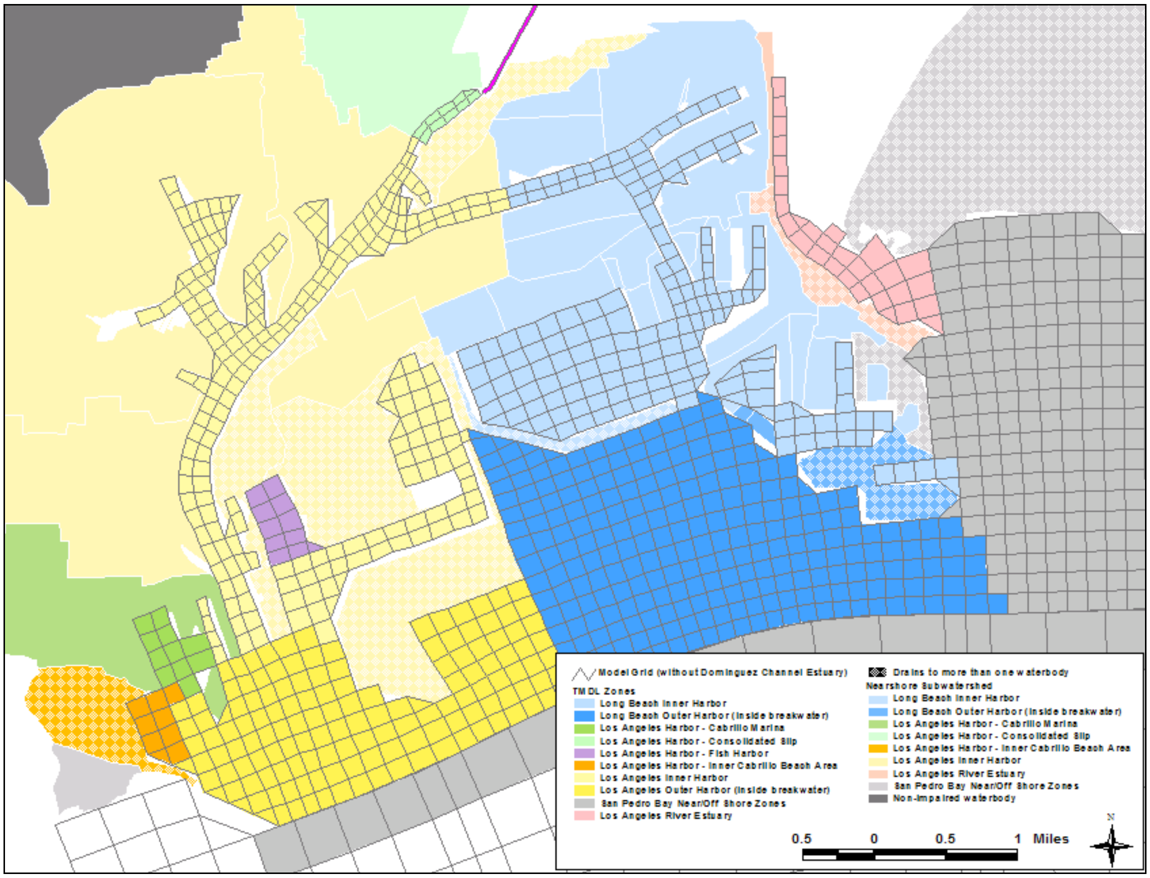

Figure 29. Nearshore Subwatersheds and Waterbody Designations

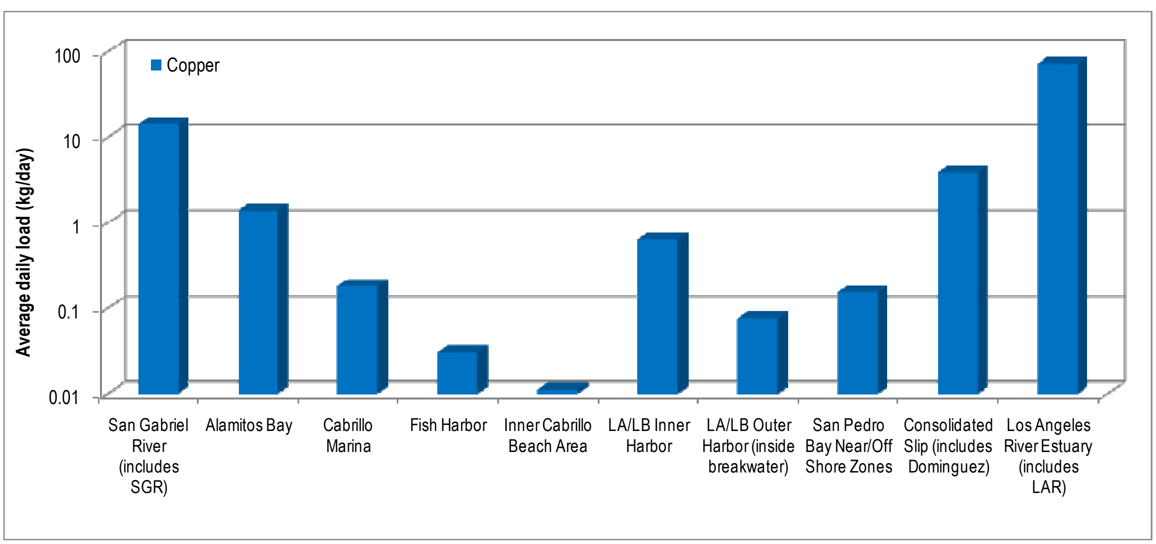

Figure 30. Average Daily Copper Loads

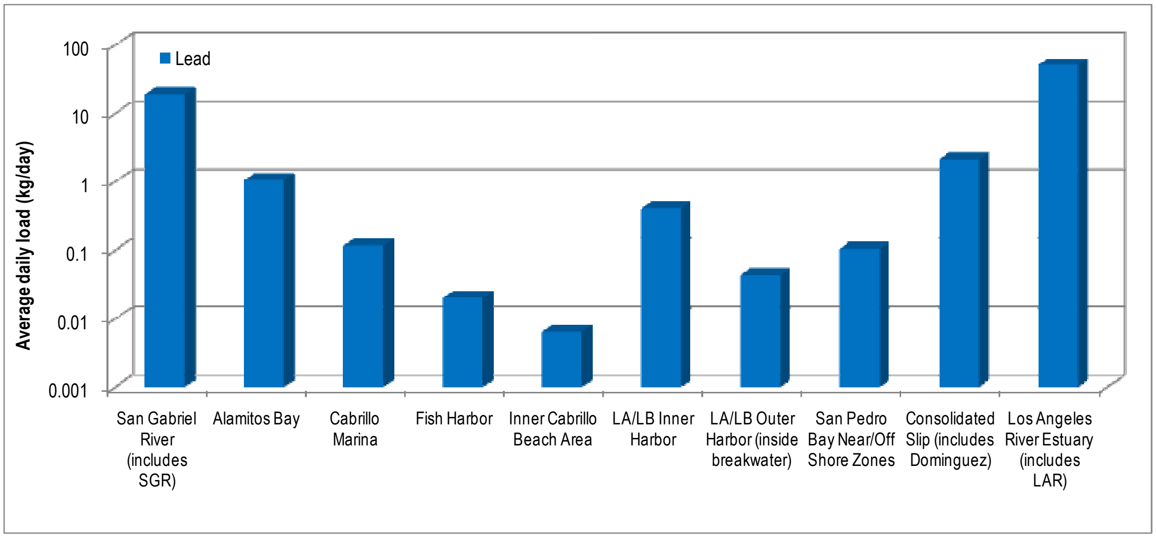

Figure 31. Average Daily Lead Loads

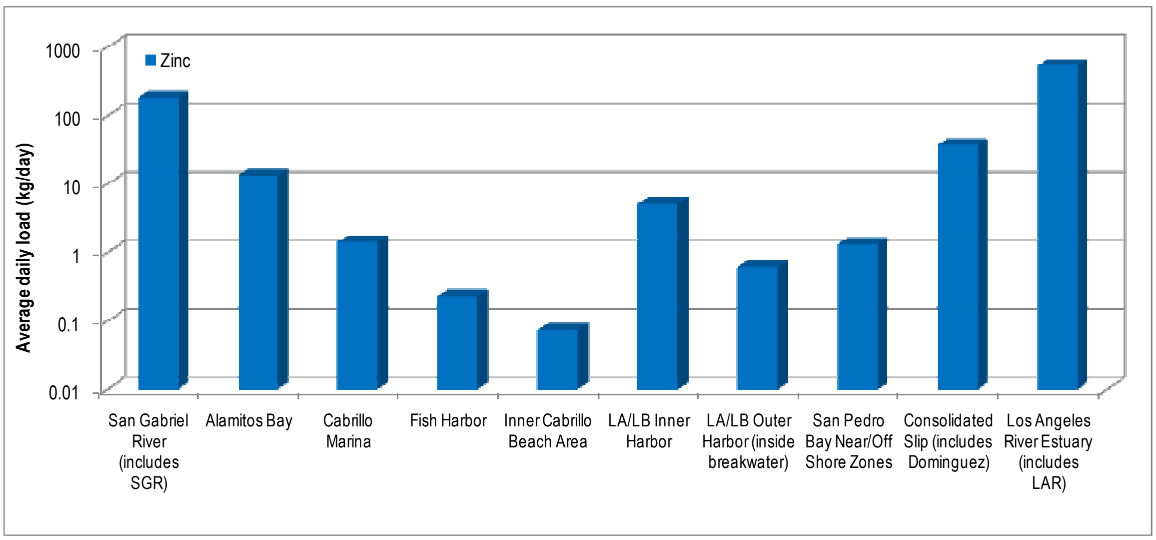

Figure 32. Average Daily Zinc Loads

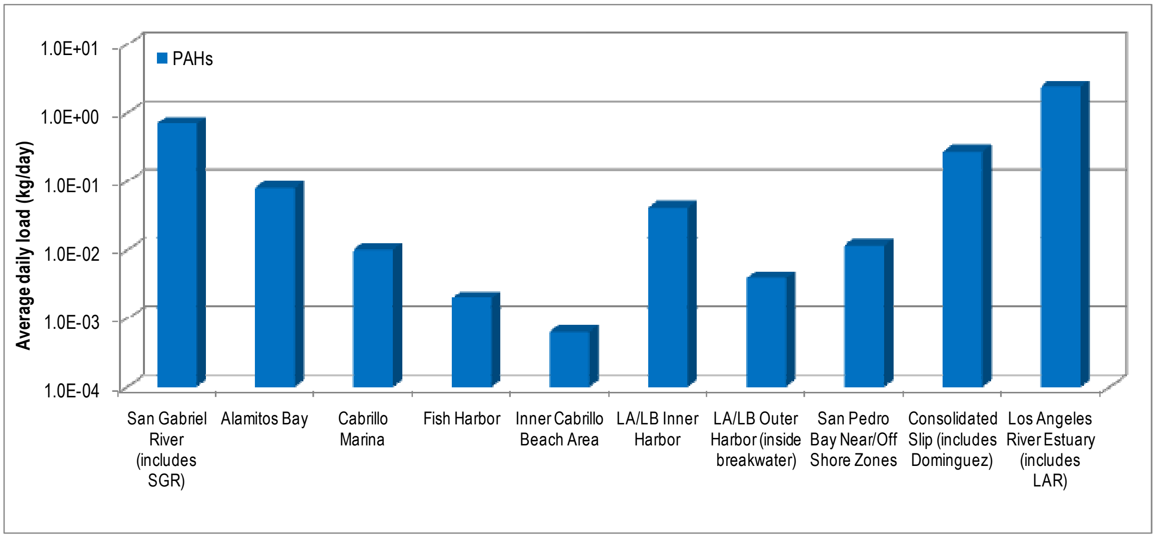

Figure 33. Average Daily PAH Loads

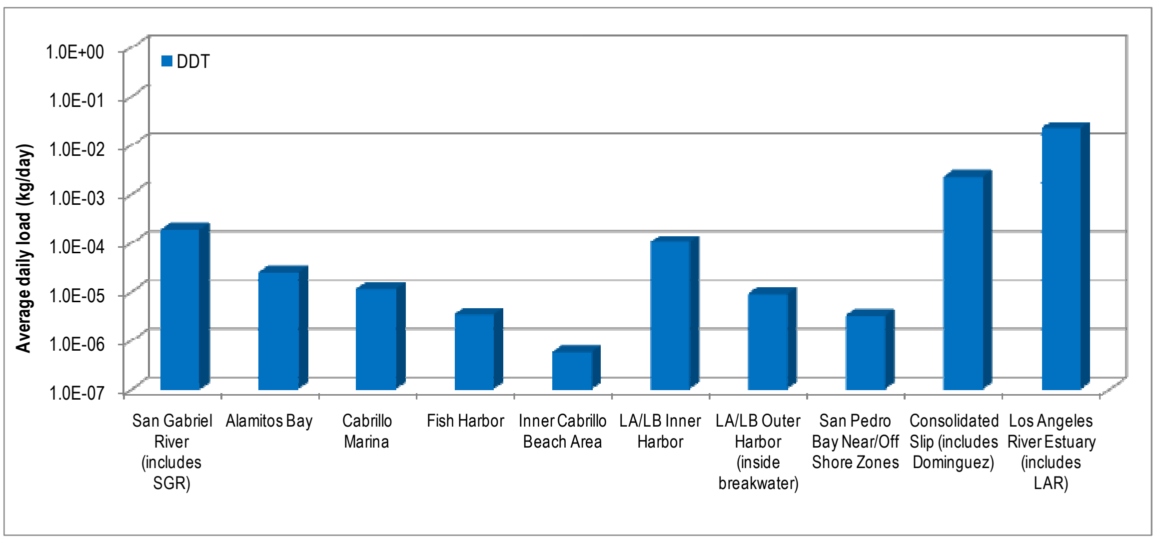

Figure 34. Average Daily DDT Loads

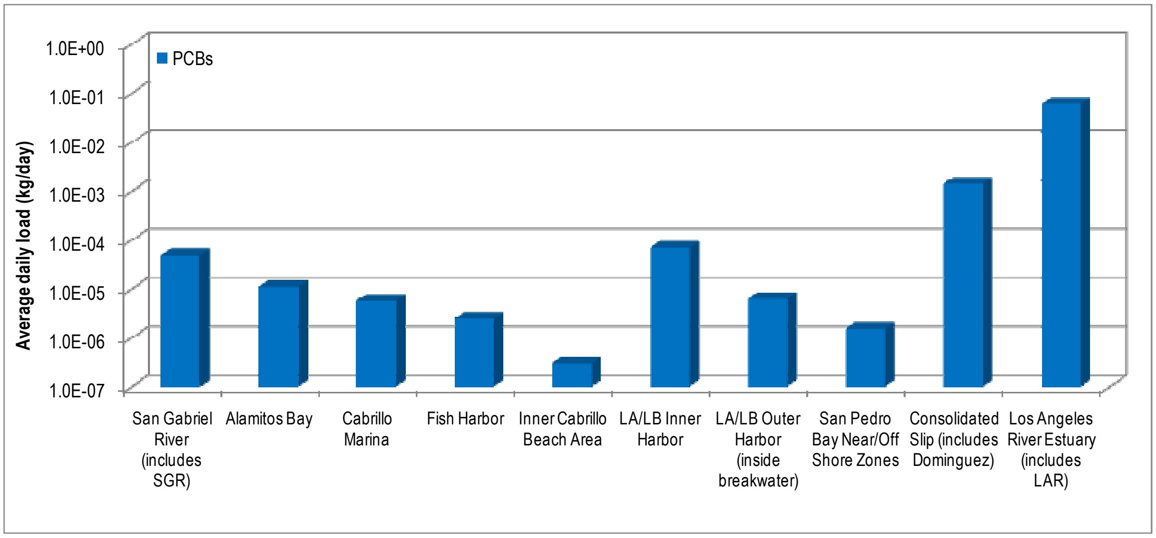

Figure 35. Average Daily PCB Loads

References

Ackerman, D., and K. Schiff. 2003. Modeling Stormwater Mass Emissions to the Southern California Bight. Southern California Coastal Water Research Project Annual Report 2001-2002. Westminster, CA.

Ackerman, D., K. Schiff, H. Trim, and M. Mullin. 2003. Characterization of Water Quality in the Los Angeles River. *Bulletin of the Southern California Academy of Sciences*, 102:1-17.

Ackerman, D., K. Schiff, and S. Weisberg. 2005a. Evaluating HSPF in an Arid, Urban Watershed. *Journal of the American Water Resources Association*, 41(2):477-486.

Ackerman, D., E. Stein, and K. Schiff. 2005b. Dry-season Water Quality in the San Gabriel River Watershed. Southern California Coastal Water Research Project Annual Report 2003-2004. Westminster, CA.

Bicknell, B. R., J. C. Imhoff, J. L. Kittle, Jr., T. H. Jobes and Anthony S. Donigian. 2001. Hydrological simulation program - FORTRAN, Version 12. AQUA TERRA Consultants. Mountain View, California. 873 pp.

Buffleben, M., K. Zayeed, D. Kimbrough, M. Stenstrom, and I. Suffet. 2002. Evaluation of Urban Non-point Source Runoff of Hazardous Metals Entering Santa Monica Bay, California. *Water Science and Technology*, Vol. 45, No. 9, pp 263-268.

CALTRANS. 2003. A Review of Contaminants and Toxicity Associated With Particles in Stormwater Runoff. California Department of Transportation, Sacramento, CA.

Dunne, T. and L. B. Leopold. 1978. Water in Environmental Planning. W.H. Freeman and Company. San Francisco, California. 818 pp.

Hoffman, E., J. Latimer, G. Mills, and J. Quinn. 1982. Petroleum Hydrocarbons in Urban Runoff from a Commercial Land Use Area. *Journal WPCF*, Vol. 54, No. 11.

LADPW. 2006. Historic mass emissions data in Los Angeles County from 5/11/88 to 7/18/2005, provided by the Los Angeles County Department of Public Works, Alhambra, CA.

LARWQCB. 2005a. Total Maximum Daily Load for Metals in Ballona Creek. Los Angeles Regional Water Quality Control Board, Los Angeles, CA.

LARWQCB. 2005b. Total Maximum Daily Load for Toxic Pollutants in Ballona Creek Estuary. Los Angeles Regional Water Quality Control Board, Los Angeles, CA.

LARWQCB. 2005c. Total Maximum Daily Load for Metals – Los Angeles River and Tributaries. Los Angeles Regional Water Quality Control Board, Los Angeles, CA.

LARWQCB. 2006. Total Maximum Daily Loads for Metals and Selenium – San Gabriel River and Impaired Tributaries. Los Angeles Regional Water Quality Control Board, Los Angeles, CA. Approved by the Regional Board July 2006; pending State Board and EPA approval).

Lau, S., and M. Stenstrom. 2005. Metals and PAHs Adsorbed to Street Particles. *Water Research*, 39 (2005) 4083-4092.

Longanathan, B., K. Irvine, K. Kannan, V. Pragatheeswaran, and K. Sajwan. 1997. Distribution of Selected PCB Congeners in the Babcock Street Sewer District: A Multimedia Approach to Identify PCB Sources in the Combined Sewer Overflows (CSOs) Discharging to the Buffalo River, New York. *Archives of Environmental Contamination and Toxicology*, 33, 130-140.

McPherson, T., S. Burian, M. Stenstrom, H. Turin, M. Brown, and I. Suffet. 2005a. Trace Metal Pollutant Load in Urban Runoff from a Southern California Watershed. *Journal of Environmental Engineering*, July 2005.

McPherson, T., S. Burian, M. Stenstrom, H. Turin, M. Brown, and I. Suffet. 2005b. Dry and Wet Weather Flow Nutrient Loads from a Los Angeles

Watershed. *Journal of the American Water Resources Association*, August 2005.

SARWQCB. 2000. Final Problem Statement for the Total Maximum Daily Load for Toxic Substances in Newport Bay and San Diego Creek. Santa Ana Regional Water Quality Control Board, Riverside, CA.

SCCWRP. 2004. Model Development for Trace Metals Loading in an Arid Urbanized Watershed. Prepared for USEPA Region 9 and the Los Angeles Regional Water Quality Control Board by the Southern California Coastal Water Research Project, Los Angeles, CA.

SCCWRP. Unpublished Results. Stormwater Inputs to the Dominguez Channel.

Shen, J., A. Parker, and J. Riverson. 2004. A New Approach for a Windows-based Watershed Modeling System Based on a Database-supporting Architecture. Environmental Modeling and Software, July 2004.

Stein, E. 2006. Personal communication from Eric Stein, Southern California Coastal Water Research Project, to Stephen Carter, Tetra Tech, Inc. June 2006.

Stein, E., and D. Ackerman. 2007. Dry Weather Water Quality Loadings in Arid, Urban Watersheds of the Los Angeles Basin, California, USA. *Journal of American Water Resources Association,* 43(2), 398-413.

Stein, E., D. Ackerman, and K. Schiff. 2003. Watershed-based Sources of Contaminants to San Pedro Bay and Marina del Rey: Patterns and Trends. Report prepared for the Los Angeles Contaminated Sediments Task Force by the Southern California Coastal Water Research Project, Westminster, CA.

Stein, E., and L. Tiefenthaler. 2005. Characterization and Source Identification of Dry-weather Metals and Bacteria in Ballona Creek. Southern California Coastal Water Research Project Annual Report 2003-2004. Westminster, CA.

Stein, E., L. Tiefenthaler, and K. Schiff. 2005. Watershed-based Sources of Polycyclic Aromatic Hydrocarbons in Urban Stormwater. *Environmental Toxicology and Chemistry*, Vol. 25, No. 2, pp 373-385.

Tetra Tech, Inc. 2004. Model Development for Simulation of Wet-Weather Metals Loading from the Los Angeles River Watershed. Prepared for USEPA Region 9 and the Los Angeles Regional Water Quality Control Board by Tetra Tech, Inc., San Diego, California.

Tetra Tech, Inc, 2005a. Model Development for Simulation of Wet-Weather Metals Loading from the San Gabriel River Watershed. Report prepared for

USEPA Region 9 and the Los Angeles Regional Water Quality Control Board by Tetra Tech, Inc, San Diego, CA.

Tetra Tech, Inc, 2005b. Model Development for Simulation of Dry-Weather Metals Loading from the San Gabriel River Watershed. Report prepared for USEPA Region 9 and the Los Angeles Regional Water Quality Control Board by Tetra Tech, Inc, San Diego, CA.

United States Department of Agriculture (USDA). 1986. Urban Hydrology for Small Watersheds. Soil Conservation Service, Engineering Division, Technical Release 55 (TR-55).

USEPA (U.S. Environmental Protection Agency). 2003a. Fact Sheet: Loading Simulation Program in C++. USEPA, Watershed and Water Quality Modeling Technical Support Center, Athens, GA. Available at http://www.epa.gov/athens/wwqtsc/LSPC.pdf (accessed in January 2005).

USEPA (U.S. Environmental Protection Agency). 2003b. Fact Sheet: Overview of the TMDL Toolbox. USEPA, Watershed and Water Quality Modeling Technical Support Center, Athens, GA. Available at http://www.epa.gov/athens/wwqtsc/Toolbox-overview.pdf (accessed in January 2005).

USEPA (U.S. Environmental Protection Agency). 2007. Total Maximum Daily Loads for Metals and Selenium – San Gabriel River and Impaired Tributaries. Approved March 26, 2007.

Yunker, M., R. Macdonald, R. Vingarzan, R. Mitchell, D. Goyette, and S. Sylvestre. 2002. PAHs in the Frasier River Basin: A Critical Appraisal of PAH Ratios as Indicators of PAH Source and Composition. *Organic Geochemistry*, 33 (2002) 489-515.

Appendix A: Water Quality Validation Time-series Plots for the Nearshore Watersheds

FINAL

October 2010

Prepared for:
USEPA Region 9
Los Angeles Regional Water Quality Control Board

Prepared by:
Tetra Tech, Inc.

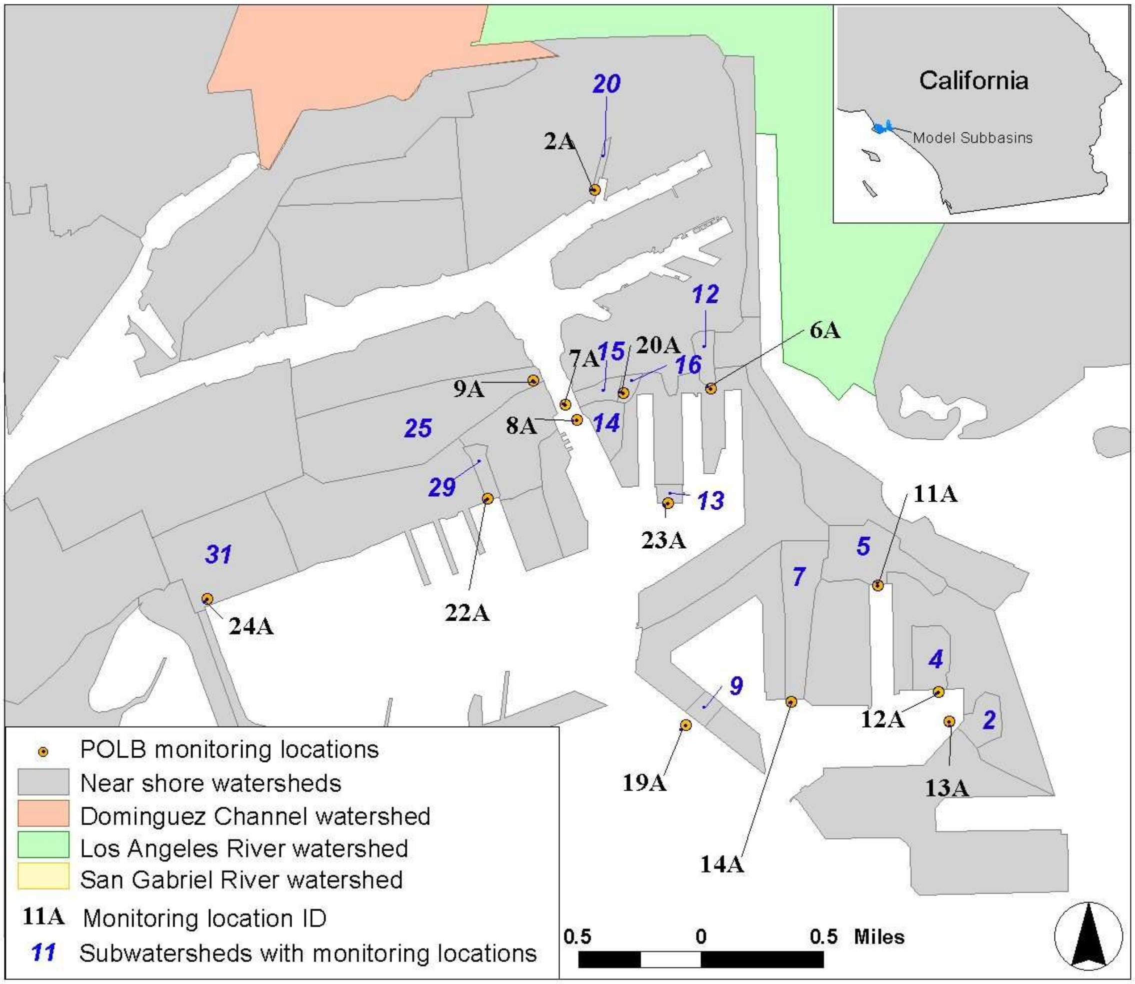

Figure A-1. Sampling Locations Used for Water Quality Validation

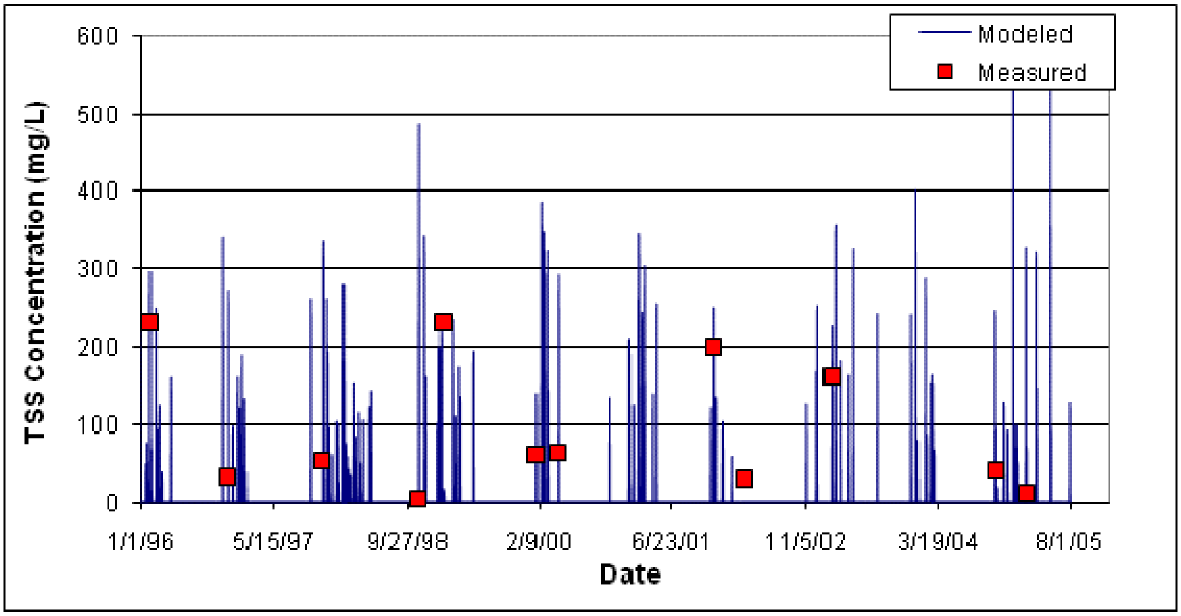

Figure A-2. Modeled and Observed TSS Concentrations for Subwatershed 2 (POLB Station 13A)

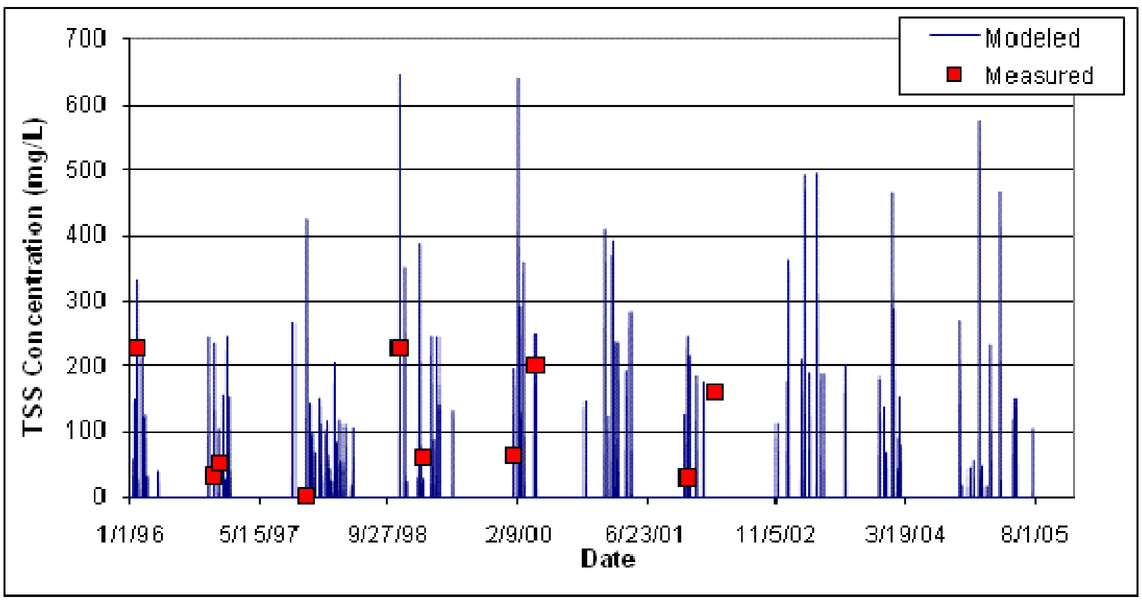

Figure A-3. Modeled and Observed TSS Concentrations for Subwatershed 4 (POLB Station 12A)

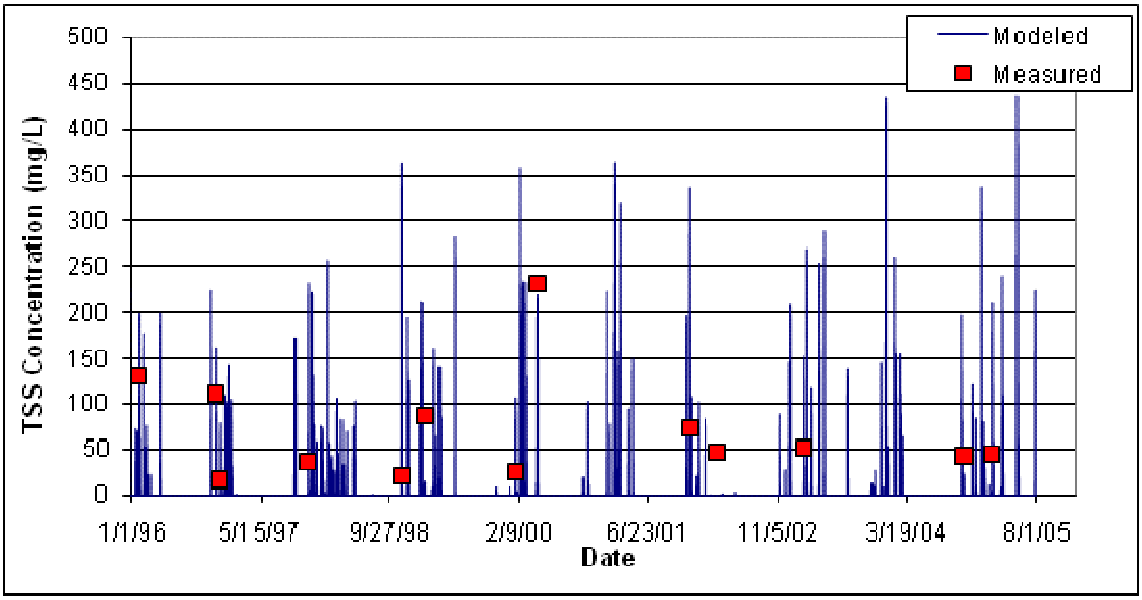

Figure A-4. Modeled and Observed TSS Concentrations for Subwatershed 5 (POLB Station 11A)

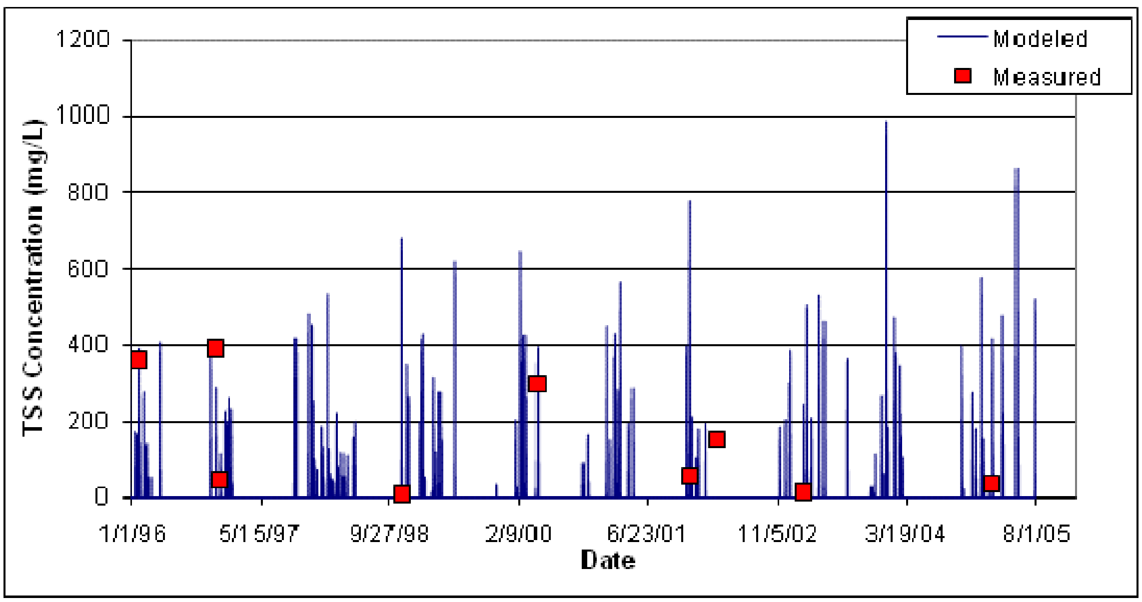

Figure A-5. Modeled and Observed TSS Concentrations for Subwatershed 7 (POLB Station 14A)

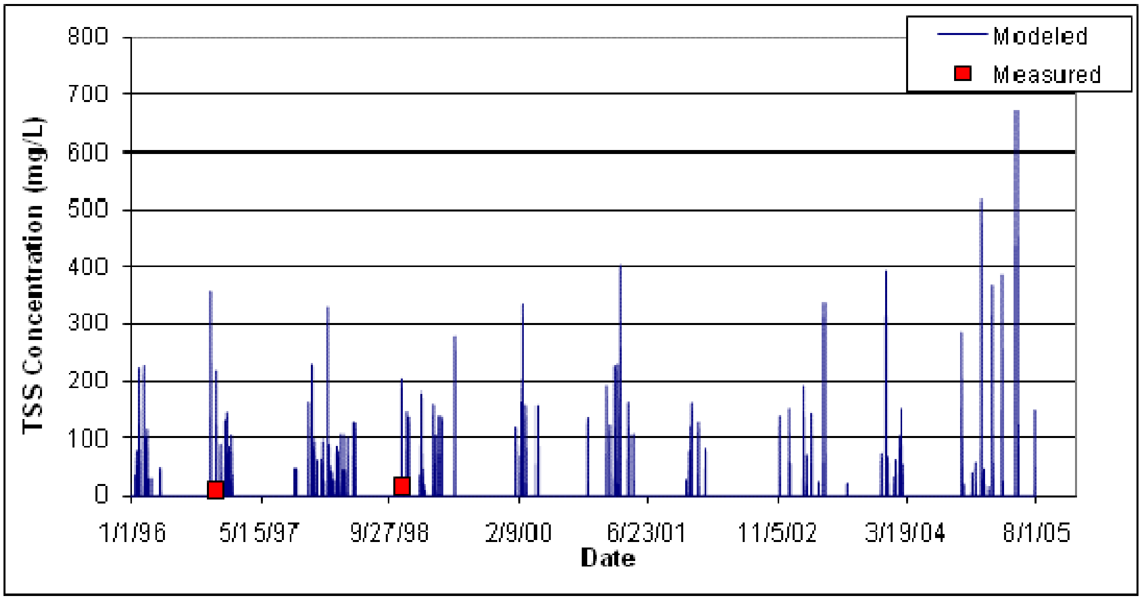

Figure A-6. Modeled and Observed TSS Concentrations for Subwatershed 9 (POLB Station 19A)

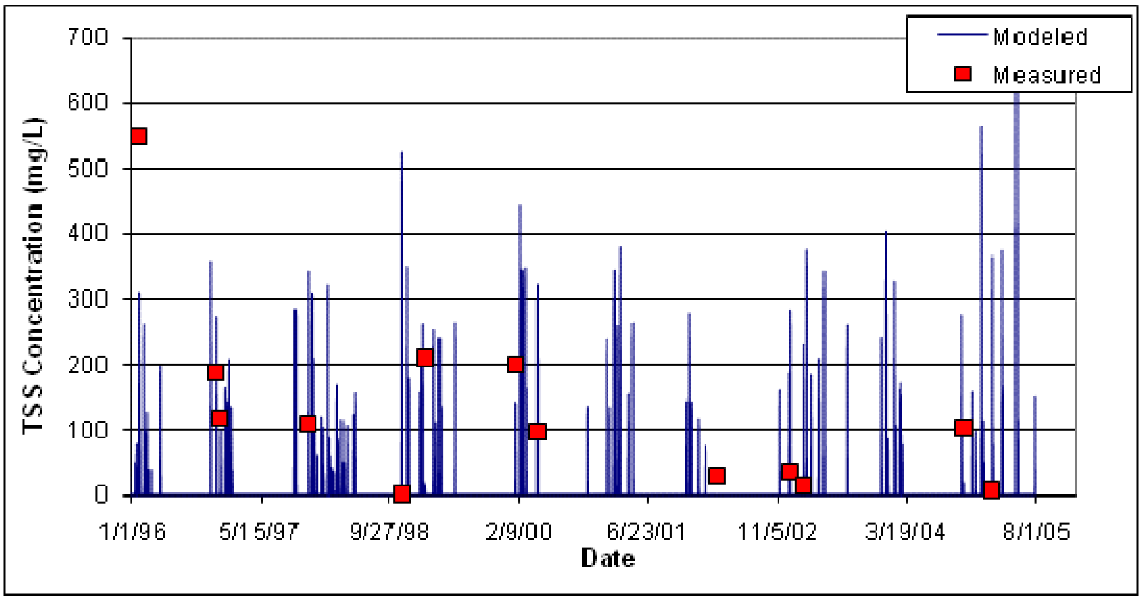

Figure A-7. Modeled and Observed TSS Concentrations for Subwatershed 12 (POLB Station 6A)

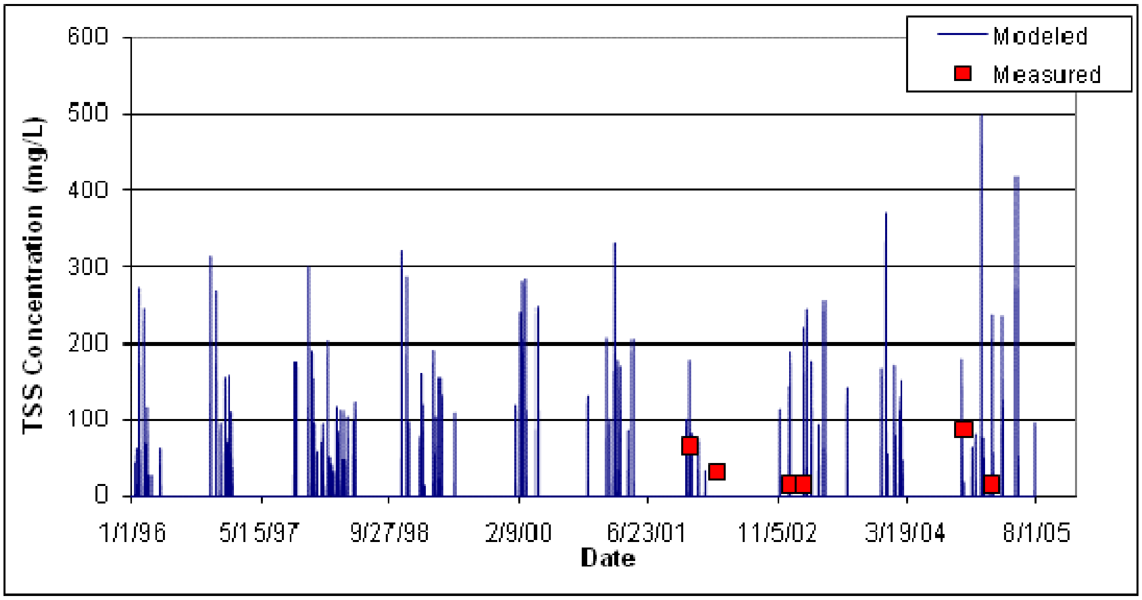

Figure A-8. Modeled and Observed TSS Concentrations for Subwatershed 13 (POLB Station 23A)

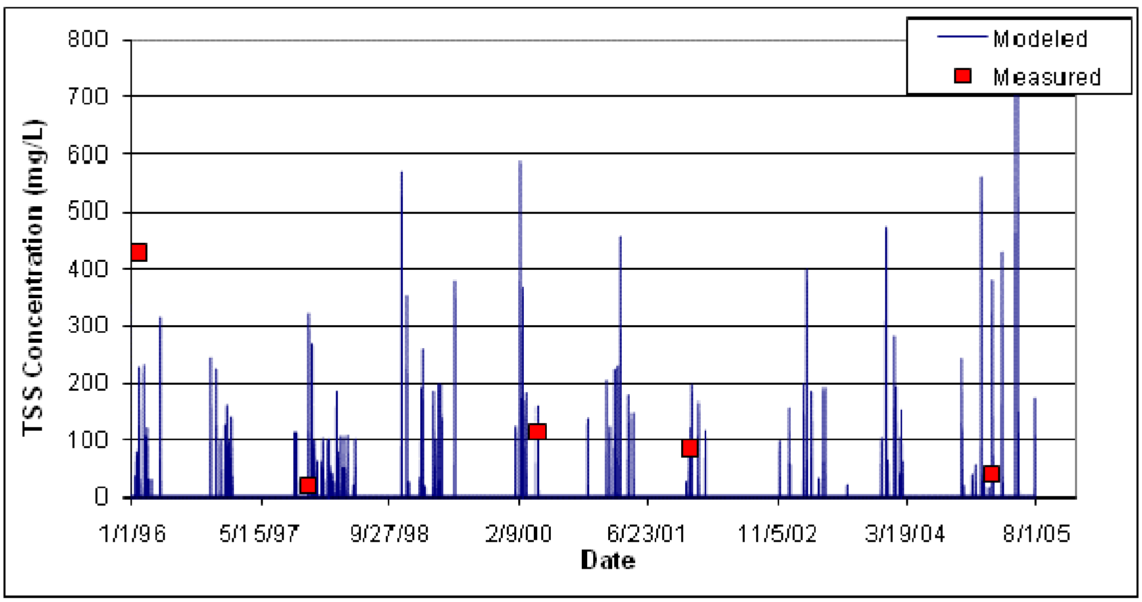

Figure A-9. Modeled and Observed TSS Concentrations for Subwatershed 14 (POLB Station 8A)

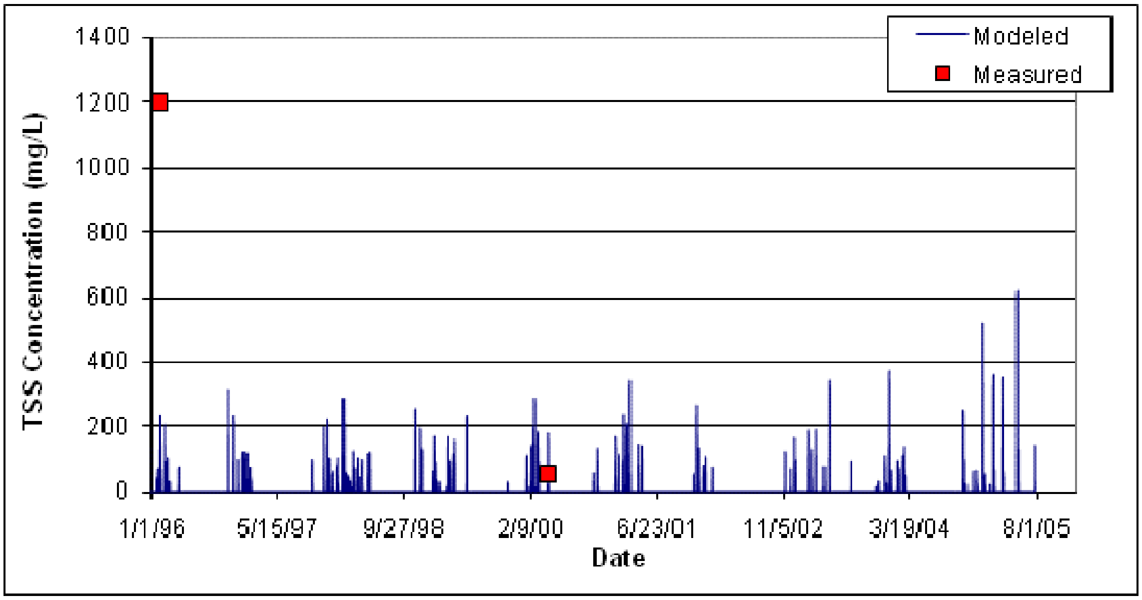

Figure A-10. Modeled and Observed TSS Concentrations for Subwatershed 15 (POLB Station 7A)

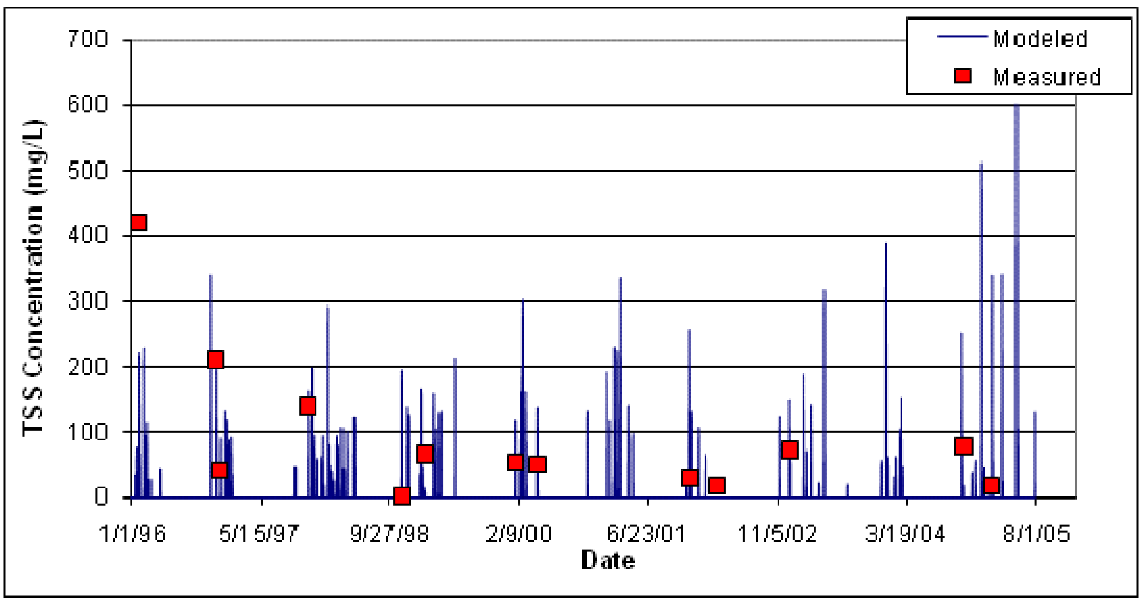

Figure A-11. Modeled and Observed TSS Concentrations for Subwatershed 16 (POLB Station 20A)

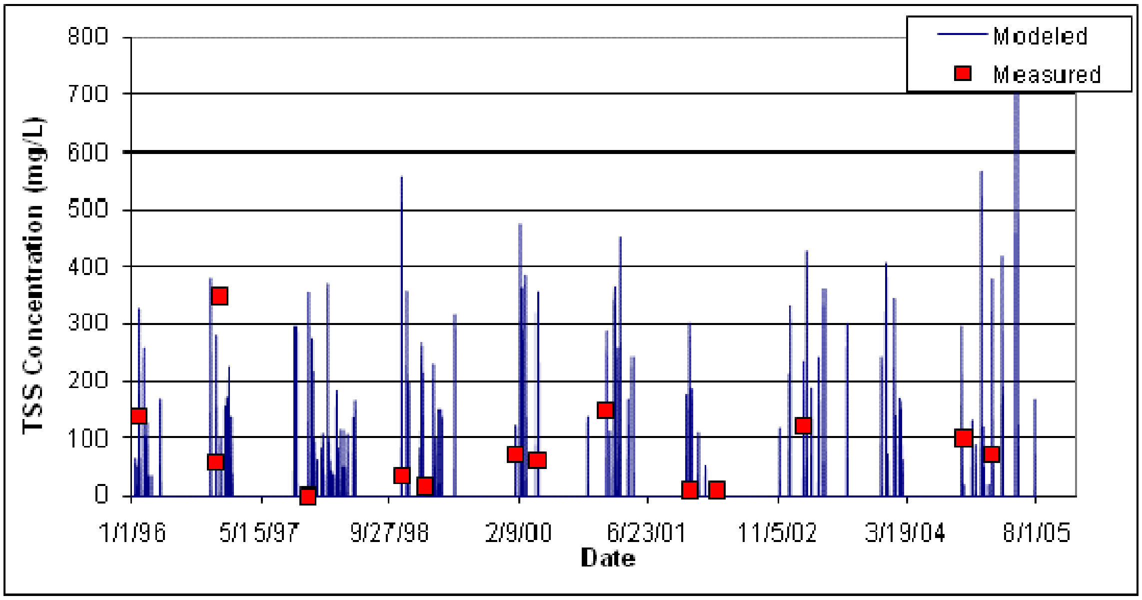

Figure A-12. Modeled and Observed TSS Concentrations for Subwatershed 20 (POLB Station 2A)

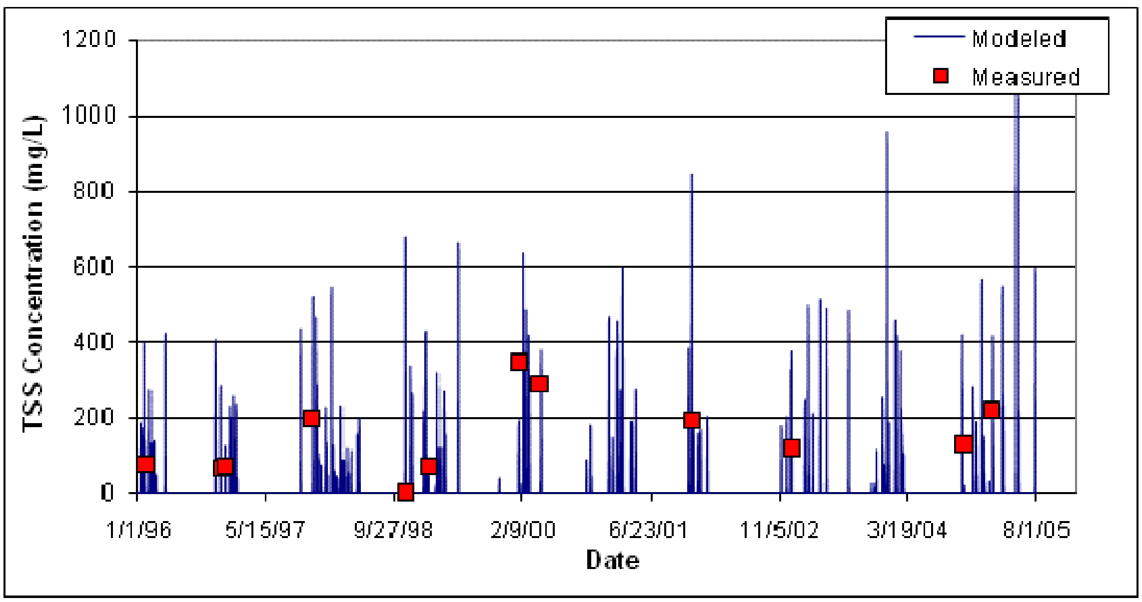

Figure A-13. Modeled and Observed TSS Concentrations for Subwatershed 25 (POLB Station 9A)

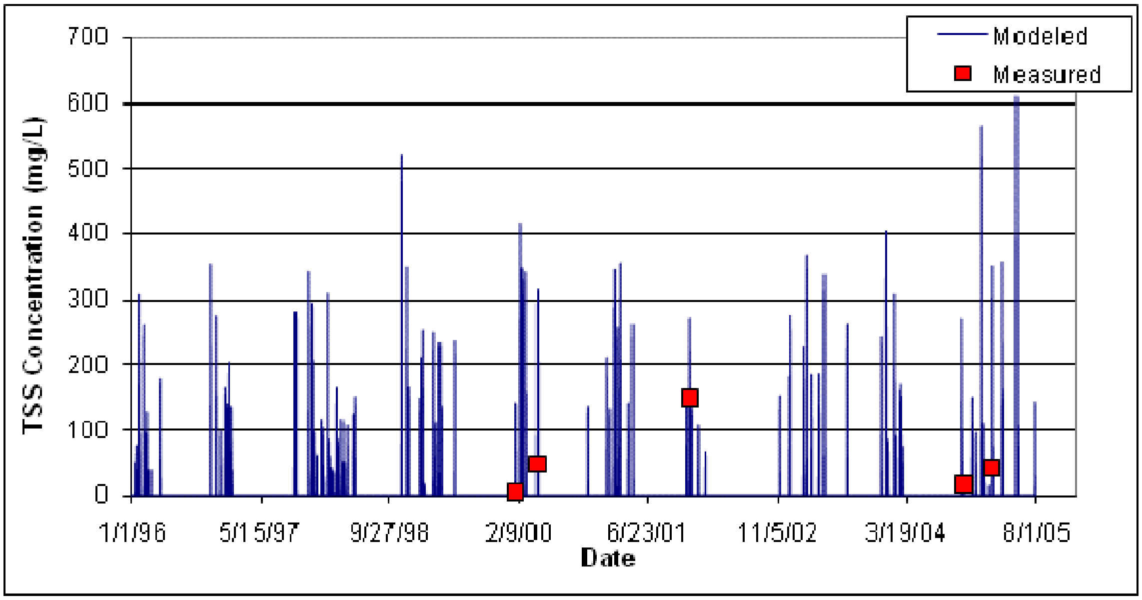

Figure A-14. Modeled and Observed TSS Concentrations for Subwatershed 29 (POLB Station 22A)

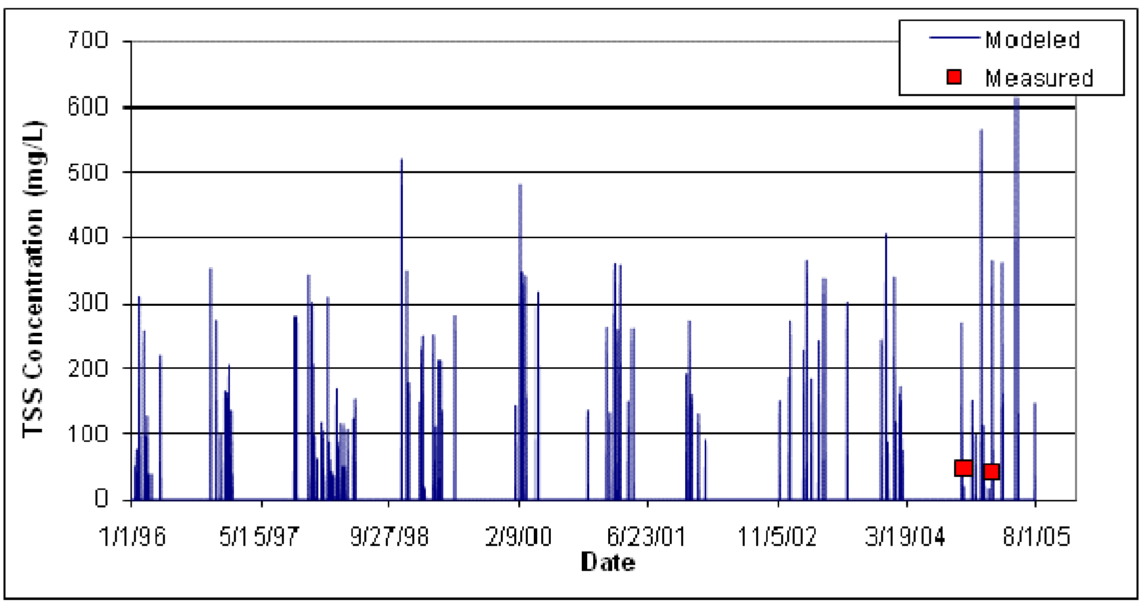

Figure A-15. Modeled and Observed TSS Concentrations for Subwatershed 31 (POLB Station 24A)

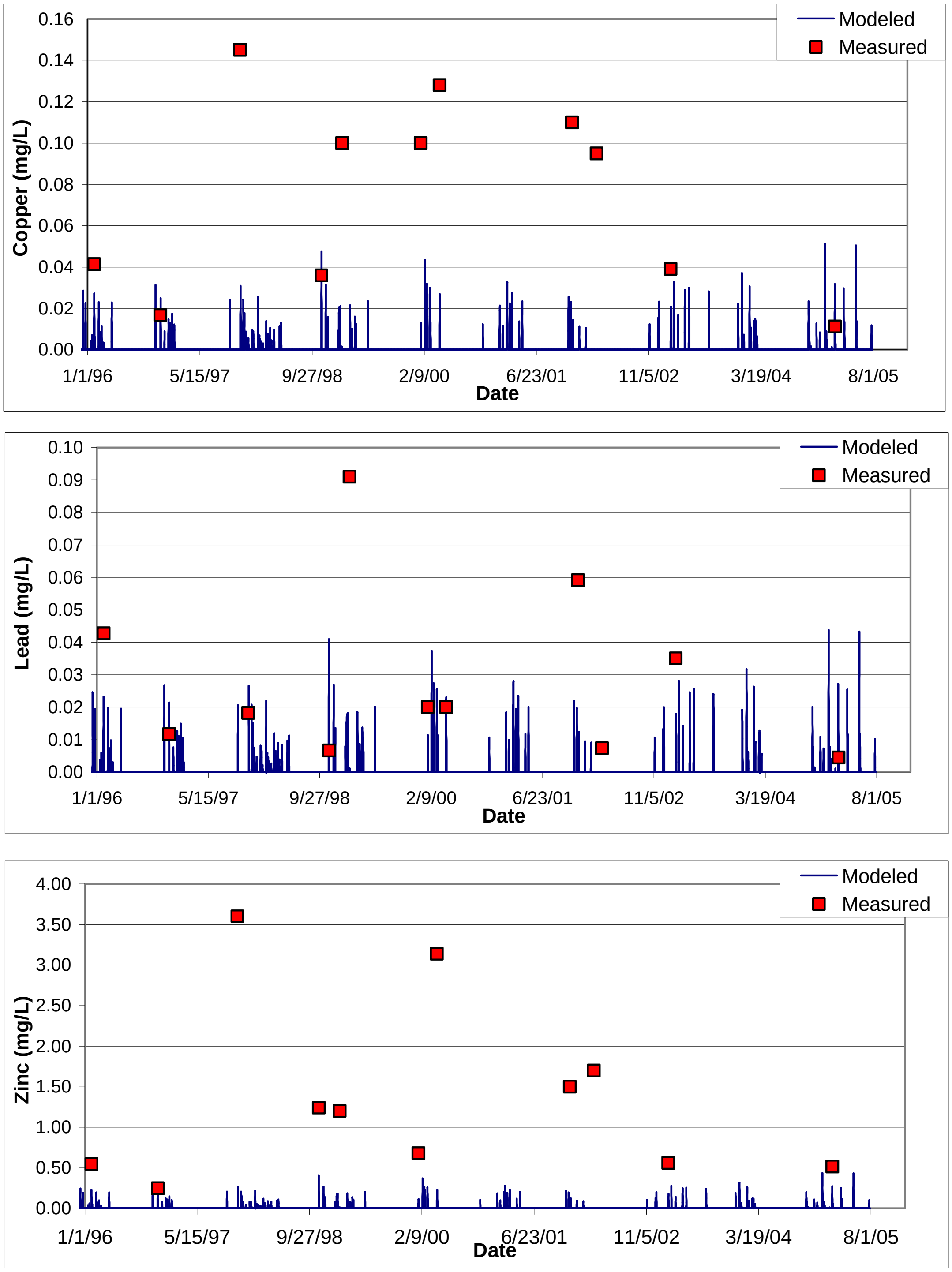

Figure A-16. Modeled and Observed Metal Concentrations for Subwatershed 2 (POLB Station 13A)

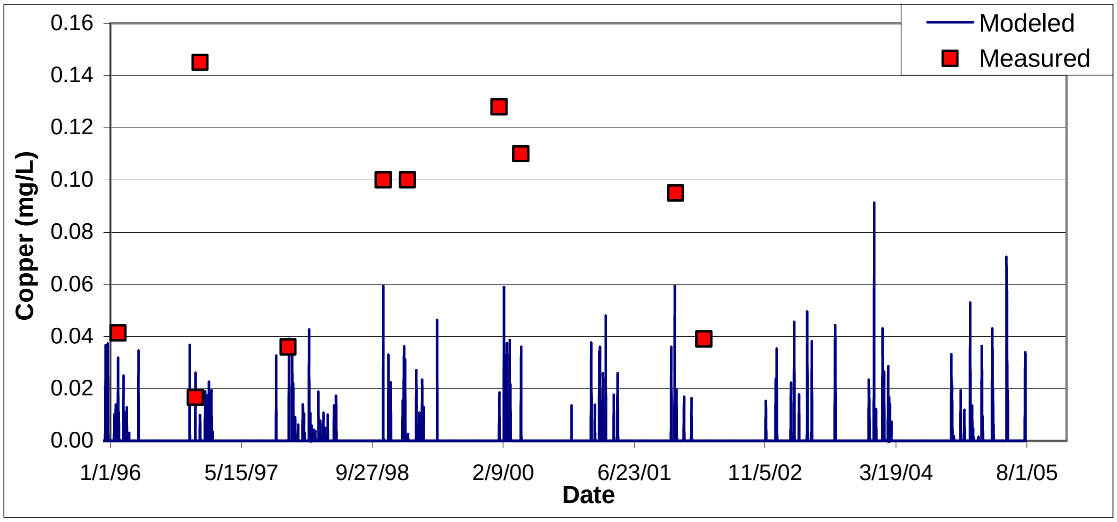

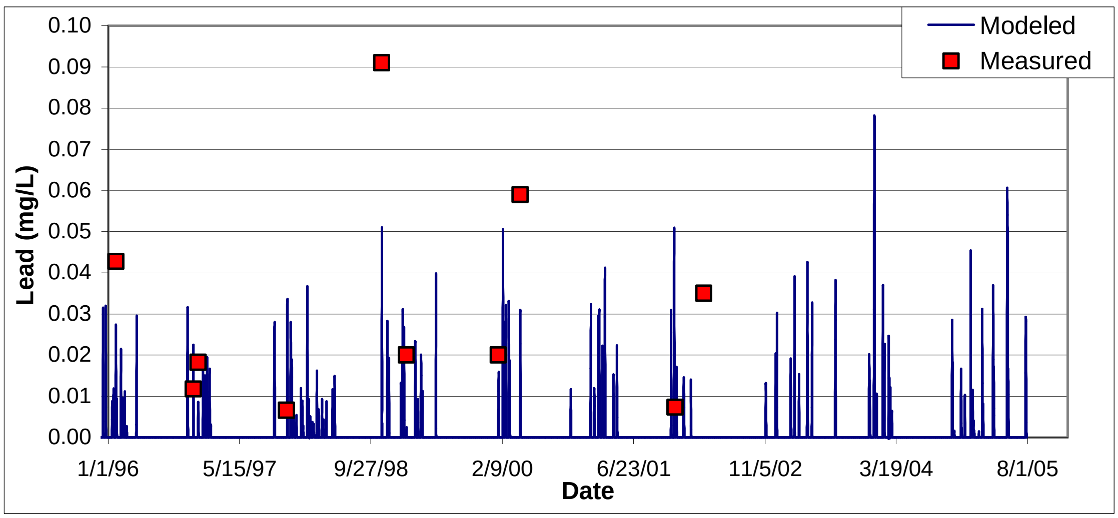

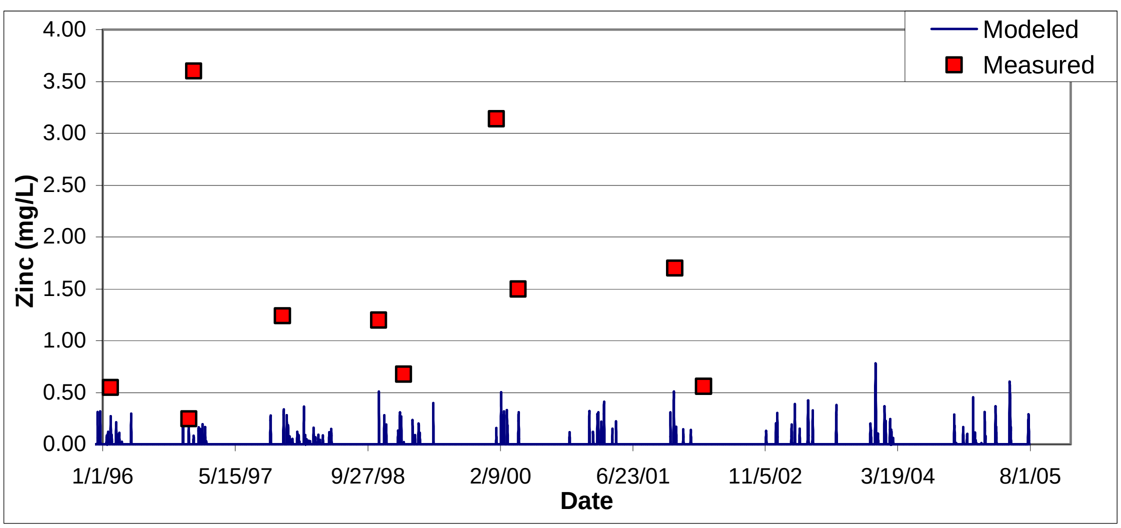

Figure A-17. Modeled and Observed Metal Concentrations for Subwatershed 4 (POLB Station 12A)

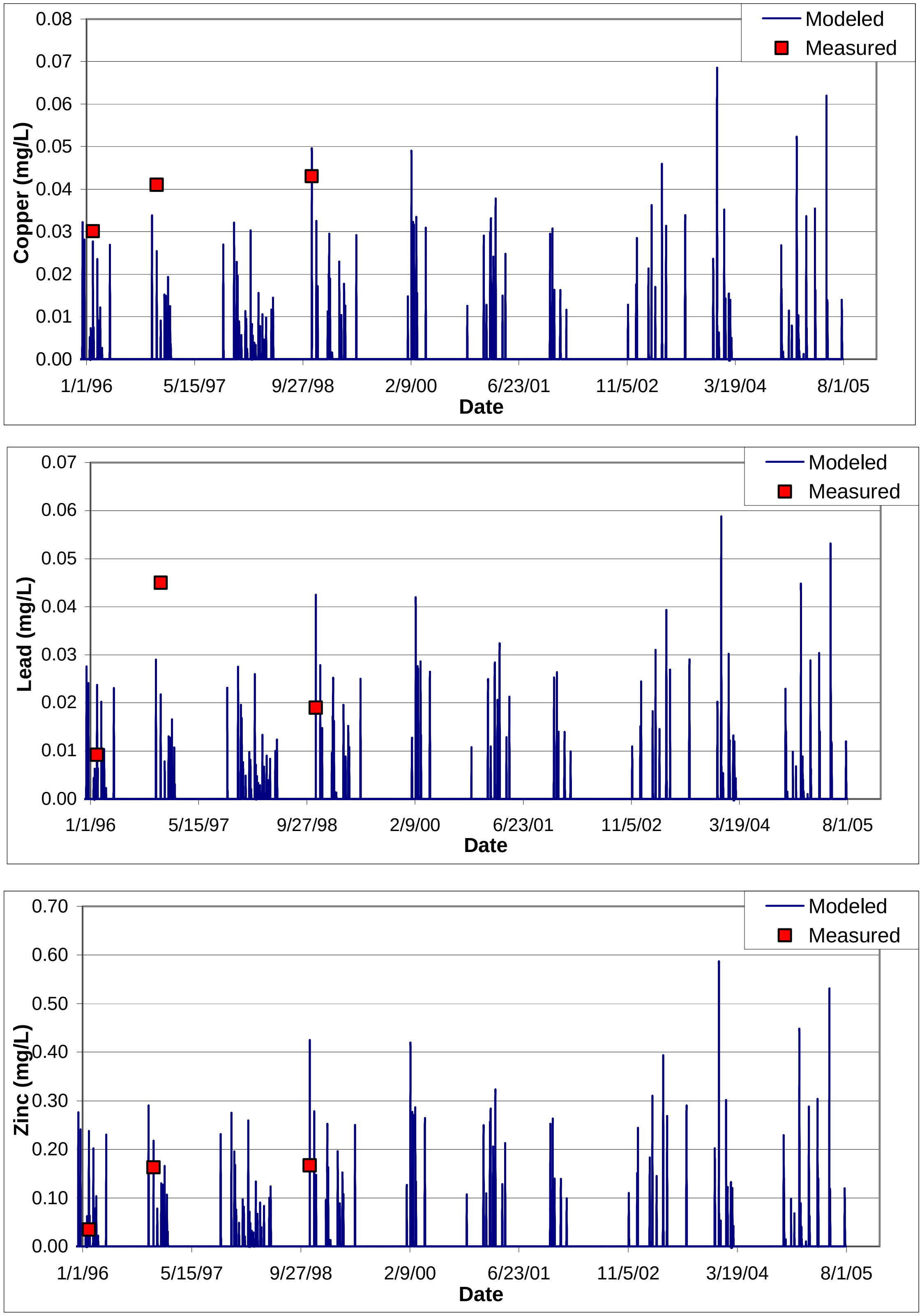

Figure A-18. Modeled and Observed Metal Concentrations for Subwatershed 9 (POLB Station 19A)

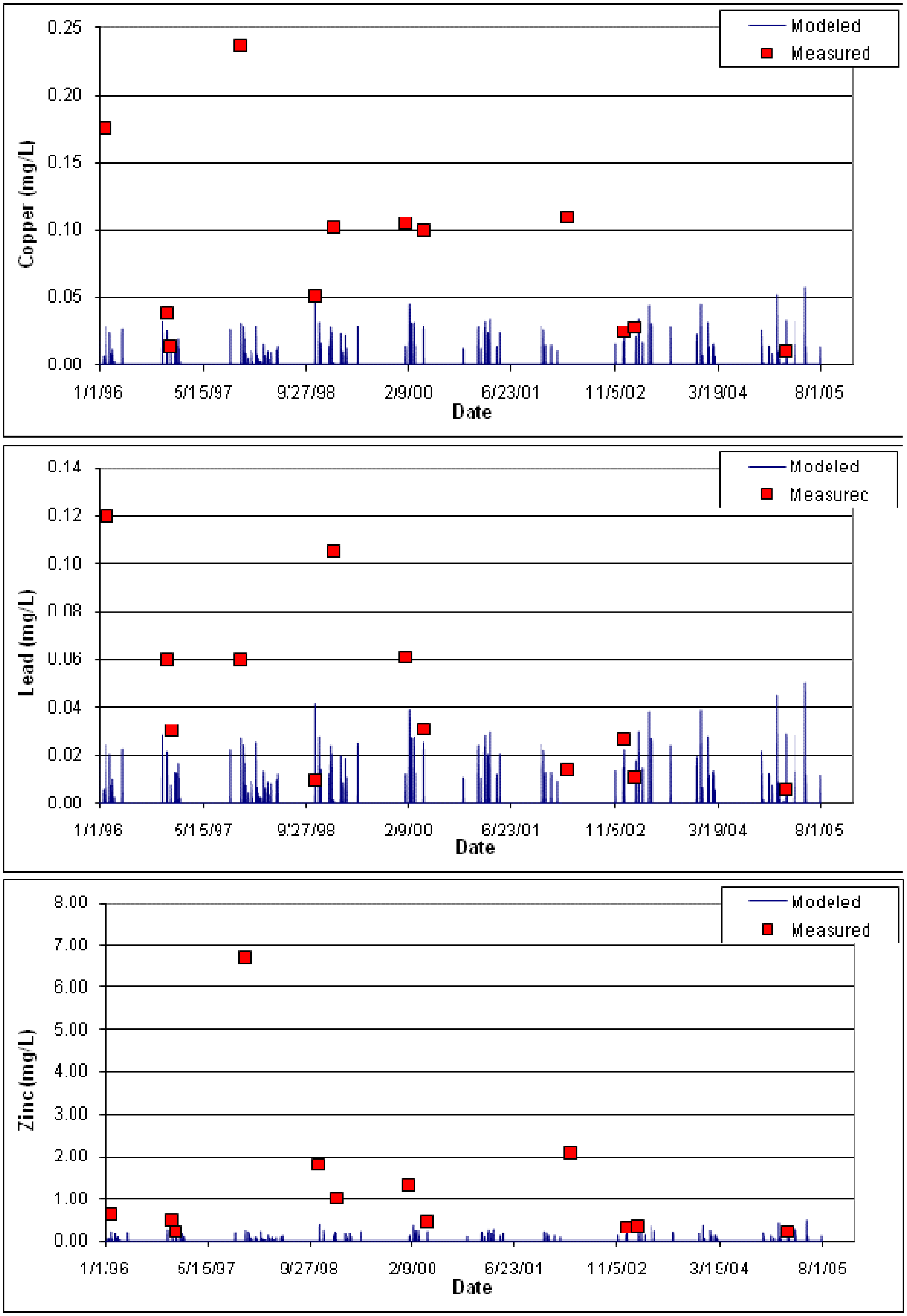

Figure A-19. Modeled and Observed Metal Concentrations for Subwatershed 12 (POLB Station 6A)

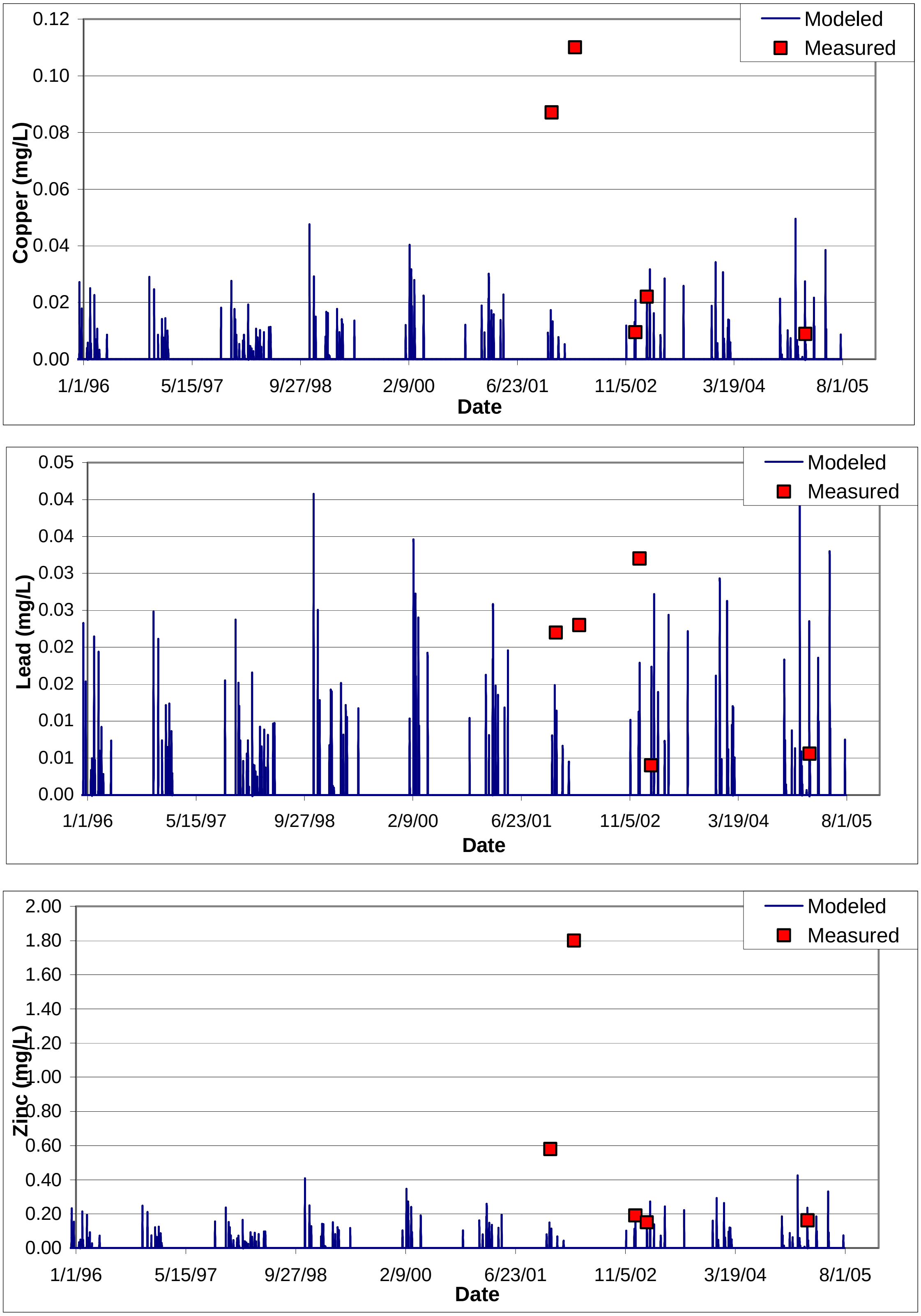

Figure A-20. Modeled and Observed Metal Concentrations for Subwatershed 13 (POLB Station 23A)

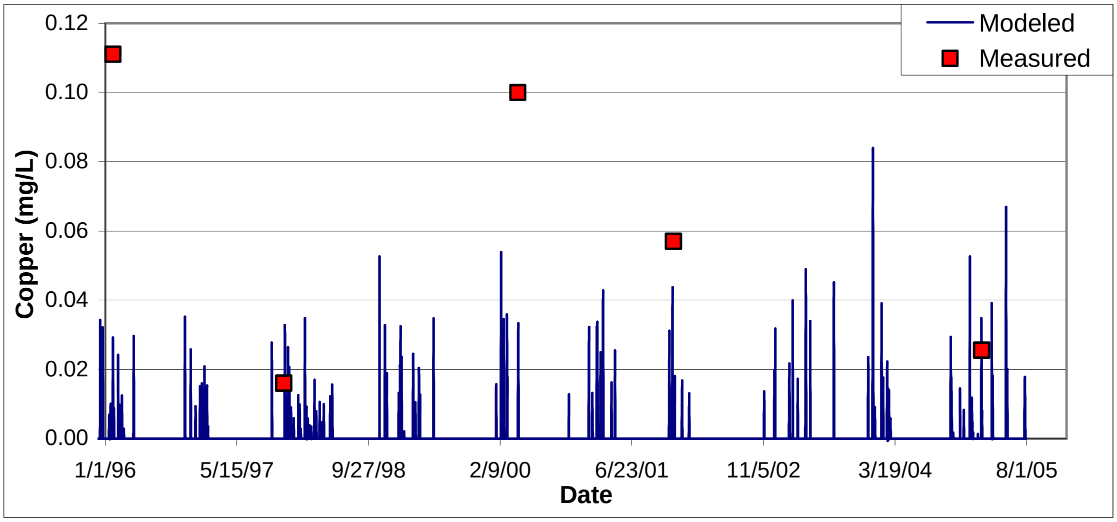

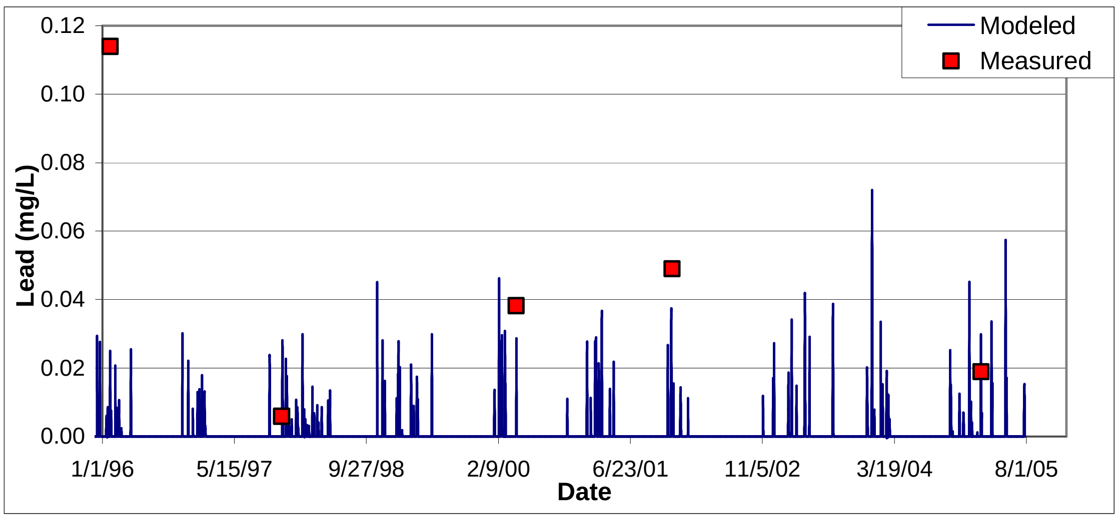

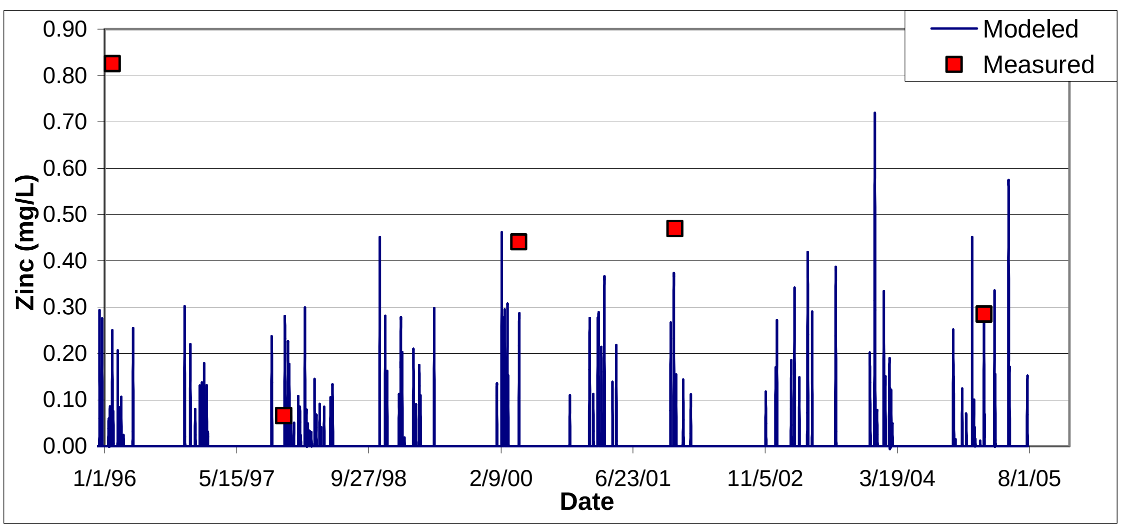

Figure A-21. Modeled and Observed Metal Concentrations for Subwatershed 14 (POLB Station 8A)

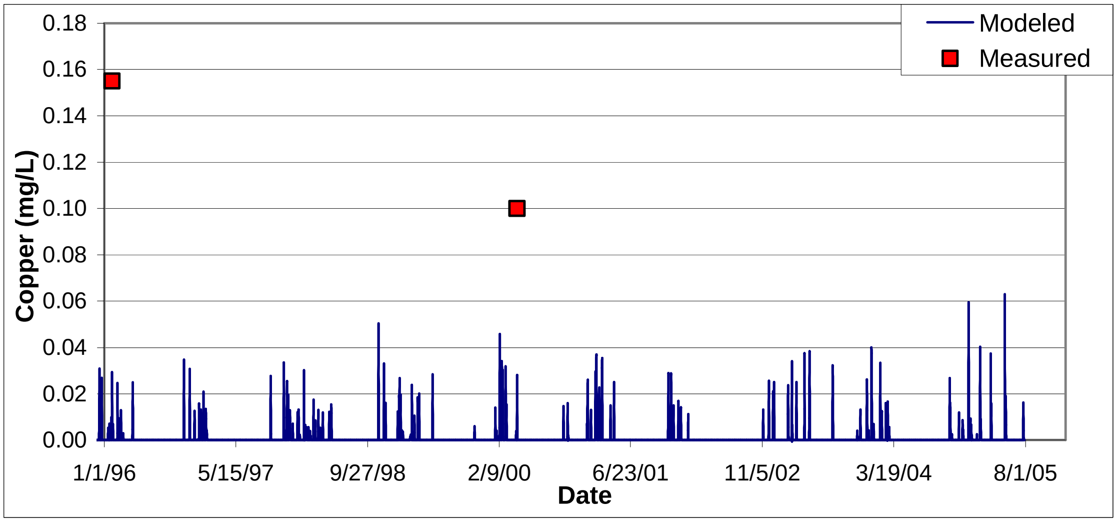

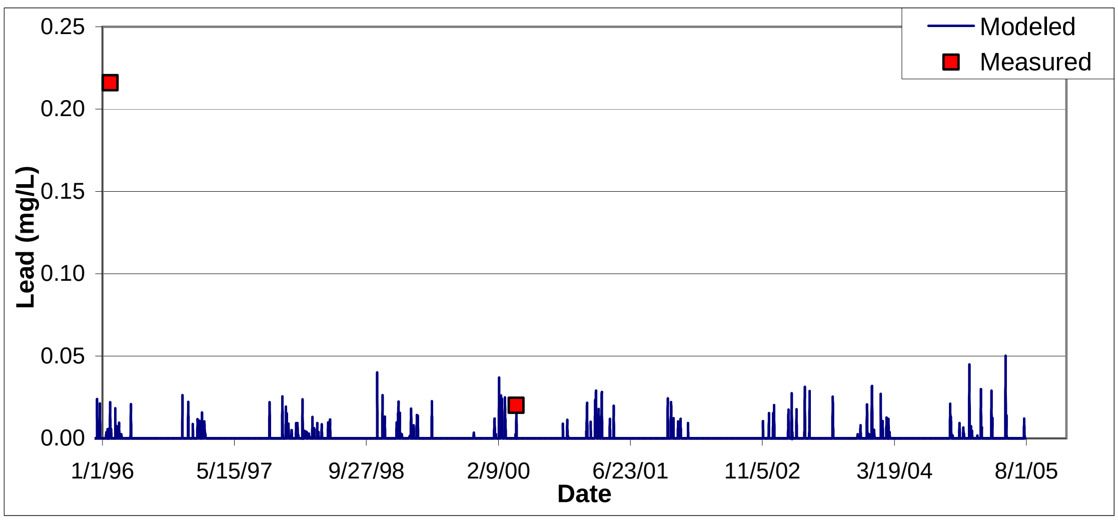

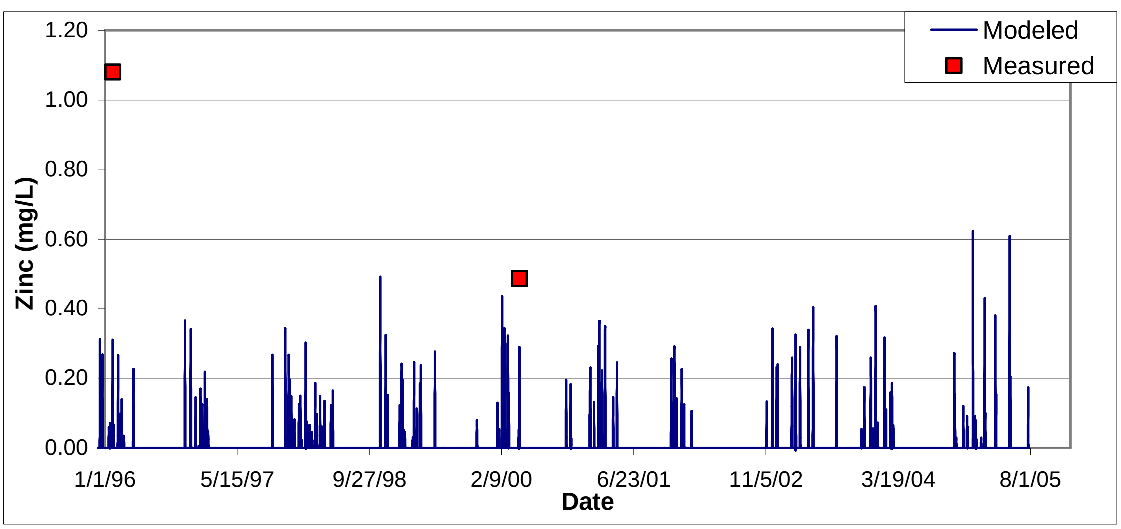

Figure A-22. Modeled and Observed Metal Concentrations for Subwatershed 15 (POLB Station 7A)

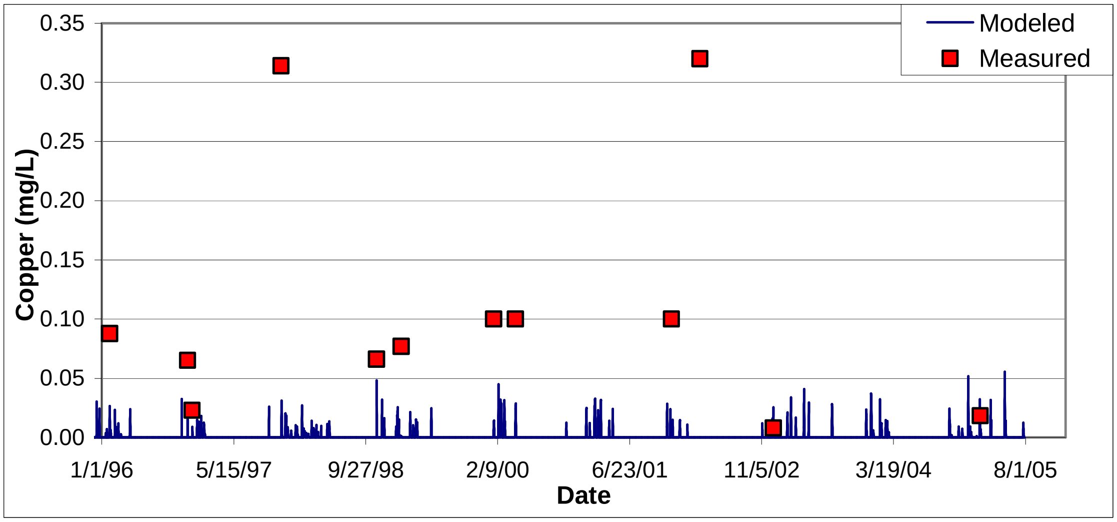

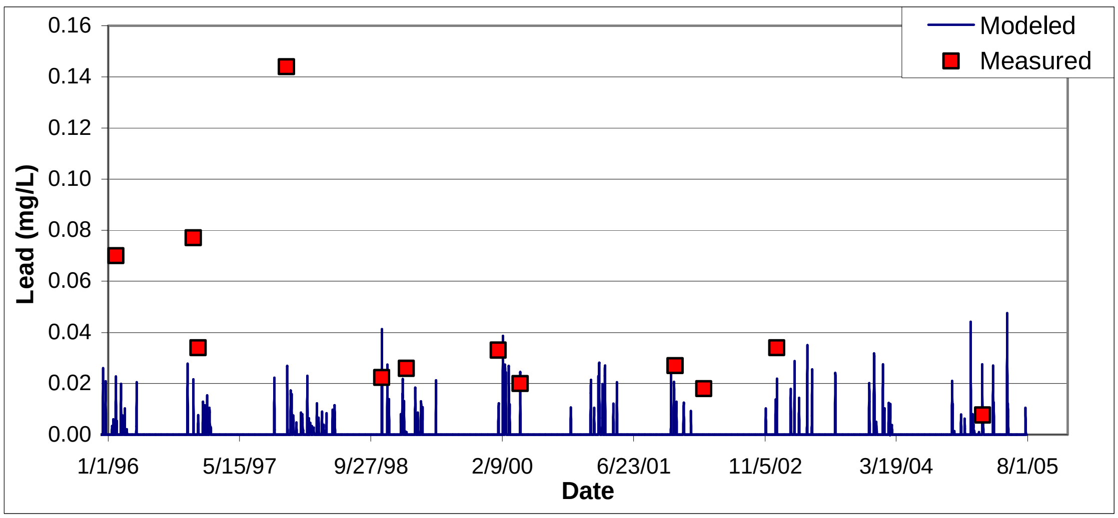

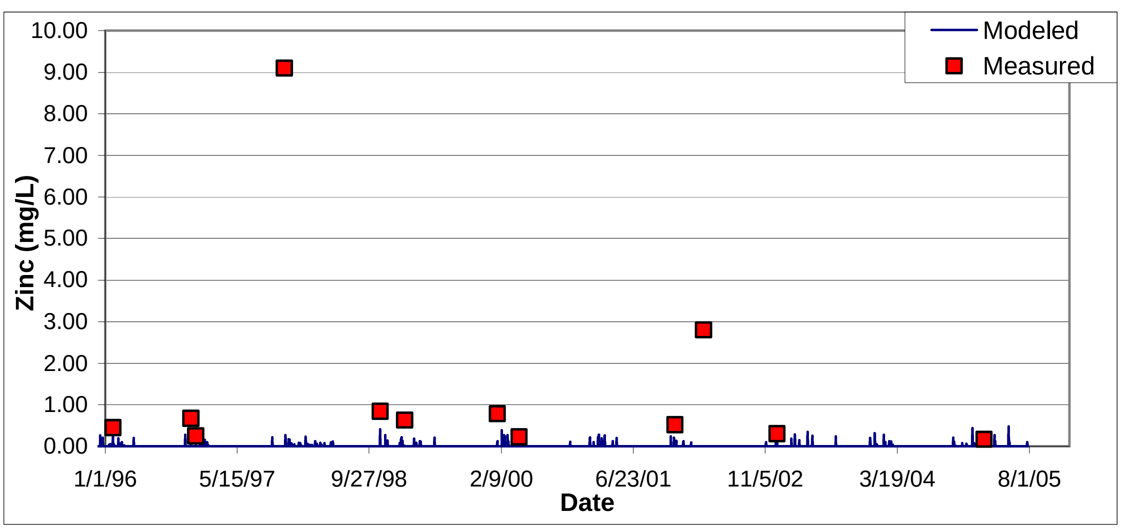

Figure A-23. Modeled and Observed Metal Concentrations for Subwatershed 16 (POLB Station 20A)

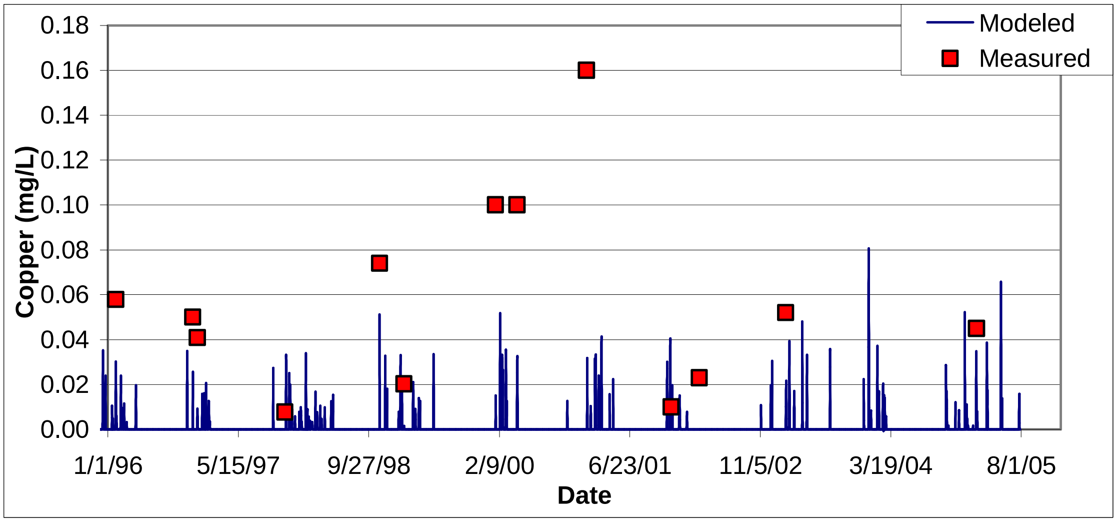

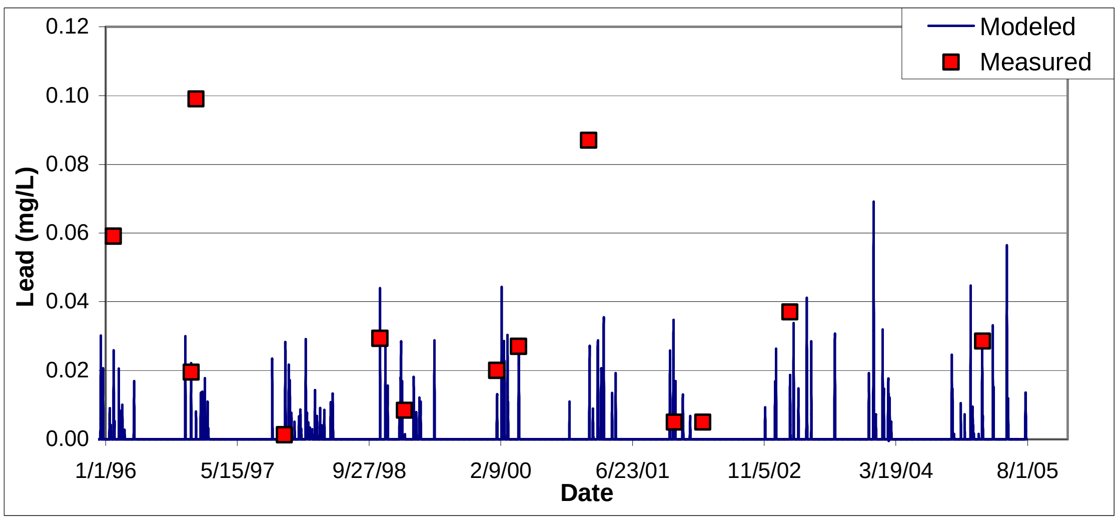

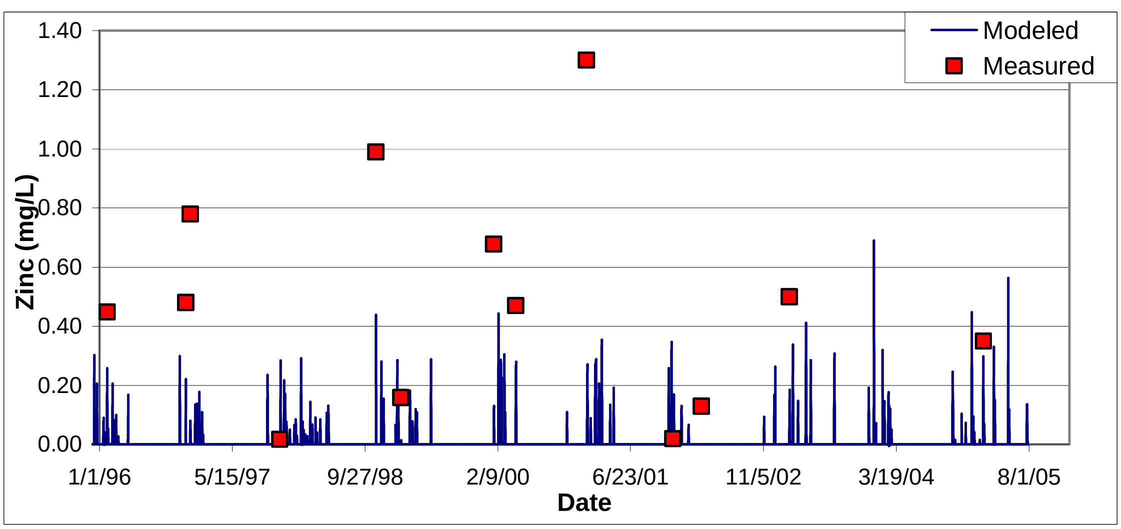

Figure A-24. Modeled and Observed Metal Concentrations for Subwatershed 20 (POLB Station 2A)

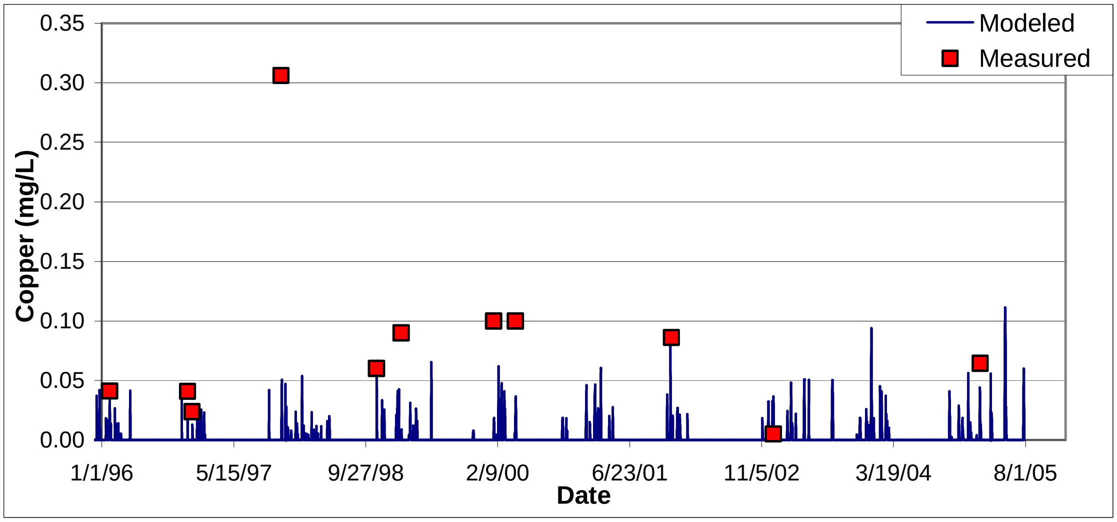

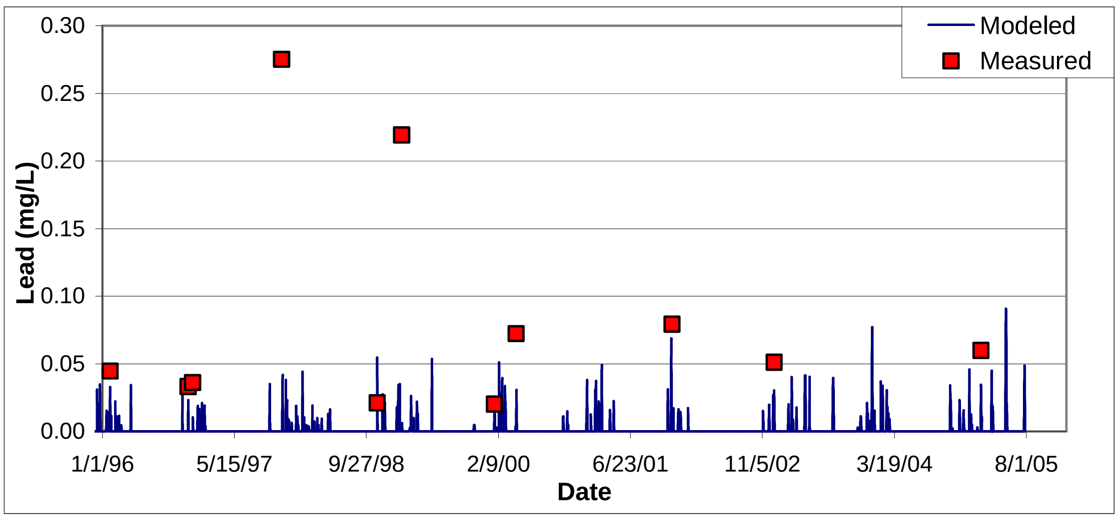

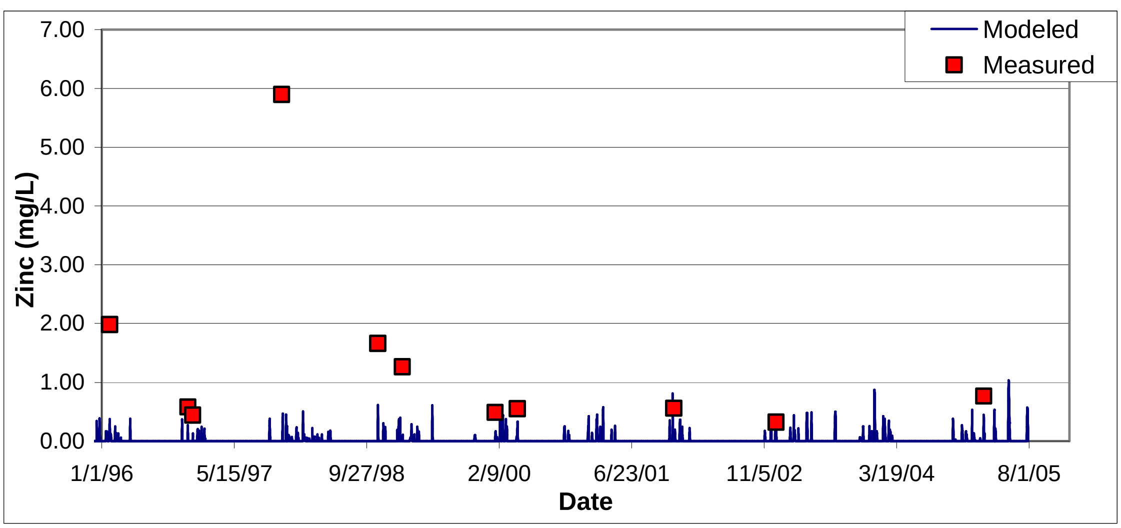

Figure A-25. Modeled and Observed Metal Concentrations for Subwatershed 25 (POLB Station 9A)

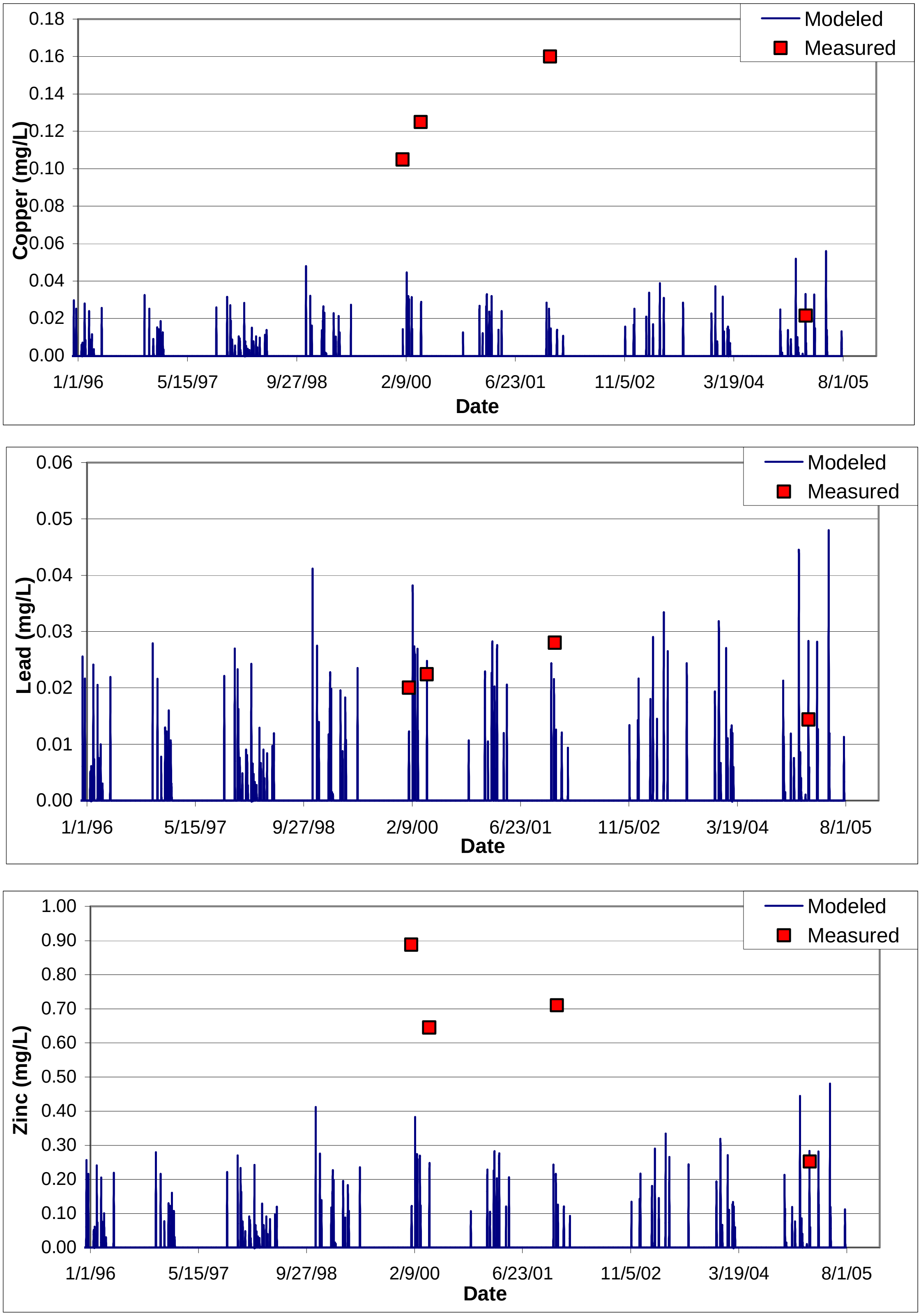

Figure A-26. Modeled and Observed Metal Concentrations for Subwatershed 29 (POLB Station 22A)

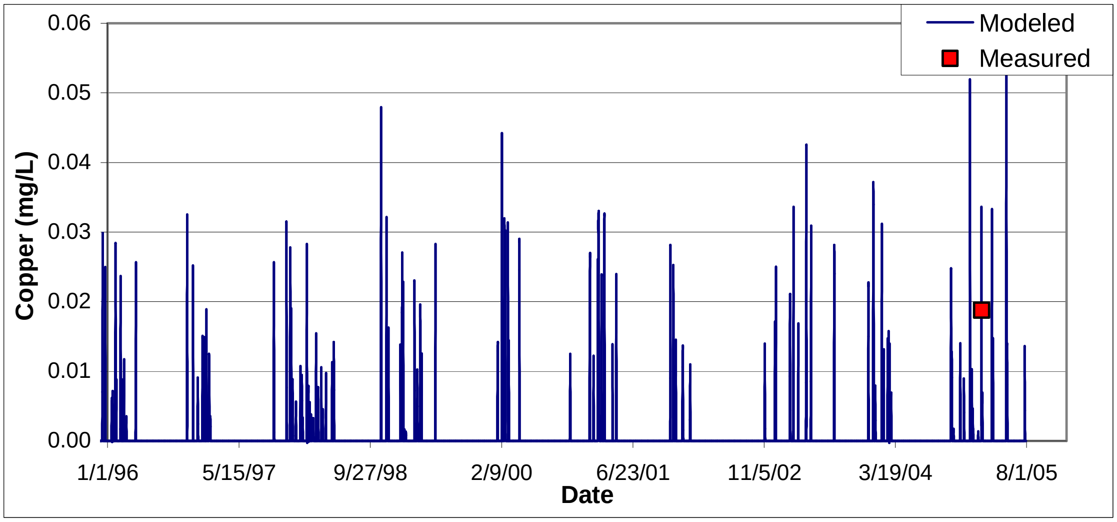

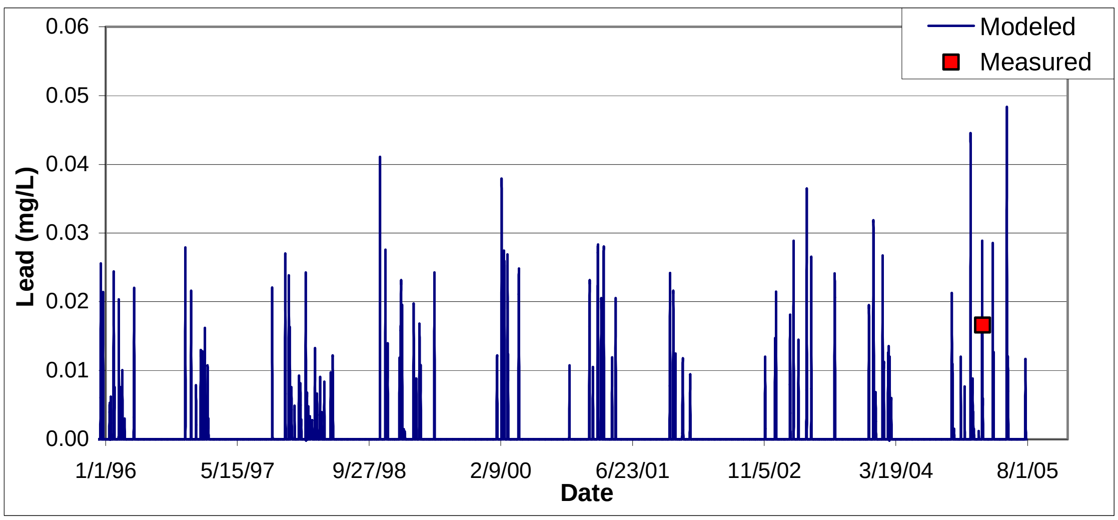

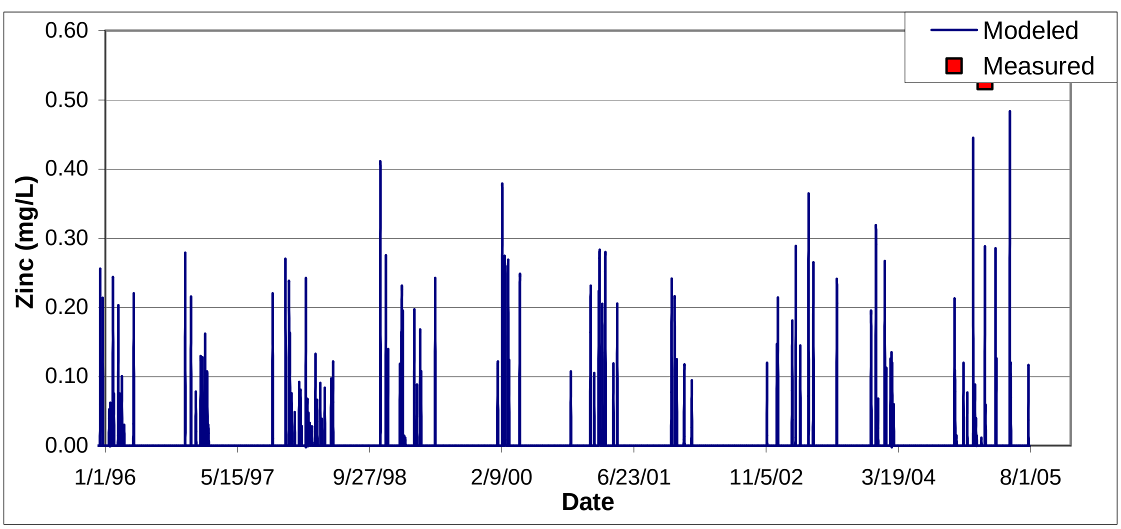

Figure A-27. Modeled and Observed Metal Concentrations for Subwatershed 31 (POLB Station 24A).

Appendix B: Annual Loads for Watersheds Draining to the Harbors & San Pedro Bay

FINAL

October 2010

Prepared for:
USEPA Region 9
Los Angeles Regional Water Quality Control Board

Prepared by:
Tetra Tech, Inc.

Table B-1. Annual Loads (kg/yr) for Subwatersheds Draining to Alamitos Bay

Year	Copper	Lead	Zinc	DDT	PAHs	PCBs
1995	699	560	6,937	0.015	55.56	0.007
1996	579	471	5,766	0.013	34.59	0.006
1997	503	399	4,818	0.008	29.47	0.004
1998	647	536	6,678	0.013	65.92	0.006
1999	258	157	2,169	0.004	13.18	0.002
2000	423	316	3,970	0.008	18.20	0.004
2001	650	544	6,184	0.009	17.47	0.004
2002	211	111	1,511	0.002	4.74	0.001
2003	472	363	4,485	0.009	19.56	0.004
2004	542	417	5,295	0.010	34.19	0.005
2005	482	366	4,536	0.008	30.03	0.004

Table B-2. Annual Loads (kg/yr) for Subwatersheds Draining to Los Angeles/Long Beach Inner Harbor

Year	Copper	Lead	Zinc	DDT	PAHs	PCBs
1995	332	216	2,719	0.061	28.24	0.041
1996	275	181	2,260	0.054	17.58	0.036
1997	239	154	1,888	0.035	14.98	0.024
1998	307	206	2,617	0.054	33.51	0.037
1999	122	60	850	0.017	6.70	0.011
2000	201	122	1,556	0.033	9.25	0.022
2001	309	210	2,424	0.036	8.88	0.025
2002	100	43	592	0.008	2.41	0.005
2003	224	140	1,758	0.039	9.94	0.026
2004	257	161	2,075	0.042	17.38	0.029
2005	229	141	1,778	0.034	15.26	0.023

Table B-3. Annual Loads (kg/yr) for Subwatersheds Draining to Los Angeles/Long Beach Outer Harbor (inside the breakwater)

Year	Copper	Lead	Zinc	DDT	PAHs	PCBs
1995	40	23	324	0.005	2.67	0.004
1996	33	19	269	0.005	1.67	0.003
1997	29	17	225	0.003	1.42	0.002
1998	37	22	311	0.005	3.17	0.003
1999	15	6	101	0.001	0.63	0.001
2000	24	13	185	0.003	0.88	0.002
2001	37	23	288	0.003	0.84	0.002
2002	12	5	70	0.001	0.23	0.000
2003	27	15	209	0.003	0.94	0.002
2004	31	17	247	0.004	1.65	0.003
2005	27	15	212	0.003	1.45	0.002

Table B-4. Annual Loads (kg/yr) for Subwatersheds Draining to Los Angeles Harbor—Consolidated Slip (including Dominguez Channel)

Year	Copper	Lead	Zinc	DDT	PAHs	PCBs
1995	2,078	1,217	19,565	1.086	171.71	0.720
1996	1,553	864	15,801	1.080	109.44	0.684
1997	1,306	694	11,853	0.763	84.68	0.477
1998	2,352	1,463	23,417	1.380	171.22	0.897
1999	699	370	6,825	0.472	53.38	0.296
2000	1,220	650	11,721	0.805	76.78	0.494
2001	1,293	671	11,510	0.581	90.34	0.338
2002	569	280	5,344	0.373	42.08	0.230
2003	1,034	521	9,909	0.681	72.45	0.428
2004	1,736	912	15,540	0.863	93.63	0.516
2005	1,664	963	15,354	0.919	119.80	0.586

Table B-5. Annual Loads (kg/yr) for Subwatersheds Draining to Los Angeles Harbor—Inner Cabrillo Beach Area

Year	Copper	Lead	Zinc	DDT	PAHs	PCBs
1995	5.72	3.44	38.98	0.0003	0.45	0.0002
1996	4.74	2.90	32.39	0.0003	0.28	0.0002
1997	4.12	2.46	27.07	0.0002	0.24	0.0001
1998	5.30	3.30	37.52	0.0003	0.53	0.0002
1999	2.11	0.96	12.19	0.0001	0.11	0.0000
2000	3.47	1.94	22.31	0.0002	0.15	0.0001
2001	5.32	3.35	34.74	0.0002	0.14	0.0001
2002	1.73	0.68	8.49	0.0000	0.04	0.0000
2003	3.87	2.23	25.20	0.0002	0.16	0.0001
2004	4.44	2.57	29.75	0.0002	0.27	0.0001
2005	3.95	2.25	25.48	0.0002	0.24	0.0001

Table B-6. Annual Loads (kg/yr) for Subwatersheds Draining to Los Angeles River Estuary (including Los Angeles River)

Year	Copper	Lead	Zinc	DDT	PAHs	PCBs
1995	71,111	50,199	497,457	21.29	1,336	59.28
1996	18,286	12,172	139,851	5.45	850	15.16
1997	13,098	8,293	96,314	3.72	644	10.34
1998	64,902	45,751	458,350	19.45	1,515	54.16
1999	5,948	3,281	43,544	1.70	380	4.73
2000	13,437	8,654	100,428	3.90	647	10.85
2001	21,404	14,905	165,034	6.37	917	17.74
2002	10,178	6,590	77,724	2.96	433	8.25
2003	16,149	11,111	126,157	4.78	673	13.30
2004	23,131	16,365	179,538	6.80	884	18.94
2005	36,597	25,632	265,994	11.31	1,379	31.48

Table B-7. Annual Loads (kg/yr) for Subwatersheds Draining to San Pedro Bay Nearshore/ Offshore Zones

Year	Copper	Lead	Zinc	DDT	PAHs	PCBs
1995	78.97	54.95	691.80	0.0019	7.90	0.0009
1996	65.42	46.20	575.00	0.0017	4.92	0.0008
1997	56.83	39.20	480.46	0.0011	4.19	0.0005
1998	73.20	52.57	665.95	0.0017	9.38	0.0008
1999	29.14	15.37	216.29	0.0005	1.87	0.0003
2000	47.87	30.97	395.91	0.0010	2.59	0.0005
2001	73.49	53.42	616.71	0.0011	2.49	0.0005
2002	23.84	10.85	150.66	0.0002	0.67	0.0001
2003	53.38	35.65	447.23	0.0012	2.78	0.0006
2004	61.27	40.95	528.03	0.0013	4.86	0.0006
2005	54.53	35.89	452.34	0.0011	4.27	0.0005

Table B-8. Annual Loads (kg/yr) for Subwatersheds Draining to San Gabriel River Estuary (includes San Gabriel River)

Year	Copper	Lead	Zinc	DDT	PAHs	PCBs
1995	5,801	7,997	78,117	0.09	444.19	0.025
1996	6,558	8,977	84,054	0.08	291.41	0.023
1997	3,867	4,533	46,291	0.04	203.14	0.010
1998	8,813	13,265	126,696	0.16	446.80	0.043
1999	2,418	2,739	26,793	0.02	153.65	0.006
2000	3,871	4,981	47,002	0.04	192.84	0.012
2001	5,119	6,515	61,860	0.06	239.91	0.015
2002	2,380	2,608	25,803	0.02	103.95	0.006
2003	4,909	6,375	59,336	0.05	186.94	0.014
2004	7,179	9,758	91,344	0.09	237.97	0.024
2005	6,136	8,121	77,256	0.08	309.26	0.021